CHALMERS
UNIVERSITY OF TECHNOLOGY

Battery Electric Vehicle with a Fuel Cell Stack

A System Study of Propulsion Concepts and Scenarios

Master's thesis in Electrical Engineering

SHAOHANG WANG
YIWEN XU

Department of ELECTRICAL ENGINEERING
CHALMERS UNIVERSITY OF TECHNOLOGY
Gothenburg, Sweden 2019

Master's thesis 2019

Battery Electric Vehicle with a Fuel Cell Stack

A System Study of Propulsion Concepts and Scenarios

SHAOHANG WANG
YIWEN XU

CHALMERS
UNIVERSITY OF TECHNOLOGY

Department of Electrical Engineering
Division of Systems and Control
Chalmers University of Technology
Gothenburg, Sweden 2019

Battery Electric Vehicle with a Fuel Cell Stack
A System Study of Propulsion Concepts and Scenarios
SHAOHANG WANG
YIWEN XU

Supervisor:
Roy Ogink, China Euro Vehicle Technology AB
Bengt Axelsson, China Euro Vehicle Technology AB

Examiner:
Anders Grauers, Department of Electrical Engineering

Master's Thesis 2019
Department of Electrical Engineering
Division of Systems and Control
Chalmers University of Technology
SE-412 96 Gothenburg
Telephone +46 31 772 1000

Cover: Lynk & Co 01, China Euro Vehicle Technology AB

Printed by Chalmers Reproservice
Gothenburg, Sweden 2019

Battery Electric Vehicle with a Fuel Cell Stack
A System Study of Propulsion Concepts and Scenarios
SHAOHANG WANG
YIWEN XU

Department of Electrical Engineering
Chalmers University of Technology

Abstract

The long-term use of a large amount of fossil energy has broken the ecological balance of the earth and climate issue, especially global warming, has been regarded as a common problem facing the development of human society. E-mobility is developing rapidly and has recently been recognized by most people as an essential part of improving this issue. With a competitive driving range, short refueling time and zero emissions, Fuel Cell Electric Vehicles (FCEVs) have been considered as 'The real breakthrough of E-mobility' which may be a possible solution for the future vehicle.

In this thesis project, a complete fuel cell system submodel, including a fuel cell stack, supplying system, and water management system was modelled. One Fuel Cell Plug-in Hybrid Electric Vehicle (FC-PHEV) and one Fuel Cell Hybrid Electric Vehicle (FC-HEV) model, as well as different components and control strategies, were also implemented in the GT-Suite software to simulate the hydrogen consumption under various driving cycles and scenarios. Furthermore, a cost analysis model is also developed to determine the optimal battery size for the FC-PHEV. Finally, a cost comparison among FC-PHEV, FC-HEV, and Battery Electric Vehicle (BEV) was made based on current data available from the U.S market.

The Fuel Cell-PHEV model and the Fuel Cell-HEV model are validated against the WLTC and NEDC driving cycles. The functionality of the main control units is also evaluated. The simulation results show that: For the Fuel Cell-PHEV, the combined hydrogen consumption is 0.29 kg/100 km for NEDC, and 0.34 kg/100 km for WLTC. For the Fuel Cell-HEV, the hydrogen consumption is 0.68 kg/100 km for NEDC, and 0.82 kg/100 km for WLTC.

The results of the initial cost comparison of energy source, based on current data, show the ranking from the cheapest to the most expensive is FC-HEV, FC-PHEV, and BEV. The ranking of the total cost of ownership, including running cost from the cheapest to the most expensive is FC-PHEV, BEV, and FC-HEV. Overall, the Fuel Cell Plug-in Hybrid Electric Vehicle could be the best choice based on the current data.

This project also present a simple mathematical cost model for determining the optimal energy capacity of the battery pack in FC-PHEV from economic aspect through

the whole vehicle lifespan, it shows the optimal battery size of FC-PHEV based on the data of this model in the U.S market is around 10.5 kWh which equals to a 50 km driving range roughly.

Finally, future work recommendations are suggested so that this research topic can be further developed.

Keywords: Fuel Cell, Hybrid Electric Vehicle, Plug-in, Hydrogen consumption, Powertrain, Control Strategy, Battery Size, GT-Suite.

Acknowledgements

The thesis report shows the results of the master thesis project *Battery Electric Vehicle with a Fuel Cell Stack-A System Study of Propulsion Concepts and Scenarios* carried out in CAE department in cooperation with powertrain department at China Euro Vehicle Technology AB (CEVT) in Lindholmen, Gothenburg.

We want to express our gratitude to our supervisors Roy Ogink and Bengt Axelsson at CEVT for giving us the opportunity and the resources to get involved in a real early-stage development project. We would also like to thank our examiner and supervisor professor Anders Grauers in Department of Electrical Engineering, Division of Systems and Control at the Chalmers University of Technology for the technical guidance and patiently sharing his knowledge to us. Furthermore, we are very grateful to our friendly colleagues at CEVT for the efficient, harmonious and pleasant working environment.

Apart from our supervisors and colleagues, we also want to thank Peter Stopp and Jake How at Gamma Technologies for webinars and patiently answering our modeling questions.

Last but not least, we would like to thank our families for their love and their continuous support.

Shaohang Wang and Yiwen Xu, Gothenburg, Sweden, June, 2019

Acronyms

BEV Battery Electric Vehicle

HEV Hybrid Electric Vehicle

PHEV Plug-in Hybrid Electric Vehicle

FCEV Fuel Cell Electric Vehicle

PEM Proton Exchange Membrane

SOC State Of Charge

ICE Internal Combustion Engine

HHV Higher heating value

LHV Lower heating value

BCU Braking Control Unit

TCU Transmission Control Unit

FCCU Fuel Cell Control Unit

EMCU Electric Motor Control Unit

BMS Battery Management System

NEDC New European Driving Cycle

WLTC Worldwide Harmonized Light Vehicles Test Cycle

WLTP Worldwide Harmonised Light-Duty Vehicles Test Procedure

CDCS Charge Depleting Charge Sustaining

ECMS Equivalent Consumption Minimization Strategy

TCO Total Cost of Ownership

Contents

List of Figures

List of Tables

1
Introduction

1.1 Background

The Automotive industry is presently undergoing a transition from internal combustion engines towards hybridization and electrification. Adding sufficient battery capacity to pure electric vehicles to reach a driving range like that of traditional combustion engine vehicles drives up the cost and increases weight significantly, also the recharging time should take into consideration for battery electric vehicles, and it is a primary factor for consumer usage experience. According to [1], for BMW i3, which contains a 33 kWh battery pack, it takes 3 hours for regular charging and 40 minutes if using supercharger (80% charge). For Tesla S60, which contains a 60 kWh battery pack, it takes 7 hours for regular charging and 30 minutes if using supercharger (80% charge). Some manufacturers, such as Toyota, Honda, and Hyundai, are starting to offer fuel cell vehicles to their customers. With the fuel cell technology, the system efficiency will increase, and the well-to-wheel greenhouse gas (GHG) emissions will be significantly lower than traditional combustion engine vehicles.

1.1.1 Environmental problems and greenhouse emission

Fossil fuel usages in our daily life can be one of the main reasons for climate changes and pollutions, especially in the transportation field. The non-renewable energy will run out someday in the future. Moreover, the impact of these pollutions on human health is severe.

The Paris Agreement, with the long-term goal to keep the increase in global average temperature to well below 2°C above pre-industrial levels, enables all countries to work together to make ambitious efforts to address climate change and adapt to the effects of climate change. All participants should make their best efforts through Nationally Determined Contributions (NDCs) and will be assessed in every 5 years. For example, the EU's nationally determined contribution (NDC) under the Paris Agreement is to reduce greenhouse gas emissions by at least 40% by 2030 compared to 1990, under its wider 2030 climate and energy framework.

As a result, more and more policymakers and vehicle manufacturers in the world have turned to more sustainable transportation solutions due to concerns about environmental pollution and greenhouse gas (GHG) emission [2].

1.1.2 Trends in fossil fuel

According to the International Energy Agency (IEA), although renewable energy has strong growth, the total share of fossil fuel in global energy demand remained at 81% in 2017. This level is almost constant for more than three decades [3].

The world oil demand increased by 1.6% (1.5 million barrels per day) in 2017, which is much higher than the average annual growth rate 1% in the past decade. The transportation sector is one of the main reasons. This is also a factor in the European Union, where oil demand has increased by 2%, the highest growth rate since 2001 [3].

1.1.3 State of play of Electric Vehicles

The vehicle as the main transportation has been playing a really important role in people's daily life for centuries. This subsection is going to introduce the market condition of EV among some major countries around the world and discuss the positive factor for EV's development which may give a clear picture of the electric mobility situation.

Based on Global EV outlook 2018 [4], the total sales of EV through the whole year of 2017 have achieved 1 million and the total stock of EV has reached 3 million globally in 2017. In addition, more than half of the total sales in 2017 happened in the China market which is higher than the sales of any other countries sum together. But the share of EV of total car sales in China through 2017 is still only 2.2%, while the value in Norway has reached 39% which is the highest number around the world.

It's not necessary to consult a crystal ball to realize that, EV market is currently a fast growing market (Figure 1.1) and China is the largest one which owned highest stock and sales, the united states and Europe rank 2 and 3 respectively.

Additionally, an expending list of nine countries including China, Denmark, France, India, Ireland, Netherlands, Norway, Sweden and United Kingdom have announced that fossil fuels vehicles will be banned in new vehicle sales during 2025 to 2040. Costa Rica announced to remove all fossil fuel vehicles at 2021 and Israel will ban all imported fossil fuel vehicle at 2030 [5].

The trend of EV is clear, more and more nations have announced their national target for developing EV through 2020-2030 to embrace the development of EV and give policy support, especially in China and Norway. With the policy support and large demand of EV, the EV charging infrastructure has been growing into a large scale. In 2017, the installed chargers have reached around 320,000 units, including over 110,000 fast chargers and the scale is still growing fast [4].

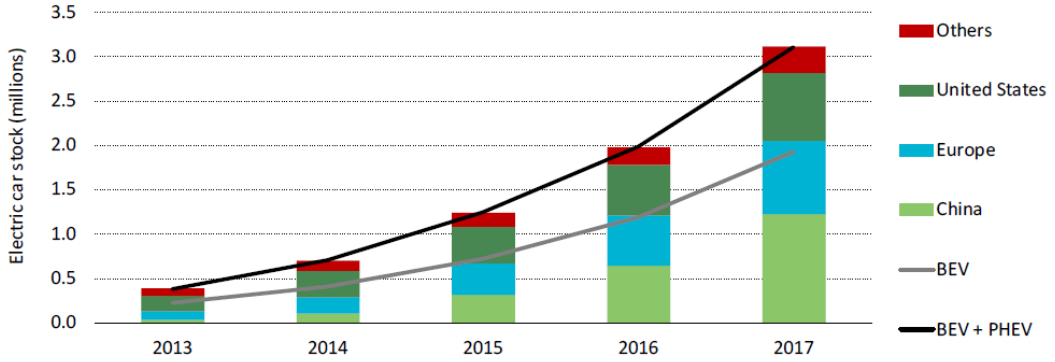

Notes: The electric car stock shown is primarily estimated on the basis of cumulative sales since 2005. Where available, stock numbers from official national statistics have been used (provided that the data can be shown to be consistent with sales evolutions).

Sources: IEA analysis based on country submissions, complemented by ACEA (2018); EAFO (2018a).

Figure 1.1: Variation trend of the global electric car stock[4]

So far the EV market is still growing fast with the cooperation of lots of countries and organizations, it is already been a common target for most people.

1.1.4 BEV Barriers

Battery Electric Vehicles (BEVs) has been recognized as the most popular electrified vehicle nowadays, but there are still some drawbacks wait for solutions. One significant factor in range limitations for BEV is the low specific energy of the battery pack, which is around 0.25 kWh/kg compared with that of diesel fuel 12.7 kWh/kg and 12.1 kWh/kg for gasoline fuel [6]. To achieve a 320 km range, the Tesla Roadster carries 450 kg of Li-ion batteries (this includes other electrical components), which is more than a third of the total vehicle weight. That same range would take around 26 kg of gasoline for a 30 mpg ICE car [7] and 3.2 kg of compressed hydrogen under the assumption that the hydrogen consumption is 1 kg/100 km (Actually this number could be even lower, the simulation results and the Fuel Cell Vehicles data on the market can be found in results chapter).

When driving a gasoline vehicle, the range is not such a big problem due to the short refueling time. However, the recharging time should take into consideration for battery electric vehicles, and it is a primary factor for consumer usage experience. According to [1], for BMW i3, which contains a 33 kWh battery pack, it takes 3 hours for regular charging and 40 minutes if using supercharger (80% charge). For Tesla S60, which contains a 60 kWh battery pack, it takes 7 hours for regular charging and 30 minutes if using supercharger (80% charge). Meanwhile, the high power DC fast charger needs the modification of the grid and a large number of DC fast chargers will be a huge load of the grid. Besides, high power fast charging is a way to reduce the charging time of BEV, but it also has a significant impact on battery degradation which is the contradiction that needs to be solved urgently.

Additionally, the cost ratio of battery in the whole vehicle manufacturing nowadays is somehow too high, and the car manufacturer is hard to earn many profits compared to conventional vehicles. Meanwhile, because of the low energy density of the battery, the rate of loading of BEVs is not competitive than other types of vehicles.

1.1.5 State of play of Fuel cell Electric Vehicles

The FCEVs has been recognized as 'the real breakthrough for e-mobility' because of its competitive performance over conventional vehicles. First, the driving range of FCEVs is comparable to the conventional vehicle thanks to the hydrogen with high energy density. Moreover, the refueling time of a FCEV with a 5kg tank can be short as 3 to 5 minutes which is similar as conventional vehicles. Considered as e-mobility, FCEVs have no emissions but heat and water vapor if made from renewable sources which makes FCEV environmentally friendly [8].

The commercialization process of FCEV has been slow and in 2017, there were more than 7,200 fuel cell vehicles in the world, far fewer than pure electric vehicles and plug-in hybrid vehicles.(Advanced Fuel Cells TCP, 2018) The U.S has more than 3,500 fuel-cell vehicles, mainly in California, accounting for nearly half the world's total. Japan has the world's second largest number of fuel-cell vehicles, at 2,300, and the highest proportion (1.1%) of electric light passenger vehicles. By the end of 2017, about 1,200 fuel-cell cars were on the road in Europe, mainly in Germany and France. Installation of hydrogenation infrastructure is currently very limited. In 2017, there were only 330 refueling stations operating around the world, mostly in Japan. On a global average, there are about four refueling stations for every 100 fuel-cell vehicles, and even fewer in countries where fuel-cell vehicle penetration is high (Japan and the United States). However, there are already encouraging signs of hydrogen infrastructure and vehicle deployment in many markets, including the united states, China, Germany, Japan and South Korea [4].

To accelerate the commercialization of hydrogen energy the support and promotion of national policies is needed. In 2019, China included the development of hydrogen stations for new energy vehicles for the first time in its Government Work Report [9] and as the largest EV market globally, China will push the development of fuel cell vehicles.

1.2 Motivation for the project

The Automotive industry is presently undergoing a transition from pure internal combustion engines towards hybridization and electrification. Unlike internal combustion engine vehicles, the battery electric vehicles are constrained by the range anxiety, the long charging time, the lack of public charging infrastructures, and the high price. By using hydrogen as fuel instead of gasoline or diesel, the vehicle can retain the potential zero tailpipe emission feature. To investigate that powertrain,

this project aims at modelling and investigating Fuel Cell Electric Vehicles, in which the fuel cell is the primary source.

The regular Fuel Cell-HEV vehicles offer fast refueling and long driving range. However, the technology is presently expensive, and the hydrogen refilling infrastructures are not yet in place. Combining a fuel cell stack with a limited size battery as range extender can potentially result in fast charging and refueling, long driving-range with cost and mass lower than pure battery electric vehicles (BEVs). Also, the vehicle fuel economy is expected to get better since the fuel cell is about 40% more efficient than the internal combustion engine [10]. Therefore the Fuel Cell-PHEV is also modeled and simulated, which uses the battery as the first energy source and the fuel cell as a range extender.

1.3 Problem definition

This project has the following goals:

1. Understand the working process of all sub-systems within a complete fuel cell vehicle's propulsion system.
2. Investigate previous studies about fuel cells.
3. Investigate previous studies of propulsion system modeling and simulation.
4. Find the optimal propulsion concept for battery size, electric motor and fuel cell power, as well as hydrogen fuel storage amount.
5. Analyze the control strategies for Fuel Cell-HEV and Fuel Cell-PHEV models.
6. Build simulation models of Battery electric vehicle with a fuel cell stack (Fuel-cell PHEV, Fuel-cell HEV) and analyze the simulation results in different driving cycles and different case studies.

1.4 Objective

The aim is to perform system studies of battery electric vehicles with a fuel cell stack. The complete propulsion system, as well as their different components and control strategies, will be built in GT-Suite to analyze and the hydrogen and electrical consumption and find optimal propulsion concept for battery size, electric motor and fuel cell power, as well as hydrogen fuel storage amount. Attributes to consider are driving range, performance, charging and refueling time, vehicle mass and cost.

Different scenarios and concepts will be studied. The results from simulations will be compared to data from actual fuel cell vehicles on the market.

1.5 Limitation

A complete propulsion system with a fuel cell will be modeled in GT-Suite. Thus it will not be tested in a real vehicle. Meanwhile, the study will only focus on the propulsion system instead of a complete vehicle. All sub-systems like chassis which are not related to the propulsion system will not be covered in this study.

1.6 Methods

In order to get an overview of a propulsion system and get familiar with the working process of all sub-systems within a complete propulsion system with a fuel cell stack, a literature study has been carried out at first. The literature study covers the control strategy which related to different propulsion concepts. The complete propulsion system, as well as their different components, will be built with GT-Suite. Different scenarios and concepts will be studied and used to optimize the model. The results from simulations will be compared to data from actual fuel cell vehicles on the market.

2

Technology review

2.1 Hybrid Electric Vehicles

A hybrid vehicle uses two or more different types of power sources, such as using an internal combustion engine to drive an electric generator that powers an electric motor to drive the vehicle.

By using hybrid configurations, different components can work more efficiently in different driving conditions. For example, using the electric motor will be more efficient at low speed and low load. The internal combustion engine is more efficient for maintaining at high speed.

2.1.1 Powertrain configurations

A hybrid powertrain transmits power to the driving wheels, which has different architectures and energy flows. There are three main powertrain configurations for HEVs and PHEVs, which are series, parallel and power-split or series-parallel hybrid powertrain configuration. For all these three configurations, one advantage is that the electric motor can work as a generator to collect the kinetic energy and store it as electric energy in the battery when braking.

2.1.1.1 Series Hybrid Vehicle

A series hybrid vehicle also called range-extended electric vehicle. The configuration can be seen in Figure.2.1 below. For a series hybrid vehicle, which is driven by an electric motor, the internal combustion engine is mechanically decoupled with the drive axle, that the engine speed can be controlled independently of the vehicle speed and can be controlled to follow its optimal operating line, which has best fuel efficiency [11].

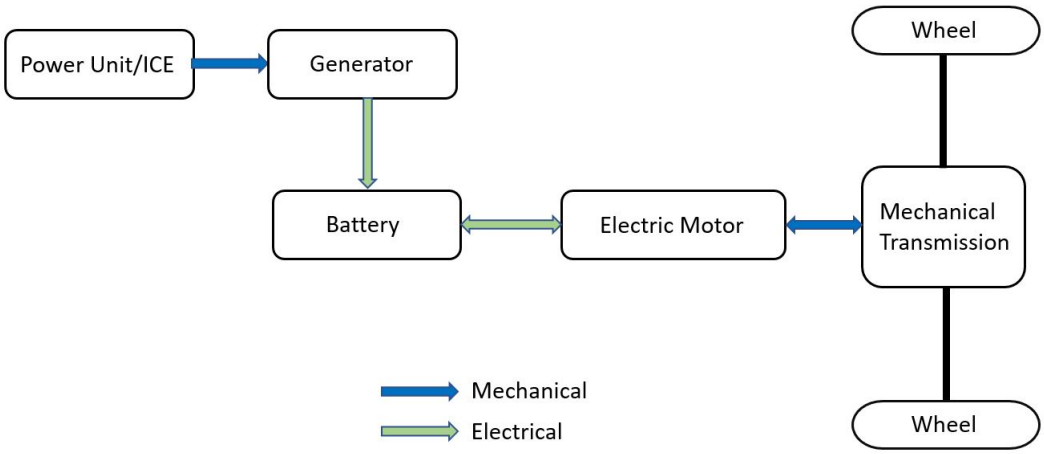

Figure 2.1: Series configuration of the powertrain for a HEV or PHEV

If the battery has sufficient electrical energy, it will drive as an electric vehicle. If the battery is insufficient, the engine will be turned on, and the mechanical output of the engine will convert to electricity by using a generator. When the power demand from the wheel is high, the engine will be turned on and both powers from the engine and battery pack will flow to the electric motor. In some situations like highway cruising, the vehicle can be driven in engine only mode, at that time the engine will run at optimal operating points. However, in some situations, if the engine is on and the power demand from the wheel is below the engine optimal operating power, and meanwhile, the battery state of charge is low, then the engine will run at optimal operating power and the extra power will be used to charge the battery.

To conclude, in a series hybrid vehicle, the electric motor can receive the energy directly from the engine, or the battery, or both. Another advantage is that it provides flexibility in locating the engine on the vehicle [11]. This configuration is considered to be the one closest to a pure electric vehicle [12].

2.1.1.2 Parallel Hybrid Vehicle

For a parallel hybrid vehicle, the configuration can be seen in Figure.2.2 below. Both electric motor and engine are mechanically connected to wheels. The vehicle can be propelled by the engine alone, by the motor alone, or by both together. Compared with a series hybrid vehicle, it has fewer components like a generator. Resulting in a more cost-effective solution. Another advantage is that the electric motor does not need to meet the peak power demand from the wheel.

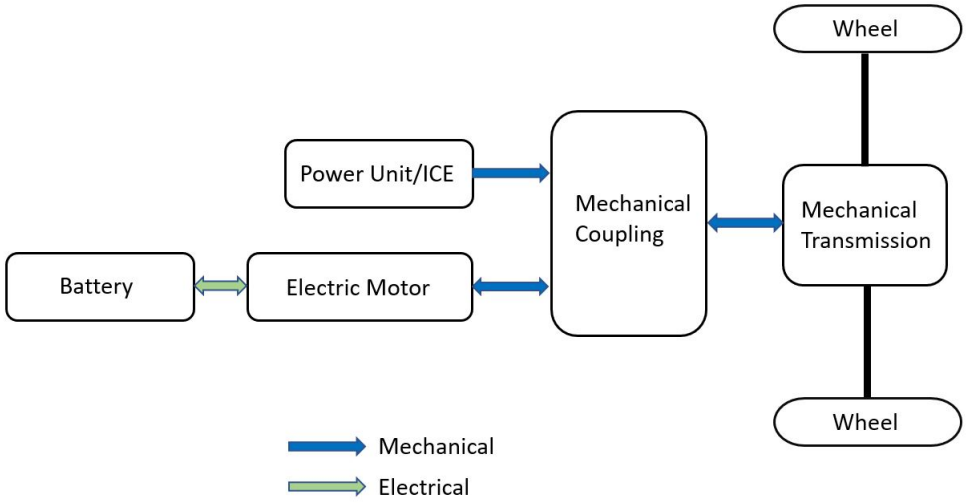

Figure 2.2: Parallel configuration of the powertrain for a HEV or PHEV

Compared with a series hybrid vehicle, the electric motor is usually smaller. When the battery has sufficient electrical energy, and the power demand from the wheel is low, it will drive like an electric vehicle and the engine will be turned off. During highway cruising, the vehicle will be driven in engine only mode. When the engine is on, but the traction power demand is low, and the battery state of charge is also low, the engine will run on the optimal operating line. The power will split, part of the power will be used for traction, the extra will be used for charging the battery. During high power demand, both the engine and electric motor will be turned on for traction [11].

2.1.1.3 Series-Parallel Hybrid Vehicle

For a series-parallel hybrid vehicle. The configuration can be seen in Figure.2.3 below. It is a combination of a series hybrid and parallel hybrid by incorporating a power split device.

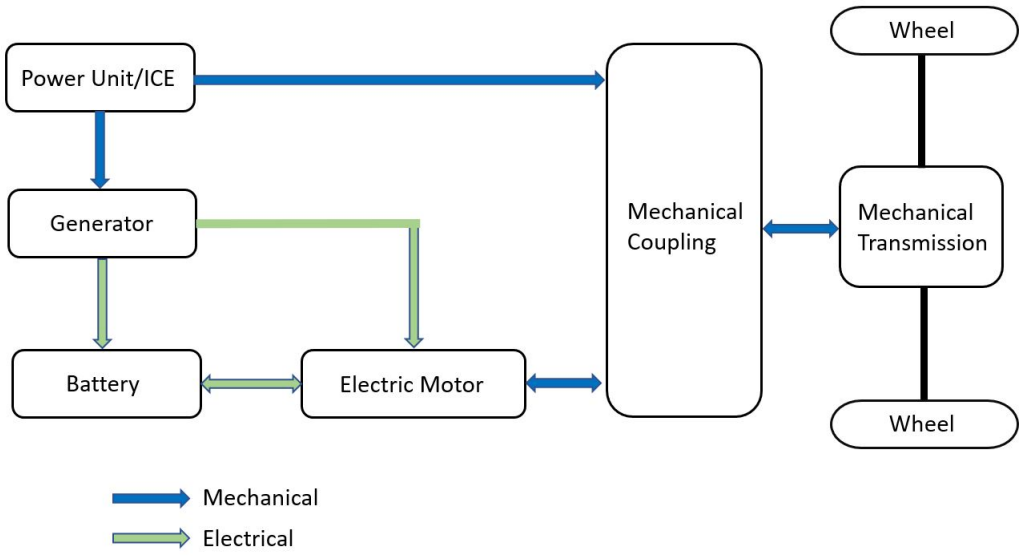

Figure 2.3: Series parallel configuration of the powertrain for a HEV or PHEV

Compared with a series hybrid, the series-parallel configuration has a mechanical connection directly from the engine to mechanical coupling part or mechanical transmission part. Compared with a parallel hybrid, the series-parallel configuration has a second electric motor which serves mostly as starter or generator [11].

2.1.1.4 HEV and PHEV

For a HEV, the battery can be recharged either by the engine or by regenerative braking when decelerating. Because of the relatively smaller battery size the electric mode is very limited. Typical HEVs today are equipped with a battery pack ranging from 1.2 to 2.2 kWh [11].

For a PHEV, a large amount of electric energy is stored in the on-board battery, which usually in the range of 7-16 kWh [11]. The largest differences compared to a HEV are that it can be recharged by using an electric outlet and it can travel powered only by the battery.

The main advantage for a PHEV is that it can be initially driven by using only electric energy from grid stored in the on-board battery, and the on-board engine or fuel cell stack can be used as a range extender for longer trips, thus the fuel economy can be improved [13].

2.2 Fuel Cell Vehicles

A fuel cell vehicle uses a fuel cell stack, which can convert the chemical energy in oxygen from the air and compressed hydrogen from on-board hydrogen tank into electrical energy to power its electric motor and propel the vehicle as can be seen

in Figure.2.4 below. Compared with conventional vehicles, most fuel cell vehicles emit only water and heat [14]. A fuel cell vehicle combines both advantages of battery electric vehicles, which are high efficiency, quiet operating, zero emission, and of conventional internal combustion engine vehicles' long driving range and short refueling time [15].

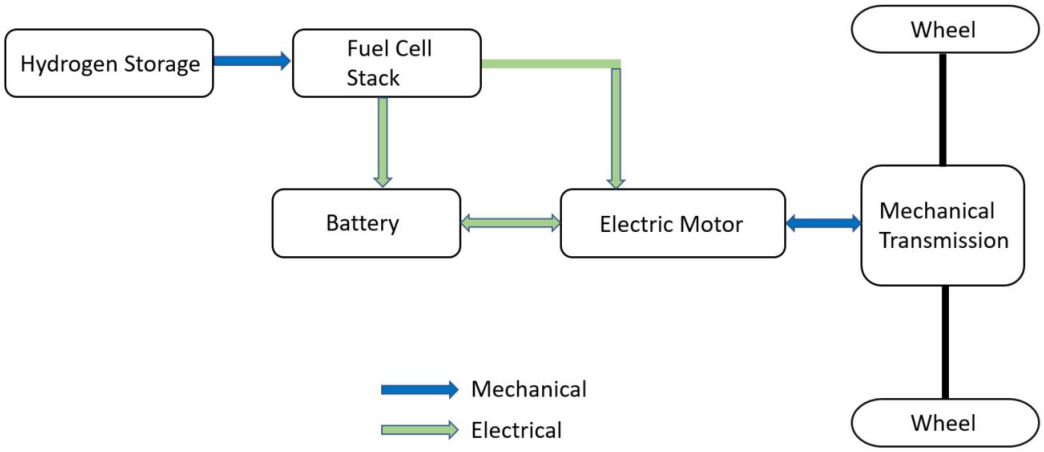

Figure 2.4: Fuel Cell Vehicle powertrain configuration for a HEV or a PHEV

The Hyundai Tucson FCV was the first commercially produced hydrogen fuel cell automobile, which was introduced in 2013. Toyota Mirai followed in 2015, and then Honda entered the market [16] [17]. Many fuel cell buses have been developed and are in operation around the world for demonstration purposes [11].

2.2.1 Examples of Fuel Cell Vehicles on the market

2.2.1.1 Toyota Mirai

The Mirai, which is shown in Figure.2.5 is a mid-size hydrogen fuel cell car manufactured by Toyota. It is also the world's first commercially available hydrogen fuel cell vehicle with the range around 500 kilometers. TFCS (Toyota Fuel Cell System) with both fuel cell technology and hybrid technology is equipped, and it only takes 3 to 5 minutes to refill the hydrogen [18][19].

Figure 2.5: Toyota Mirai [20]

In Table.2.1 below, one can observe the main parameters for Toyota Mirai.

Table 2.1: The main parameters for Toyota Mirai [18].

Toyota Mirai	
Electric Motor	113 kW
Fuel Cell	114 kW
Battery	1.6 kWh (Nickel-metal hydride)
Hydrogen Tank Capacity	5 kg Hydrogen
Tank Pressure	700 bar
Range	502 km
Hydrogen Consumption	0.76 kg/100 km

2.2.1.2 Hyundai ix35

The Hyundai ix35 FCEV is the first SUV-like vehicles sold commercially. The current version is the 2012 fourth generation ix35 FCEV, which equipped with a 100 kW motor (136 hp), enabling the maximum speed of 160 km/h. It contains two hydrogen tanks with 5.64 kg compressed hydrogen in total, which enables the vehicle to travel a total of 594 km on a single charge [18] [21]. Also, some energy is stored in a 24 kW lithium polymer battery, together with the fuel cell stack can propel the vehicle.

Figure 2.6: Hyundai ix35 [22]

In Table.2.2 below, one can observe the main parameters for Hyundai ix35.

Table 2.2: The main parameters for Hyundai ix35 [18].

Hyundai ix35	
Electric Motor	100 kW
Hydrogen Tank Capacity	5.64 kg Hydrogen
Tank Pressure	700 bar
Range	594 km
Hydrogen Consumption	1.0 kg/100 km

2.2.1.3 Mercedes-Benz GLC F-CELL

The Mercedes-Benz GLC F-CELL contains both fuel cell and plug-in battery pack that can be charged from the grid using plug-in technology. Therefore, the gradual expansion of the hydrogen infrastructure is considered in an ideal way. Also, there is an important contribution to cost reduction due to the sharing of standard components used in the drive train [23].

Figure 2.7: Mercedes-Benz GLC F-CELL [24]

In Table.2.3 below, one can observe the main parameters for Mercedes-Benz GLC F-CELL. The combined hydrogen consumption is 0.34 kg/100 km, the combined CO2 emission is 0 g/km, and the combined electrical consumption is 13.7 kWh/100 km [25].

Table 2.3: The main parameters for Mercedes-Benz GLC F-CELL [18].

Mercedes-Benz GLC F-CELL (Plug-in)	
Electric Motor	147 kW
Battery	13.8 kWh
Hydrogen Tank Capacity	4.4 kg Hydrogen
Tank Pressure	700 bar
Hydrogen Range	437 km
Battery-electric Range	49 km
Hydrogen Consumption (Combined)	0.34 kg/100 km

2.3 Hydrogen production, delivery and storage

2.3.1 Hydrogen production

Hydrogen, like electricity as an energy carrier, can be used for different applications: transportation, power systems, industries,.etc. It has very high specific energy, nearly three times that of in gasoline or diesel and nearly seven times that of in methanol[6] [8]. One can find it in Table.2.4 below. Hydrogen can be extracted from materials containing hydrogen atoms, such as the electrolysis of water and hydrocarbons. Different technologies can be used from different starting materials for the formation of the final H_2 molecule.

Table 2.4: Higher and lower heating values for various fuels [26].

Fuel	HHV (MJ/kg)	LHV (MJ/kg)
Hydrogen	141.9	119.9
Methane	55.5	50
Ethane	51.9	47.8
Gasoline	47.5	44.5
Diesel	44.8	42.5
Methanol	20	18.1

Today, hydrogen is mostly produced in the industry from fossil energy by steam methane reforming (SMR) of natural gas, which is around 48%. Then the partial oxidation (POX), which is about 30% and coal gasification, which occupies 18%. In a tiny part, only about 4% of hydrogen will be produced by water electrolysis as is shown in Table.2.5 [8] [27].

Table 2.5: The main hydrogen production methods [28].

Raw Materials	Technology	Production Percentage
Natural Gas	Steam Reforming	48%
Refinery oil	Partial Oxidation	30%
Coal	Gasification	18%
Water	Electrolysis	4%

For steam reforming (SR), the efficiency is around 74% to 85%. The significant advantage for SR is its developed technology. The disadvantage is that it has CO_2 by product and it highly depends on fossil fuels. For partial oxidation (POX), the efficiency is around 60% to 75%. The advantages of POX are the proved technology and existing infrastructures. The disadvantage is the same as the SR. For electrolysis, the efficiency is around 40% to 60%. The significant advantages for electrolysis are no pollution, if renewable electricity is used, the feedstock water is abundant, and O_2 is the only byproduct. The disadvantages are low overall efficiency and high capital cost [26].

According to [26], the capital cost for Steam Methane Reforming is 226.4 million dollars, and the hydrogen cost is 2.27 $/kg. For Coal Gasification, the capital cost is 545.6 million dollars, and the hydrogen cost is 1.63 $/kg. For Electrolysis, the cost varies in different production methods. The capital cost for Solar PV Electrolysis is from 12 to 54.5 million dollars, and the hydrogen cost is from 5.78 to 23.27 $/kg. The capital cost for Wind Electrolysis is 499.6 to 504.8 million dollars, and the hydrogen cost is 5.89 to 6.03 $/kg.

2.3.1.1 Steam Methane Reforming

Steam Reforming is a chemical process in which hydrogen is produced by hydrocarbon fuels and water steam at high temperature around 700 °C to 1100 °C and high pressure under 3 to 25 bar. Natural gas mainly consists of methane, CH_4, which has the highest H/C ratio within hydrocarbon [27]. Metal-based catalyst (Nickel) is used, and the byproducts of this reaction are hydrogen, carbon dioxide and carbon monoxide.

The chemical reactions for steam reforming process are shown below:

Ni-based (Ni-Al2O3) catalysts will enhance the reaction

$$CH_4 + H_2O \rightleftharpoons CO + 3H_2 \tag{2.1}$$

Simultaneously, the water gas shift reaction produces further H2

$$CO + H_2O \rightleftharpoons CO_2 + H_2 \tag{2.2}$$

2.3.1.2 Partial Oxidation

Partial Oxidation (POX) use fossil fuel and oxygen to get hydrogen and carbon monoxide. The byproducts are water and carbon monoxide. Then the carbon monoxide further reacts with water steam to yield hydrogen [29] .

The reactions can be expressed as

$$CH_4 + O_2 \longrightarrow CO + 2H_2 \tag{2.3}$$

$$CH_4 + 2O_2 \longrightarrow CO_2 + 2H_2O \tag{2.4}$$

$$CH_4 + H_2O \longrightarrow CO + 3H_2 \tag{2.5}$$

For higher hydrocarbons:

$$C_nH_m + (\frac{n}{2})O_2 \longrightarrow nCO + (\frac{m}{2})H_2 \tag{2.6}$$

2.3.1.3 Coal Gasification

Coal gasification consists of a series of chemical reactions producing similar products as reforming reactions: carbon monoxide and hydrogen.

The reaction happens at high pressure up to 60 bar and a temperature higher than 700 °C, with a controlled amount of oxygen and steam. The overall chemical equation (not balanced) can be written as [27]:

$$CH + O_2 + H_2O \rightleftharpoons CO + CO_2 + H_2 + other\ species \tag{2.7}$$

2.3.1.4 Water Electrolysis

Hydrogen can also be produced by water splitting such as electrolysis, which will break the water molecules into oxygen and hydrogen by electrical current. Electrolysis requires much electricity to produce enough hydrogen quantities [26]. The overall reaction is shown below.

$$2H_2O \longrightarrow 2H_2 + O_2 \tag{2.8}$$

One significant advantage is that water is far more abundant and easy to get compared with fossil fuel. If the required energy for electrolysis is from renewable energy such as solar or wind, then it will be the cleanest energy carrier that can be used.

2.3.2 Hydrogen delivery and storage

There are several hydrogen delivery methods such as pipeline, tube trailers with liquefying, and trailers without liquefying. According to [30]. Considering both cost and environment impact assessment. Hydrogen delivery with the pipeline is most suitable for large scale power plant, when the cost is 2.73$ per kg hydrogen delivery. Hydrogen delivery with tube trailers without liquefying is most suitable for small scale power plant, when the cost is 2.86$ per kg hydrogen delivery. The costs for operation and maintenance highly dependent on the served refueling stations' number.

Hydrogen can be stored in large amounts for a very long time, which is difficult for electricity. Physical-based and material based methods can be used. For physical based method, hydrogen can be stored as compressed gas, cold/cryogenic compressed hydrogen or liquid hydrogen. For material based method, hydrogen can be stored with absorbent, liquid organic, interstitial hydride or complex hydride, etc.

For compressed hydrogen, hydrogen gas will be stored from 1 to 350 bar (5,000 psi) or 700 bar (10,000 psi) under pressure, which can increase the energy density by volume. This technology has been used in fuel cell vehicles, such as Toyota Mirai and Mercedes-Benz GLC F-CELL. Composite tanks such as carbon fiber with a polymer liner are used, and the hydrogen is stored at 700 bar [31].

For liquid hydrogen, which has higher energy density than gaseous hydrogen, it requires liquefaction at –253 °C, similar to liquified natural gas (LNG) which is stored at -162°C, which needs complex process and extra cost. Also, there could be an efficiency loss of 12.79% or 4.26 kWh/kg out of 33.3 kWh/kg [32]. BMW has been working on liquid hydrogen tanks for cars (BMW Hydrogen 7).

For the material based method, hydrogen can be stored or absorbed on the surface of some solids or liquids. The storage media can be divided into hydrid storage, liquid hydrogen carrier, and surface storage. However, most of those techniques are

still being developed.

2.3.3 About the safety perspective

Security issues are also a matter of concern. For a fuel cell vehicle, the frame structure should be designed uniquely to effectively distribute the impact force. When a collision happens, the force should be dispersed around the passenger compartment and around the fuel cell stack and the hydrogen tank.

Also for the hydrogen tank, which has pressure up to 700 bar, it should be durable, lightweight and very robust. For instance, there are three layers in the Toyota Mirai hydrogen tank and can absorb five times as much energy as steel. The internal layer is a polymer layer which closest to hydrogen. The intermediate layer is made of carbon fiber that reinforces the can body. At the outermost layer, the glass fiber can reduce the wear on the outside of the can [33]. In the event of a collision, the hydrogen system will be shut off to avoid leakage. All components belonging to the hydrogen system are located outside the passenger compartment and are designed to prevent hydrogen leaks from reaching the passenger compartment. Because hydrogen is lighter than air, it dissipates quickly so that can minimize the ignition risk.

3

Fuel Cell Vehicle Modeling and Simulation

In this chapter, both Fuel Cell PHEV and Fuel Cell HEV models are built. They both include similar components and control units such as vehicle model, electric machine, driver model, brake control unit, electric machine control unit, and battery management system. However, some of the components and control units are quite different, like larger battery pack size in Fuel Cell PHEV and smaller in Fuel Cell HEV, the fuel cell control unit and the State Selection model, which is the main control for mode selection at the highest level.

The theoretical approach to design specific components such as Battery, Fuel Cell, and Electric Machine is also shown. It includes the theoretical explanation and design values given by the stakeholder.

3.1 Fuel Cell Vehicle Powertrain Layout

In this project, both Fuel Cell PHEV and HEV are involved. The powertrain configuration is shown in Figure.3.1 below. Specific components parameters and control units can be seen in the next sections.

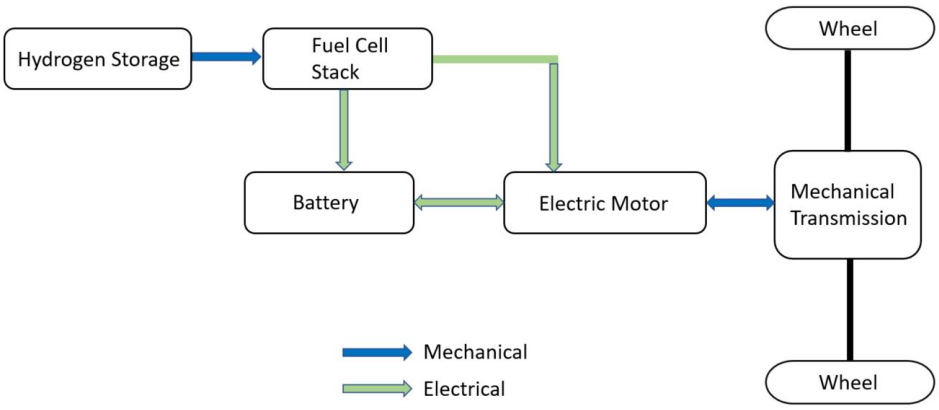

Figure 3.1: Fuel Cell Vehicle Powertrain

The Fuel Cell Vehicle Powertrain layout modeled in GT-SUITE is shown in the Figure 3.2 below. It contains a Vehicle Model, a Driver Model, an Electric Motor Model with Electric Motor Control Unit (EMCU), a Battery Model with Battery Management System (BMS), a Fuel Cell Model with Fuel Cell Control Unit (FCCU), a Brake Control Unit (BCU) and a State Selection Block, which contains the Finite State Machine (FSM) logic which has the control logic for switching between various modes.

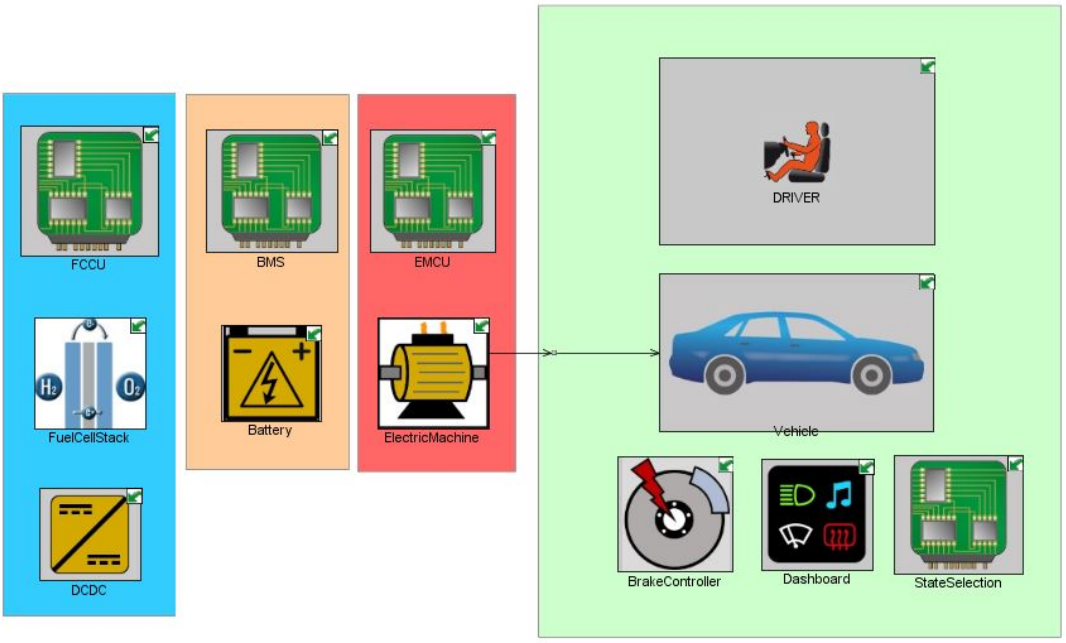

Figure 3.2: Fuel Cell Vehicle Powertrain model in GT-Suite

3.2 Vehicle Model

In this project for both Fuel Cell PHEV and Fuel Cell HEV, the car is equipped with an electric machine with 150 kW maximum power and 330 Nm maximum torque. A 30 Ah lithium-ion battery is used in Fuel Cell PHEV with 9.85 kWh. A 6.9 Ah lithium-ion battery is used in Fuel Cell HEV with 1.82 kWh.

The model has a Rear Wheel Drive (RWD) drivetrain, which has a driveshaft connecting the rear differential and the two axles. Figure 3.3 is exploded from the vehicle powertrain model in Figure 3.2.

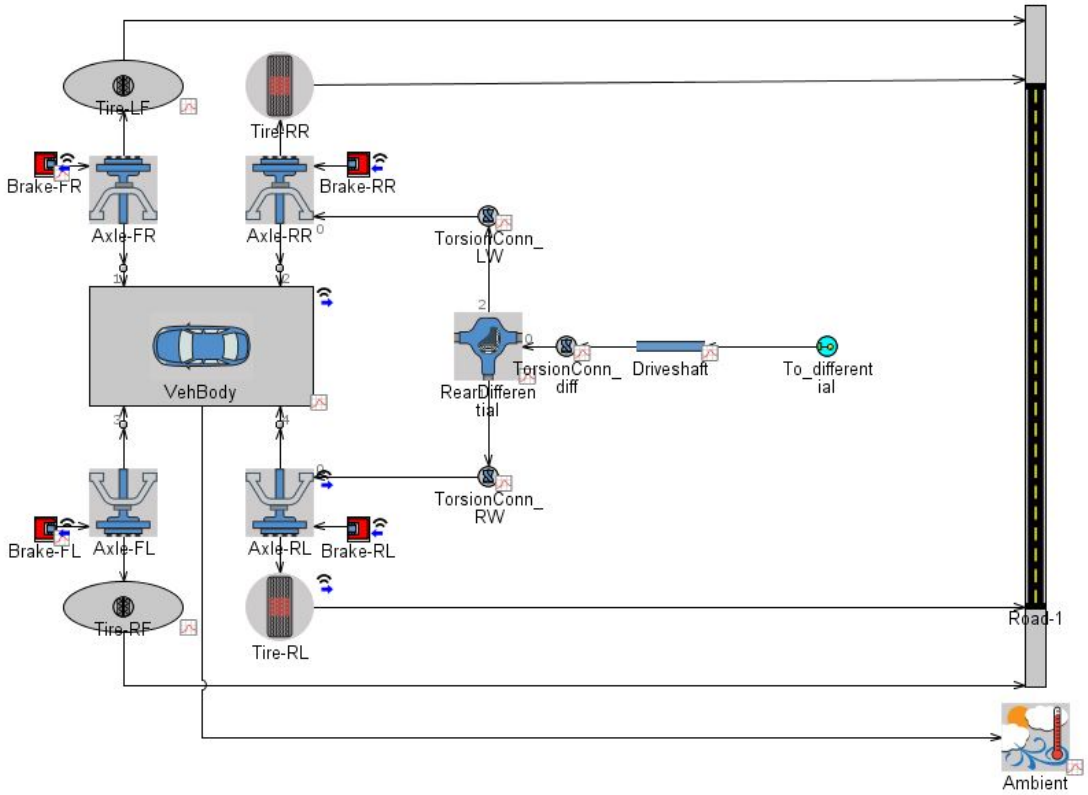

Figure 3.3: The vehicle model in GT-Suite

The Differential is currently modeled as a simple locking differential, where both the half axles connected to it rotate at the same speed. The input and output shafts to the differential are currently assumed to have a very low moment of inertia. The Axles are modeled as rigid half axles, ignoring compliance or damping. The various parameters are listed in the table 3.1 below.

Table 3.1: The main parameters for the vehicle.

Vehicle type	Fuel Cell-HEV/PHEV
Drive Axle	Rear wheel drive
Curb weight	1806 (kg)
Wheel base	2.73 (m)
Final drive ratio	8.57
Frontal area	2.58 (m^2)
Drag coefficient	0.33
Electric motor max power	150 (kW)
Electric motor max torque	330 (Nm)

The path of power flow is such that the power demand from wheel given by the driving cycle pass through the rear axles, rear differential, the driveshaft then connected with the electric motor. The power demand will split between the battery

and the fuel cell controlled by the strategies.

The basic Vehicle Model tries to describe the external resistance loads when driving on the road, which is important to know at the beginning. Since it can explain what load demands the powertrain need to deliver in order to drive. Here lateral dynamics are not considered, only longitudinal dynamics are studied.

According to Newton's second law of motion

$$m\frac{d}{dt}v(t) = F_{traction}(t) - F_{resistance}(t) \tag{3.1}$$

Which means a vehicle will accelerate when the traction force is larger than the resistance loads and will decelerates when opposite. When the two forces equal, the vehicle will run at a constant speed.

The external resistance load $F_{resistance}$ is shown in Figure. 3.4

$$F_{resistance} = F_{air} + F_{roll} + F_{grade} \tag{3.2}$$

where F_{air} refers to aerodynamic drag, F_{roll} refers to rolling resistance, F_{grade} refers to road grade resistance.

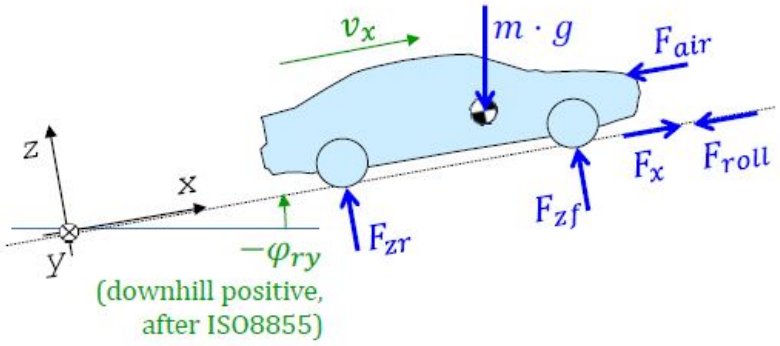

Figure 3.4: External resistance loads [34]

3.2.1 Aerodynamic drag

Aerodynamic drag F_{air} is a resistance force due to the oncoming air on the moving vehicle body, which is unavoidable during driving. Aerodynamic drag may affect the vehicle's speed and performance. It has an extreme dependence on the square of vehicle speed as is shown below

$$F_{air} = \frac{1}{2}\rho C_d A V^2 \tag{3.3}$$

Where ρ is the air density, C_d is the drag coefficient, A is the frontal cross-sectional area of the vehicle. Wind speed has not been taken into consideration here.

3.2.2 Rolling resistance

Rolling resistance F_{roll}, also called rolling friction is a force resisting the tire during rolling, which is mainly caused by non-elastic effects.

$$F_{roll} = f_r mg\cos(\varphi_y) \tag{3.4}$$

where f_r is a dimensionless rolling resistance coefficient, m is vehicle mass, g is gravity constant, φ_y is road inclination angle.

3.2.3 Road grade resistance

Road grade resistance is a gravitational force acting on a vehicle which is parallel with the road surface. It can be calculated in the following formula:

$$F_{grade} = mg\sin(-\varphi_y) \tag{3.5}$$

When the vehicle travels uphill, the F_{grade} will act as resisting force. However, when the vehicle travels downhill, this force will act as the traction force.

In this report, F_{grade} equals to zero because the driving cycles used are based on horizontal road inclination.

3.2.4 Traction force

The traction force $F_{traction}$, which comes from the powertrain to wheels is to overcome the resistance forces mentioned before and maintain certain vehicle speed or acceleration level given by

$$F_{traction}(t) = F_{acc}(t) + F_{air}(t) + F_{roll}(t) + F_{grade}(t) \tag{3.6}$$

The maximum traction force available between wheels and surface is limited by the maximum powertrain capacity and also limited by the tire and road surface adhesive capacity.

$$F_{traction} = \mu mg \tag{3.7}$$

Where μ is the friction coefficient between the wheel and the road surface.
The torque demand at wheel can be written as

$$T_{wheel}(t) = F_{traction}(t) r_{wheel} \tag{3.8}$$

Where r_{wheel} is the radius of wheel.

3.2.5 Traction power and energy demand

The traction power demand from powertrain to wheels to propel a vehicle can be calculated as

$$P_{wheel}(t) = F_{traction}(t)v(t) \tag{3.9}$$

where $v(t)$ is the vehicle speed and $\omega(t)$ is the angular wheel speed.

When P_{wheel} is positive, which means the powertrain provides positive traction force and propels the vehicle. When P_{wheel} is negative, which means braking power. If the vehicle has regenerative braking mode. Then the wasted energy can be collected.

The energy consumed during driving can then be calculated from time integral of power

$$E_{traction}(t) = \int P_{wheel}(t)dt \tag{3.10}$$

3.3 Driving cycles

Laboratory tests for vehicles include fuel consumption, CO_2 emissions, which are directly related with fuel consumption, the pollutant emissions, and energy consumption values of alternative powertrains as well as the range of electric vehicles. Driving cycles has been developed so that they can be used in different world regions, and the test results can be compared worldwide. However, studies have shown that results from some driving cycles have a significant difference compared with results from real-world driving. For example, the New European Driving Cycle (NEDC), which was designed in the 1980s. The driving conditions have become outdated today because of the newly developed technologies and more complicated driving conditions [35].

3.3.1 WLTP

From September 2017, the old NEDC lab test for vehicles has gradually been replaced by the new WLTP test (Worldwide Harmonised Light Vehicle Test Procedure), which is designed based on real driving data around the world and better matches on-road performance and everyday driving profiles [36]

Vehicles are divided into three different WLTC test classes based on power/weight ratio [kW/ton]:
For each class a different cycle is used.

- Class 1 - low power vehicles with ratio <= 22
- Class 2 - vehicles with 22 < ratio <= 34
- Class 3 - high-power vehicles with ratio > 34

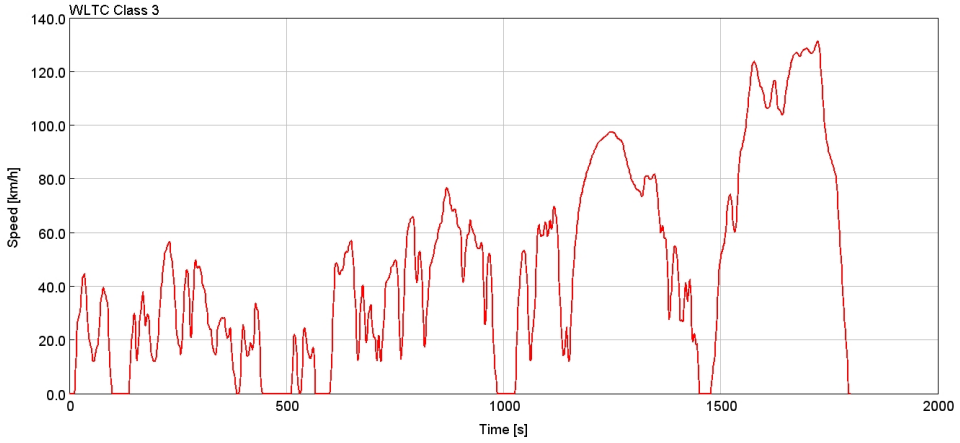

Figure 3.5: WLTC Class 3 cycle

Nowadays, most common cars' power-weight ratios belong to 40–100 kW/ton, which is class 3 as is shown in Figure. 3.5 above. Vans and buses can also belong to class 2.

In each class, there are several driving tests designed to represent real-world vehicle operation on urban, extra-urban roads, motorways, and freeways. The duration of each part is fixed between classes. However, the acceleration and speed curves are shaped differently. The sequence of tests is further restricted by maximum vehicle speed V_{max} [37]. One can observe the main parameters for the WLTP Class 3 driving cycle below.

Table 3.2: The WLTP Class 3 cycle: selected parameters[38].

WLTP Class 3 cycle									
Phase	**Duration (s)**	**Stop Duration (s)**	**Distance (m)**	**Stop Percentage**	**Maximum Velocity (km/h)**	**Average Velocity without stops (km/h)**	**Average Velocity with stops (km/h)**	**Minimum Acceleration (m/s2)**	**Maximum Acceleration (m/s2)**
Low	589	156	3095	26.5%	56.5	25.7	18.9	-1.47	1.47
Medium	433	48	4756	11.1%	76.6	44.5	39.5	-1.49	1.57
High	455	31	7162	6.8%	97.4	60.8	56.7	-1.49	1.58
Extra-High	323	7	8254	2.2%	131.3	94.0	92.0	-1.21	1.03
Total	1800	242	23266						

Compared with NEDC, WLTC has the following properties:
- 4 more dynamic phases, 52% urban and 48% non-urban, more representative of real driving.
- Longer test distance.
- Shorter stops.
- Higher average and maximum speed.
- Higher average and maximum drive power.
- More accelerations and decelerations.

From the regulation point of view, from September 2017, cars type approved using NEDC before September 2017 can still be sold. WLTP type approval testing will be introduced for new car types. From September 2018, all new cars must be certified

according to the WLTP test procedure, and no longer on NEDC. An exception should be made for end-of-series vehicles to allow for a limited number of unsold vehicles in stock that were approved under the old NEDC test to be sold for one more year. From January first, 2019, all cars in dealerships should have WLTP-CO2 values only to avoid any confusion among consumers, in the view of the automobile industry. During 2020, the European Commission will convert today's (NEDC-based) CO2 targets to specific WLTP-CO2 targets of comparable stringency. These new WLTP targets will apply for monitoring car fleet compliance [36].

3.4 Fuel Cell Electric Vehicle Model Control Strategy

In this chapter, the operation and the control strategies for Fuel Cell-HEV and Fuel Cell-PHEV are described and presented. Also, Volvo XC90 Twin Engine PHEV and Toyota Mirai Fuel Cell-HEV are studied and see what lessons can be learned.

3.4.1 Volvo XC90 Twin Engine PHEV

First, the Volvo XC90 Twin Engine PHEV is studied and to see what can be learned from this successful vehicle. Some components size can be seen in Table 3.3 below.

Table 3.3: The Volvo XC90 Twin Engine PHEV components size [39].

Engine maximum power	233 kW
Electric Motor maximum power	65 kW
Battery size	9.2 kWh

There are mainly four driving modes in Volvo XC90 PHEV, which are Hybrid mode, Pure mode, Save mode, and Power mode. Selecting a drive mode affects the vehicle's driving characteristics to help make driving more enjoyable or more fuel can be saved in certain types of situations.

In Hybrid mode, which is also the default mode, the amount of driving using only the electric motor is determined by the hybrid battery's charge level and the need for heating or cooling in the passenger compartment. If sufficient electrical energy is available, only the electric motor will be activated. However, when the driver presses the accelerator pedal above a certain level when the response required cannot be provided by the electric motor alone, the gasoline engine will be turned on. When the battery SOC level is low, the gasoline engine will start more often to help conserve electrical energy or switch to the save mode [39].

In Pure mode, which activates the electric motor only with as low energy consumption as possible and the lowest possible carbon dioxide emissions. Pure mode is

available when the hybrid battery is sufficiently charged. If the battery SOC level gets too low, the gasoline engine will be turned on. The gasoline engine will also be turned on if the vehicle's speed goes above approximately 125 km/h or if the driver wants more response than the electric motor alone can provide [39].

Using only the electric motor saves more fuel at low speeds than at high speeds. Therefore, use the SAVE mode primarily when the hybrid battery's charge level is high and driving will initially be at highway speeds but will end with city driving when electric driving is preferable. If the battery SOC level is low when this mode is selected, the gasoline engine will start and charge the battery up to approximately 33%. If the battery's charge level is already above 33%, this level will be maintained by the engine management system, which will start or stop the engine in the same way as in Hybrid drive mode. This mode increases fuel consumption because the gasoline engine is used to conserve battery charge for later use [39].

Power mode is intended for more aggressive driving. This mode maximizes the combined effects of the electric motor and the gasoline engine. Response to pressure on the accelerator pedal is more immediate. In this mode, both the electric motor and the gasoline engine are used continuously, which results in higher fuel consumption [39].

From report [40], how customers use their XC90 Plug-in Hybrid in daily life is studied by analyzing diagnostic readout (DRO) data, which is logged in cars and extracted at repair shops. The statistics show that driving behavior when using hybrid functions does not have much difference in different markets like Sweden, Germany, and China. Hybrid mode is most commonly used, which is larger than 80% from a time perspective. Then followed with Pure mode which is around 8% from a time perspective. In average, customers drive 44% from a time perspective and 33% from distance perspective electrically. At that time the engine will be turned off. During driving and standstill, sustaining mode occupies 61%, and depletion mode occupies 39% from a time perspective, and at 56% of the time, the battery SOC is lower than 35% [40].

3.4.2 Fuel Cell-PHEV Control Strategy

For a Fuel Cell-PHEV, the main difference with PHEV like Volvo XC90 T8 is that it does not have an internal combustion engine, which can provide power together with an electric motor. All the traction power will come from a 150 kW electric motor in this Fuel Cell-PHEV model. The energy will come from either a 9.85 kWh battery or a 45 kW fuel cell stack or from both in some situations.

If the minimum fuel consumption wants to be achieved and does not know how long the trip will be, the safest strategy is to first use battery only mode and after that, start the fuel cell as a range extender. So any trip shorter than the maximum range in battery electric-only mode will be driven with no hydrogen consumption.

When the battery is almost empty. The fuel cell will be started. One reason why the battery should not be empty before the fuel cell started is the battery needs to provide extra power during acceleration and gradients. So there must be sufficient energy remaining to handle a few minutes high power demand without discharge the battery completely.

Basically, the charge depleting and charge sustaining (CDCS) control strategy is implemented, which can be seen in Figure 3.6 below.

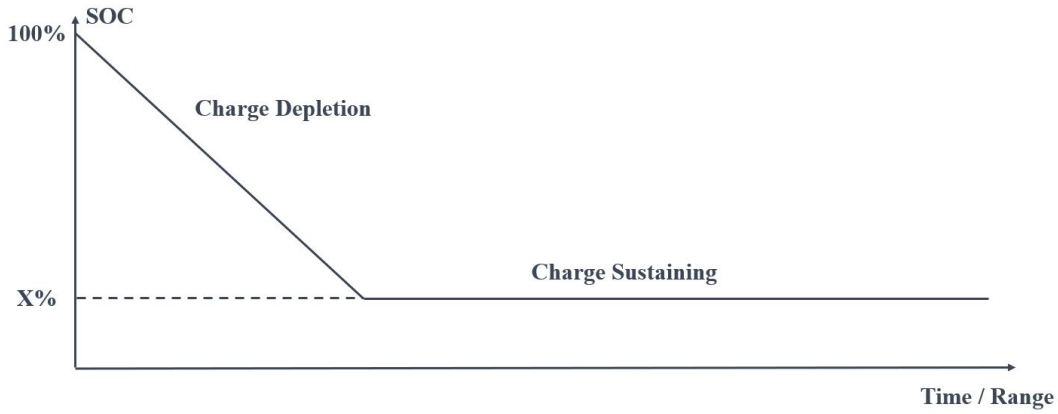

Figure 3.6: The charge depletion and charge sustaining (CDCS) control strategy

In charge depletion mode (CD), there is no need for any control. Since all the energy comes from the battery and the fuel cell should be turned off except if the requested speed or acceleration forces the fuel cell system to assist. In charge sustaining mode (CS), the battery will sustain at about the same charge level. How to control the fuel cell power to keep the SOC level fairly constant should be determined.

As is shown in Figure 3.7 below. The efficiency of the fuel cell is between 42% and 53.8%. The power efficiency curve for the fuel cell stack is just like the brake specific fuel consumption (BSFC) map in an internal combustion engine, which shows for one kWh energy, how much grams of fuel will be consumed. And based on that map, some control strategies can be designed and implemented so that the fuel cell system can work at optimal operating points. The maximum power for the fuel cell stack is 45 kW, and the maximum system efficiency is 53.8% when the power is at 16.5 kW. And the high-efficiency region is from 12.3 kW to 25 kW, where the system efficiency is 52.8%. Taken both power and efficiency into consideration. The trade-off optimal point is set to be 25 kW.

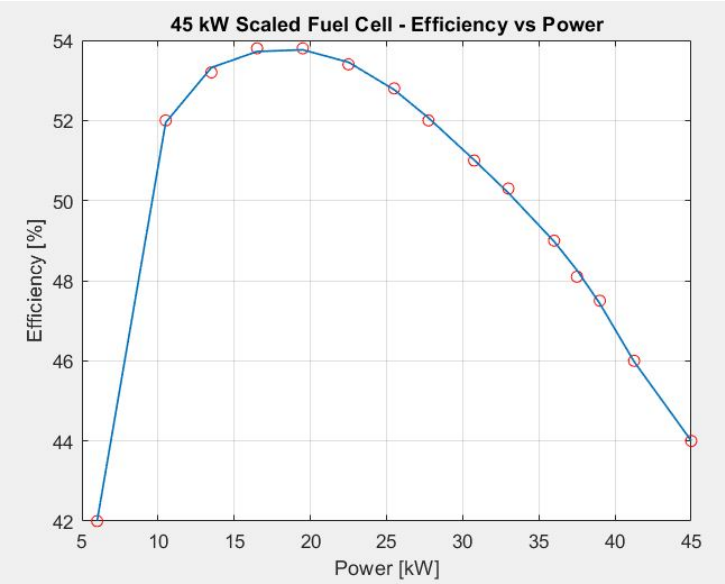

Figure 3.7: The power efficiency curve for the 45 kW fuel cell stack

One really simple control is that due to the characteristic of the fuel cell stack system, the fuel cell will be switched on and off in cycles which can be seen in Figure 3.8. And the battery SOC is sustained between lower limit 30% to upper limit 33%. With this controller, the fuel cell power output will only switch between two fixed values 0 and 45 kW and this controller will repeat itself.

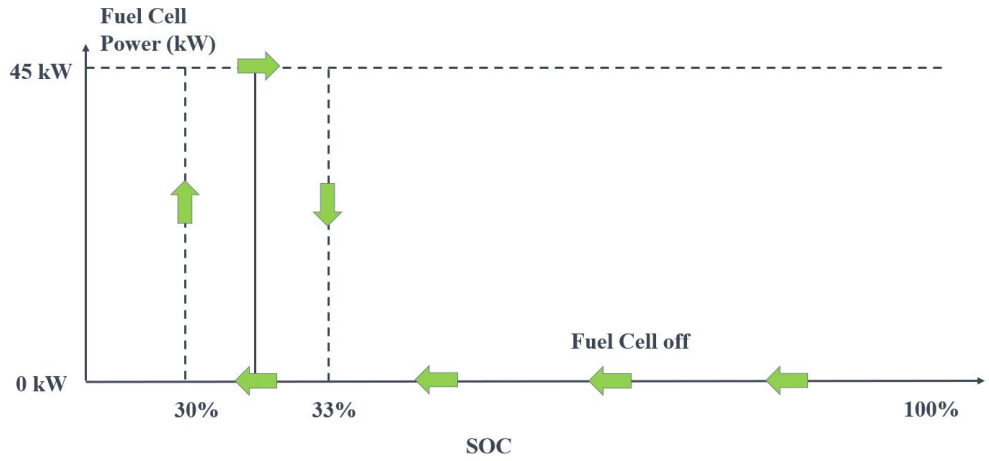

Figure 3.8: One really simple CDCS control strategy

As is shown in Figure 3.9. The system could run more efficiently if the fuel cell can switch between 0 or the optimal operating power (which is 25 kW in this fuel cell stack system). For power demands up to 25 kW, the controller only use the peak efficiency operating point, and the fuel cell will be switched between on and off in order to produce the right power request by the electric motor and to charge the battery.

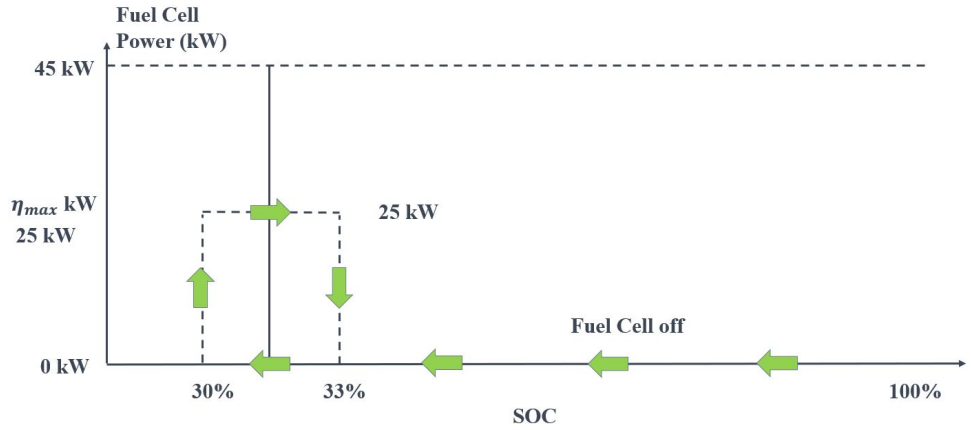

Figure 3.9: One simple but more efficient CDCS control strategy

The control strategy could be more complex and more realistic. If the battery SOC level is lower than the lower limit, which is at 30%. Then the fuel cell stack will be turned on and start to charge the battery at max efficiency power to see whether it is enough. If the battery SOC continues to decrease, the decreasing SOC leads to increasing fuel cell charging power. Then the battery SOC continues to decrease but slower and slower until it reaches the level that the fuel cell charging power equals the power demand from the wheel and to charge the battery. As is shown in Figure 3.23. If the battery SOC level reaches between 25% and 30%. The fuel cell output power will increase linearly from the most efficient point 25 kW to maximum power point 45 kW. If the SOC level decreases lower than 25%, which is a very urgent situation, then the fuel cell will operate with maximum power.

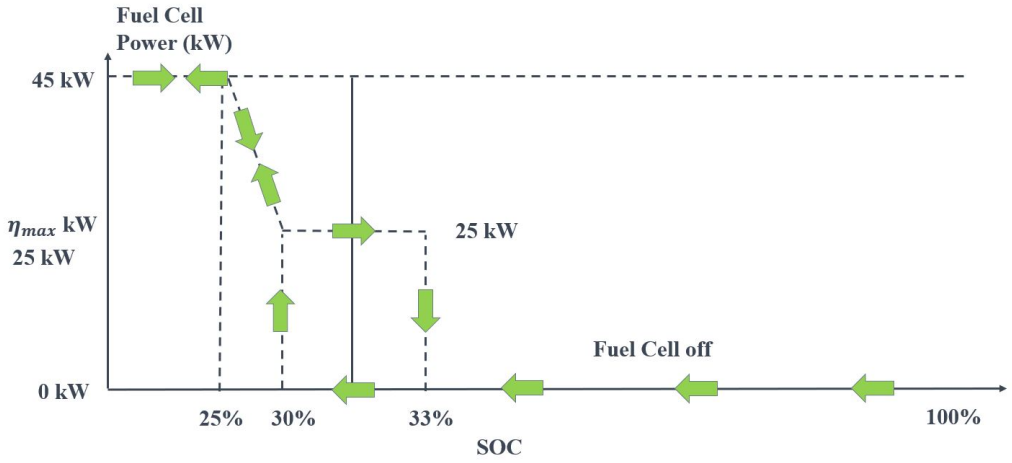

Figure 3.10: One more complex and more realistic CDCS control strategy

The aim for this Fuel Cell-PHEV model is that all power demand from the wheel will come from the electric motor with as low energy consumption as possible and the lowest possible carbon dioxide emissions. The battery usable SOC window is set from 20% to 95%. If the hybrid battery is sufficiently charged the vehicle will

run at charge depletion mode until the battery SOC reaches 30%, then the fuel cell stack system will be switched on and start to charge the battery and the vehicle will run at charge sustaining mode. The fuel cell stack system will also be turned on when the traction power demand from the wheel is larger than 65 kW which is the maximum power limit from the battery.

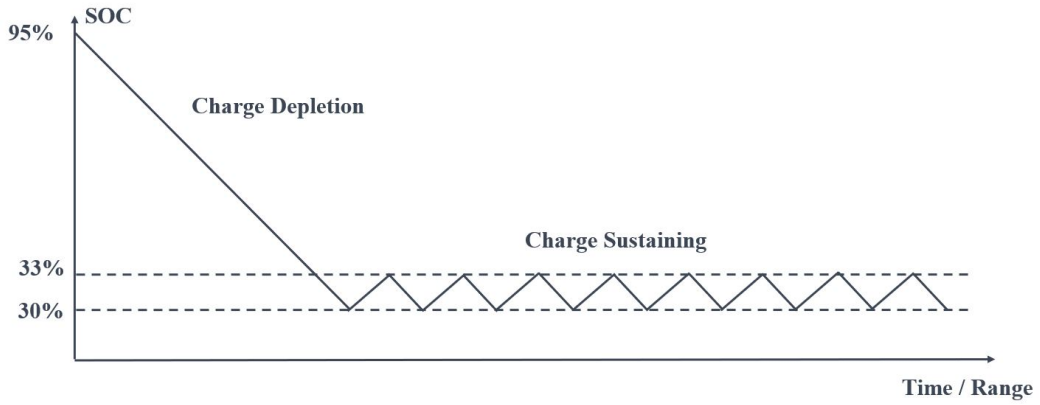

Figure 3.11: One more complex and more realistic CDCS control strategy

3.4.3 Toyota Mirai Fuel Cell-HEV

According to the 'Technology Assessment of a Fuel Cell Vehicle: 2017 Toyota Mirai' from U.S. Department of Energy, Argonne National Laboratory [41]. The test vehicle is Toyota Mirai, which is a fuel cell dominant hybrid electric vehicle with a strong load following control strategy and some main vehicle parameters are shown in Table 3.4 below.

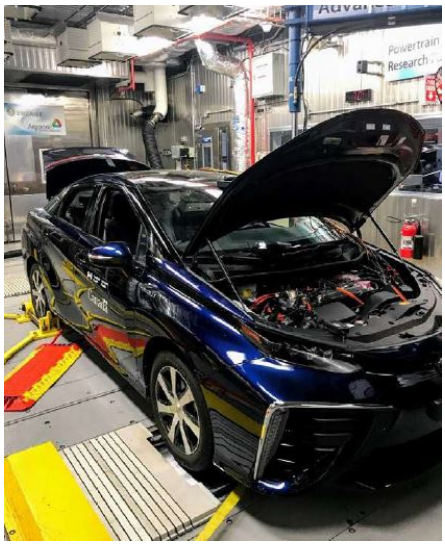

Figure 3.12: The test vehicle in Argonne National Laboratory[41]

Table 3.4: Main parameters for the test vehicle (Toyota Mirai).

Vehicle specification	
Vehicle type	Fuel Cell Series Hybrid
Nickel-metal Hydrid Battery	1.6 kWh
PEM Fuel Cell	114 kW, 370 cells
Hydrogen storage	690 bar, 5 kg H2

The fuel cell system peak efficiency for the test vehicle is 63.7% at around 7 kW.

During the test in the NEDC driving cycle, several interesting control logic can be learned:

1. No power comes from fuel cell stack while the vehicle stopped.
2. Battery power is used for electric launch.
3. Fuel cell stack provides the majority of power during acceleration. For example, during one acceleration 15 kW power comes from the fuel cell stack and 5 kW power comes from the battery. Another case is that 20 kW power comes from the fuel cell stack and 10 kW power comes from the battery.
4. The fuel cell will recharge the battery when traction power is low.
5. When traction power is low, the vehicle will run like a battery electric vehicle.
6. Fuel cell stack provides the power to cruise at steady state speed and the battery is inactive.
7. Fuel cell stack will close when there is large regenerative braking power. But when regenerative braking power is low, fuel cell stack still provides some power (maybe for charging the battery).

During the test in aggressive driving (US06), several control logic can be learned:

1. Highly dynamic speed changes while cruising and the power from fuel cell stack follows the dynamic load changes.
2. Regenerative braking limited by battery maximum power limit.
3. When really large regenerative braking, the fuel cell stack will be forced to close.
4. Large peak power demand during acceleration at high speed. (High power from the fuel cell stack assisted with low power from the battery).

During the special 1 hour idle test to quantify the idle hydrogen consumption, these control rules can observe:

1. When idling, stack stops producing power. The hydrogen flow is stopped.
2. The hydrogen consumption is zero most of the time when the fuel cell idles.
3. Fuel cell system recharges the battery at 5 to 10 kW when the battery SOC level is low.
4. Fuel cell system will start once the battery SOC drops to 45.5%. The charging power will change from 10 kW to 6 kW when the battery SOC level reaches to 50%.

The battery polarization curve, which is a plot of current density versus electrode potential for a specific electrode-electrolyte combination and the battery and fuel cell system power graphs can be observed in Figure 3.13 and Figure 3.14 below. The operating points are the 10 Hz data from NEDCx2, UDDSx3, Highwayx2, US06x2, maximum acceleration x3, and steady-state speed tests. [41]

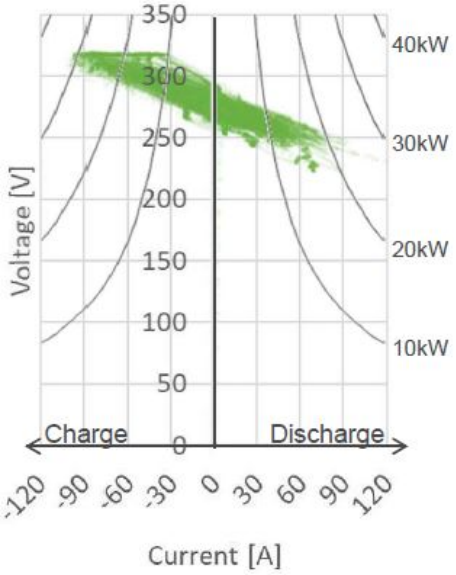

Figure 3.13: The battery polarization curve for the test vehicle [41]

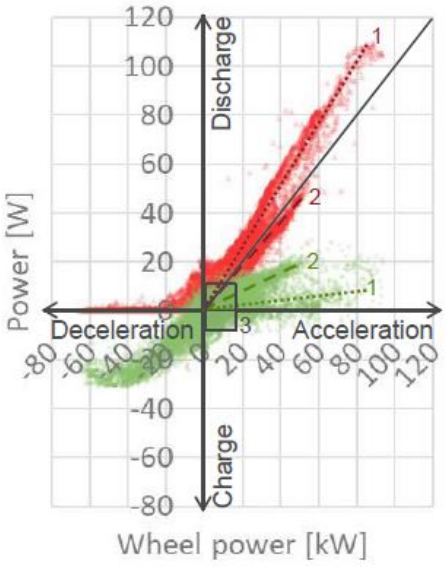

Figure 3.14: The battery (green) and fuel cell (red) power operating points for the test vehicle [41]

One can observe in the battery polarization curve (figure 3.13) that the charging power is from 0 to -30 kW and the discharging power is from 0 to 20 kW. The power range is wider on charging side for the test fuel cell hybrid.

In Figure 3.14, the green points represent battery operating points and the red points represent fuel cell operating points. One can observe that the battery can collect a maximum of 30 kW braking power and can provide a maximum of 20 kW for traction. When traction power demand is low, the fuel cell system can charge the battery and the maximum charge power from the fuel cell system to the battery is around 10 to 15 kW. At that situation, the fuel cell system will provide 20 kW and the extra 5 to 10 kW will be used as traction power. When traction power demand is below 10 kW, use battery only.

The combined fuel economy for the tested Toyota Mirai vehicle is 106.22 km/kg.

3.4.4 Fuel Cell-HEV Control Strategy

For a Fuel Cell-HEV, the fuel cell system works as the primary power source and all the traction power will come from a 150 kW electric motor. The main differences with a Fuel Cell-PHEV are: the battery size will be much smaller. The battery pack for the Fuel Cell-PHEV is 9.85 kWh and the battery pack for the Fuel Cell-HEV is 1.82 kWh. However, the fuel cell stack size is much bigger than that of a Fuel Cell-PHEV, which is around 100 kW.

Table 3.5: The main differences between Fuel Cell-PHEV and Fuel Cell-HEV.

	Fuel Cell-HEV	**Fuel Cell-PHEV**
Fuel cell stack size	100 kW	45 kW
Battery size	1.82 kWh	9.85 kWh
Battery maximum power	50 kW	65 kW

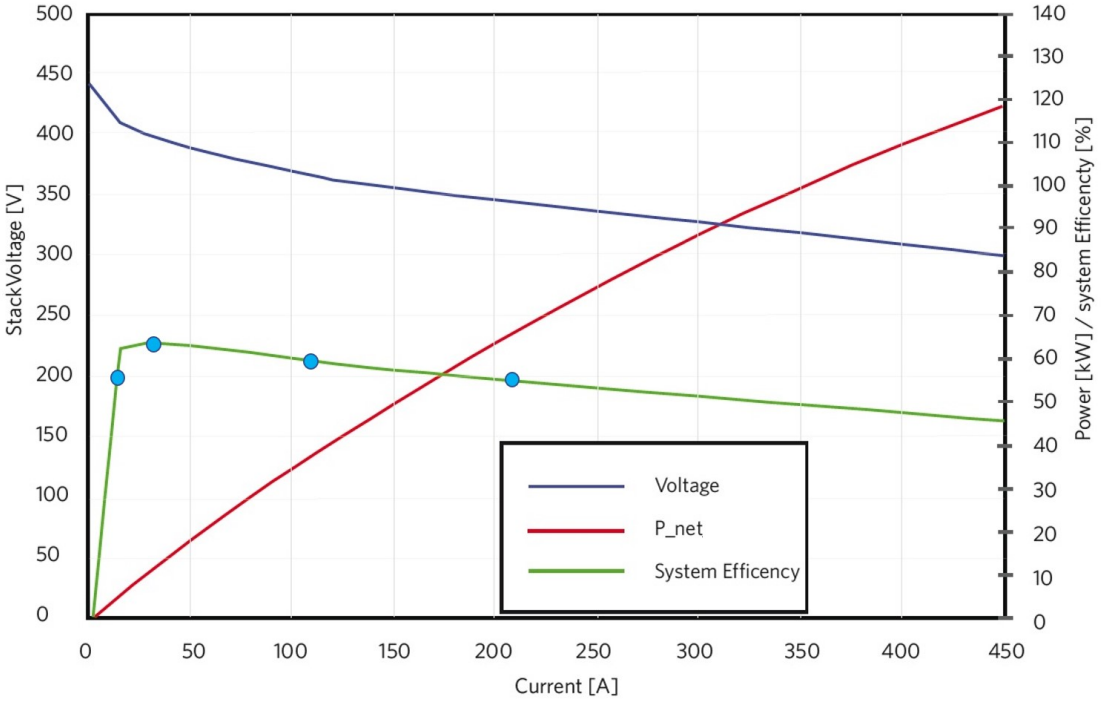

Figure 3.15: The operating characteristics of the 100 kW fuel cell system

For a fuel cell vehicle, if the fuel cell system is the only power source, then there could have several drawbacks. For example, in high accelerations or driving aggressively, the fuel cell system could have problems like long start-up time, and slow power response. Moreover, as shown in Figure 3.15, if the power request from the fuel cell system is too low or extremely high, then the fuel cell system will run in the very low-efficiency region leads to higher hydrogen consumption [42].

One can observe the fuel cell stack operating characteristics for the fuel cell-HEV in Figure 3.15. The x-axis represents the stack current [A], the Y-axis on the left side represents the stack voltage [V] and the Y-axis on the right side represents the stack power [kW] and the fuel cell system efficiency [%]. The red curve is the power curve. The maximum power is 118 kW at the beginning of life (BOL) and will reduce to 105 kW at the end of life (EOL). The usable power window for this fuel cell stack is set from 0 kW to 100 kW. The green curve is the efficiency curve. The first blue dot and the fourth blue dot represent the optimal operating region for this fuel cell stack, which has at least 55% system efficiency and the corresponding power is 5 kW and 64 kW respectively. The second blue dot shows the most efficient power, which has 64% system efficiency and the corresponding power is 12 kW. The third blue dot represents power with 60% system efficiency and the corresponding power is 38 kW. Based on the power and efficiency of this fuel cell stack system, the trade-off optimal operating range is set from 12 kW to 64 kW, which means the fuel cell system can run with at least 55% system efficiency. The more detailed control strategy will be described below.

The state selection model and the fuel cell control unit will provide signals to different sub-modules like the battery, the electric motor, the fuel cell, etc. The power demand can be split, either only from the battery or from the fuel cell system or from both when large power is needed. The battery SOC level is detected every second and the controller will keep it in a specific SOC window, which is from 30% to 70% for the HEV-battery here. The fuel cell control unit will monitor different signal values and make decisions when the battery needs to be charged and how much power is needed and when the fuel cell system needs battery to assist in order to run as efficiently as possible and when it is suitable for using fuel cell only mode to meet the traction power demand from the wheel.

The control strategy here is used to manage the power flow between the fuel cell stack, the battery and the traction power demand from the wheel, which should make sure that the power flow to the electric motor should always meet the traction power demand and the SOC level in the battery should always be maintained in a certain region, which has the ability to meet the power demand in sharp acceleration and has the SOC-reserve to collect the potential regenerative braking energy in the future. Another essential feature is that the fuel cell stack should run in the optimal operating region which is shown in Figure 3.15 above as much as possible.

As shown in Figure 3.16, there are various operating modes based on different power request from the wheel, the battery SOC level, the fuel cell optimal operating region, etc.

The driving modes are decided by the State Selection Controller at first, which is a Finite State Machine (FSM). It is a logic tool that allows for control algorithms to have pre-determined modes that it can operate in. The modes and basic control strategies are explained below.

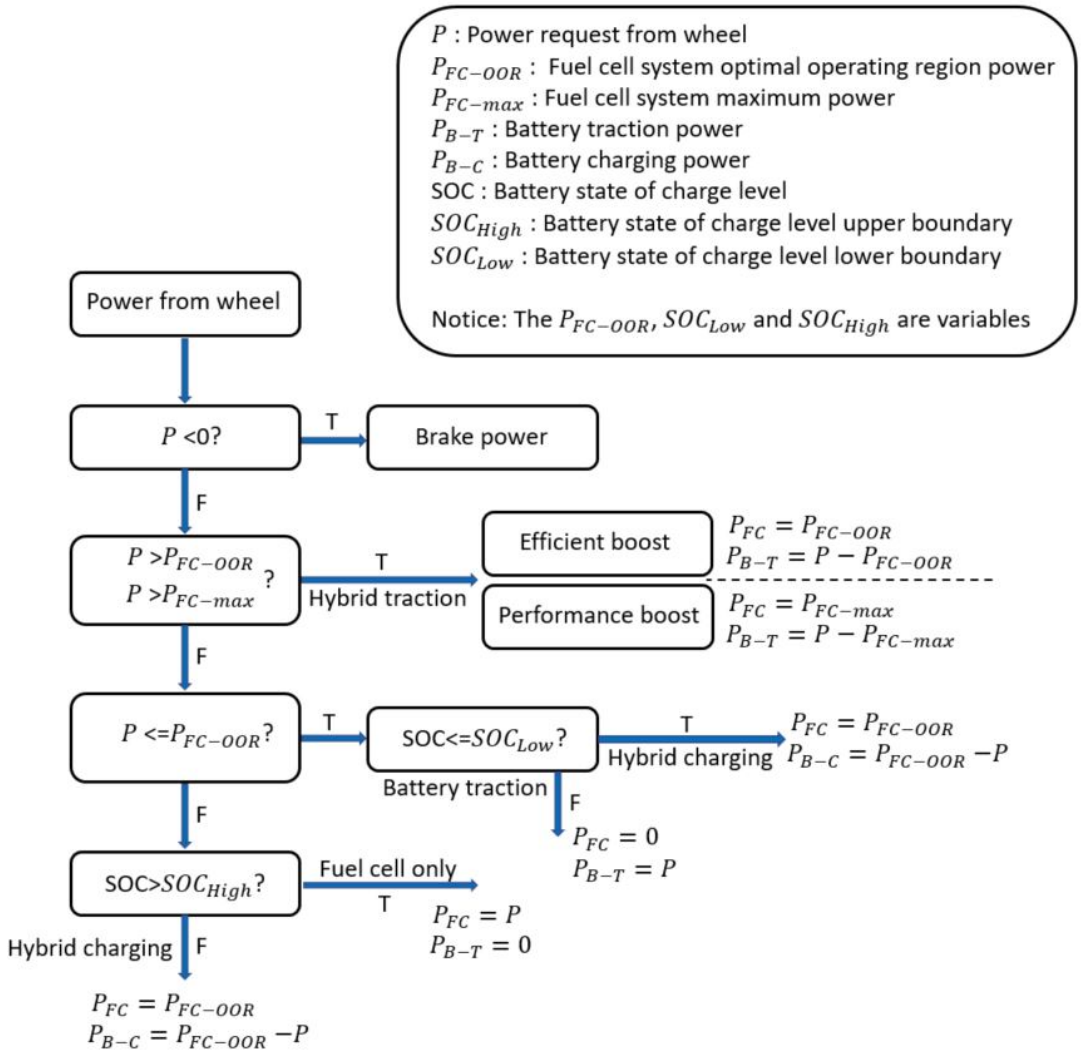

Figure 3.16: The flowchart for the fuel cell-HEV basic control strategy.

Standstill mode: There will be no power flow from the fuel cell system or from the battery. As mentioned in the Technology Assessment of Toyota Mirai chapter, the fuel cell system could be turned off or idling. When idling, stack stops producing power. The hydrogen flow is stopped. The hydrogen consumption is zero most of the time when the fuel cell idles.

Braking mode: When braking, the detailed control logic can be found in the Brake Controller Model section. The fuel cell system could work at idling and the battery will absorb the regenerative braking energy. But if the SOC level is below the lower limit, then the fuel cell system will be switched on and recharge the battery. When the regenerative braking power is really large, the fuel cell stack can be forced to close.

In order to meet the driving performance demand, keep the battery SOC at a certain level and run the fuel cell in the optimal operating region as much as possible. The

traction mode is divided into four situations as following:

Performance boost mode: If the power demand from the wheel is larger than the maximum power of the fuel cell system, then the performance boost mode is used. The fuel cell will work at its maximum available power and the battery will assist to provide traction power to propel the electric motor.

Efficient boost mode: If the power demand from the wheel is larger than the fuel cell system optimal operating power range upper limit, then the efficient boost mode is used. The fuel cell will work at its optimal operating power range and the battery will assist to provide the rest of traction power to propel the electric motor so that the hydrogen efficiency can be improved.

Standard power mode: If the power demand from the wheel falls into the fuel cell system optimal operating power range, then the standard power mode is used. At the same time if the battery SOC below a certain value, then the fuel cell system will provide more power but still working in the optimal operating range. Part of the power will go to the wheel while the other part of the power will be used to charge the battery. However, if the battery SOC is quite high at that time. Then the fuel cell system will work alone to propel the vehicle. In this mode, all power comes from the fuel cell system.

Low power mode: If the power demand from the wheel is below the lower boundary of the fuel cell system optimal operating power range, then the low power mode is used. At the same time, if the battery SOC level is high, which means it does not need charging, then the fuel cell system will idle and the vehicle will drive like a battery electric vehicle. Otherwise, the fuel cell system will operate at the optimal operating range and part of the power flow will charge the battery.

The Fuel Cell-HEV controller combines two rule-based control strategies. The first one is the power following (maximum SOC of battery) control strategy, the other one is the thermostat control strategy.

In the power following (maximum SOC of battery) control strategy. The fuel cell system works as the main power source, follows the traction power from the wheel and run at the optimal operating line as much as possible. The battery SOC level will be kept at a high level for the future pure electric driving or hybrid driving with battery assists. The battery will be charged when the vehicle speed is higher than a certain value and the traction power demand is lower than the fuel cell optimal operating power and the battery SOC level does not reach the upper limit. But if the battery SOC level is already high and the traction power is low, then the fuel cell will run away from the optimal operating points thus leads to lower efficiency.

In the thermostat control strategy, which is also called fuel cell on-off control strategy. The on-off state of the fuel cell is controlled by the battery SOC level like the temperature control of a thermostat. If the battery SOC reaches below the

lower limit, the fuel cell will be switched on and work at the optimal operating region, which is the same as the power following (maximum SOC of battery) control strategy. When the battery SOC reaches above the upper limit, the fuel cell will be turned off and all the traction power will come from the battery until the SOC reaches the lower limit again. By using this control strategy, the fuel cell will either run in the optimal operating region or be turned-off. However, the battery needs to meet all the instantaneous power demand. The current fluctuation of the battery will be very large and there are a lot of large current charge and discharge conditions, which is detrimental to the service life of the battery. Also, there are more energy losses during energy conversion.

SOC / P_{demand}	*Low* [30%-45%)	*Medium* [45%-55%]	*High* (55%-70%]
Low Power (P_L) 0-12 kW	$P_{FC} = P_{Low}$ $P_{B-C} = P_{Low} - P_L$	$P_{FC} = P_{Low}$ $P_{B-C} = P_{Low} - P_L$	$P_{FC} = 0$ $P_{B-T} = P_L$
Medium Power (P_M) 12-38 kW	$P_{FC} = P_{Mid}$ $P_{B-C} = P_{Mid} - P_M$	$P_{FC} = P_{Mid}$ $P_{B-C} = P_{Mid} - P_M$	$P_{FC} = P_M$ $P_B = 0$
High Power (P_H) 38-64 kW	$P_{FC} = P_{High}$ $P_{B-C} = P_{High} - P_H$	$P_{FC} = P_H$ $P_B = 0$	$P_{FC} = P_H$ $P_B = 0$

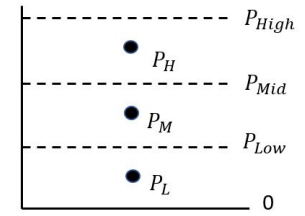

FC optimal operating power:

P_{Low} = 12 kW, η_{FC} = 64%

P_{Mid} = 38 kW, η_{FC} = 60%

P_{High} = 64 kW, η_{FC} = 55%

Figure 3.17: The combined power following and thermostat control strategy for Fuel Cell-HEV.

Combining the advantages and disadvantages of these two control strategies, the high-efficiency range of fuel cell system and battery operation can be fully utilized to make the overall efficiency better. This control strategy is based on the power following strategy, assisted by the thermostat control strategy. One can observe in Figure 3.17 above, the fuel cell optimal operating power is divided into three regions, which are low power region from 0 kW to P_{Low} kW, middle power region from P_{Low} kW to P_{Mid} kW and high power region from P_{Mid} kW to P_{High} kW. Points P_L P_M P_H are the demanded traction powers and P_{Low} P_{Mid} P_{High} are the fuel cell optimal operating power, which are 12 kW and 38 kW and 64 kW respectively. At those points, the corresponding fuel cell system efficiency is 64%, 60%, and 55% respectively. Similarly, the battery SOC level is also separated into three regions, which are low SOC from 30% to 45%, medium SOC from 45% to 55% and high SOC from 55% to 70%, so that the control is based on the real-time traction power demand and the battery SOC level.

For example, when the traction power demand is at point P_L as shown on the left in Figure 3.17, which is less than the fuel cell optimal operating power P_{Low}, the fuel cell system can be operated at optimal power and charge the battery or turned off, depending on the battery SOC level. When the traction power demand is at

point P_M, if the battery SOC is in the high region, the fuel cell will provide the power exact equal to the traction power and no power will flow in or out from the battery. Otherwise, if the SOC level is in medium or low level, the fuel cell will run at P_{Mid}, and the charging power is $P_{Mid} - P_M$. When the traction power demand is at point P_H, if the battery SOC is in either high region or medium region, the vehicle will run in fuel cell-only mode. Otherwise, the fuel cell will run at P_{High}, and the charging power is $P_{High} - P_H$.

3.5 Powertrain components design and control units

This section covers the main parameters for the powertrain components and how the control units are designed and worked.

3.5.1 Driver Model

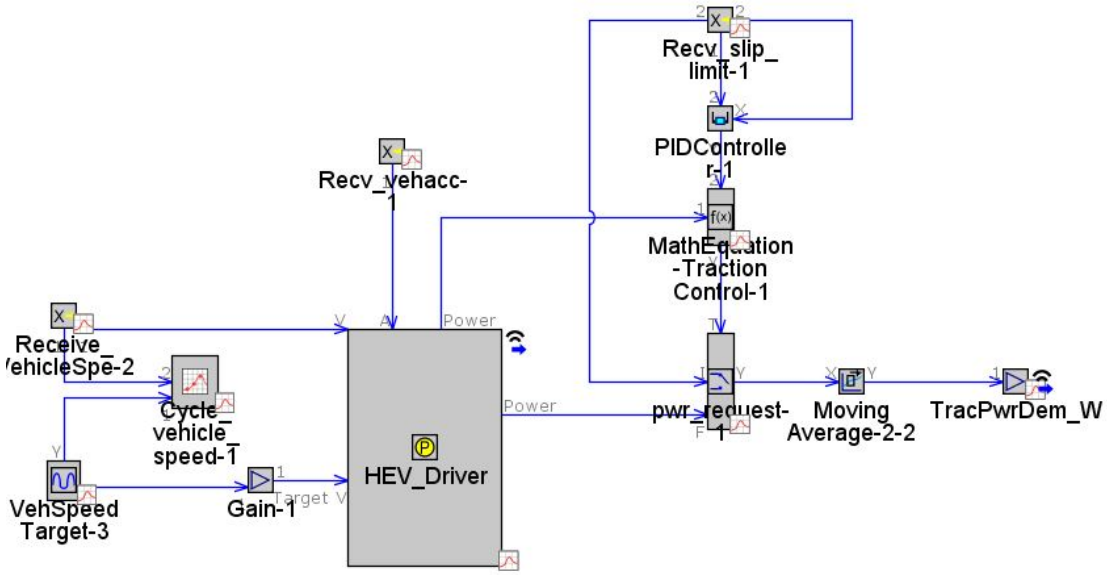

Figure 3.18: The driver model in GT-Suite

The HEV Driver controller is used for performing dynamic driving cycle analysis with hybrid vehicles. The input signals are target vehicle speed from driving cycle, the actual vehicle speed from the vehicle body and some vehicle parameters such as vehicle mass, vehicle frontal area, drag coefficient, tire rolling radius, etc. The Driver Model calculates required power to follow the drive cycle, which is the target speed.

The equations for traction force and the power demand to follow the driving cycle are shown below. The road grade resistance force is neglected.

$$F_{traction}(t) = F_{acc}(t) + F_{air}(t) + F_{roll}(t) \tag{3.11}$$

$$P_{wheel}(t) = F_{traction}(t)v(t) \tag{3.12}$$

3.5.2 State Selection Controller Model

State selection controller is the main control (also called Supervisory controller) for mode selection, which has the highest level. It mainly consists of two modes: driving mode and electric mode, which can be found in Table 3.6.

Table 3.6: The operating modes from the State selection controller.

Determines the operating mode	
Driving Mode	**Electric Mode**
	0. Stand still
1. Stand still	1. Electric-tractive
2. Electric	2. Electric-regeneration
3. HEV	3. HEV
4. Fuel cell	4. Fuel cell

The control logic for the State Selection controller model is defined in a Finite State Machine (FSM), which is a logic tool that allows for control algorithms to have pre-determined modes that it can operate in.

A FSM consists of States and Transitions. States are pre-defined modes that the machine can change into depending upon the conditions which match. Transitions are conditions under which a FSM can change from one state to another depending on the pre-defined logical statements. It is often represented graphically using a series of circles and arrows. In these graphical representations, circles represent states and arrows represent transitions as shown in Figure 3.19 below.

Figure 3.19: The Finite State Machine graphical representation

3.5.2.1 State Selection Controller for FC-PHEV Model

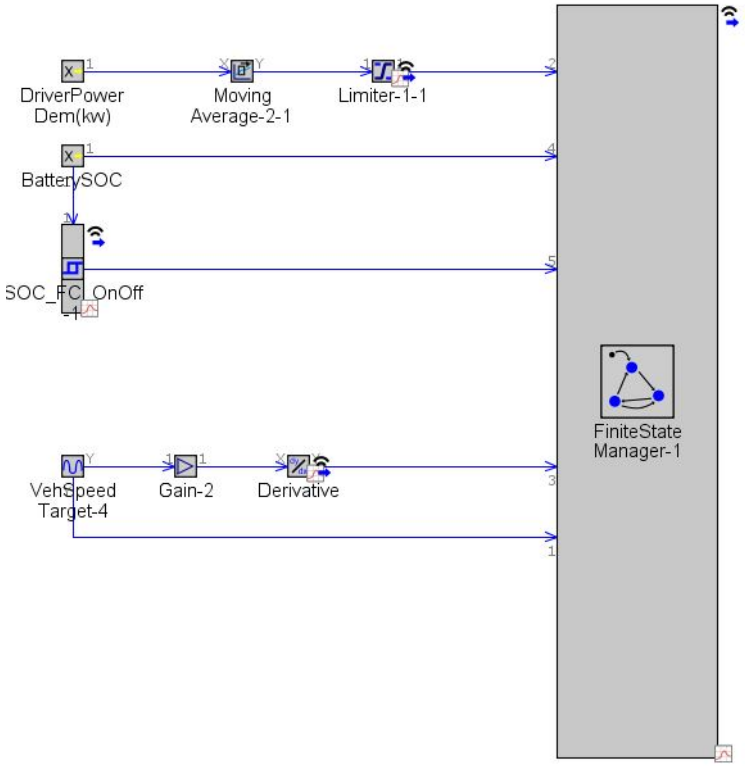

Figure 3.20: The State Selection Controller for FC-PHEV Model in GT-Suite

The Finite State Machine (FSM) receives input signals from different submodules like vehicle module or battery module as described in the Table 3.7 which compares with the logical statements upon the conditions being satisfied the necessary actions are performed. For example, for the finite state machine to switch from Electric Tractive mode to Electric Regenerative mode the traction power should be less than 0 kW. When these conditions are satisfied the modes will be switched.

Table 3.7: The input signals in FSM.

Input signals	Signals from
Vehicle speed	Driving cycle
Tractive power demand	Driver model
Acceleration	Derivative of Driving cycle
Battery SOC	Battery
Fuel cell on-off trigger for charging (0=off, 1=on)	Hysteresis control

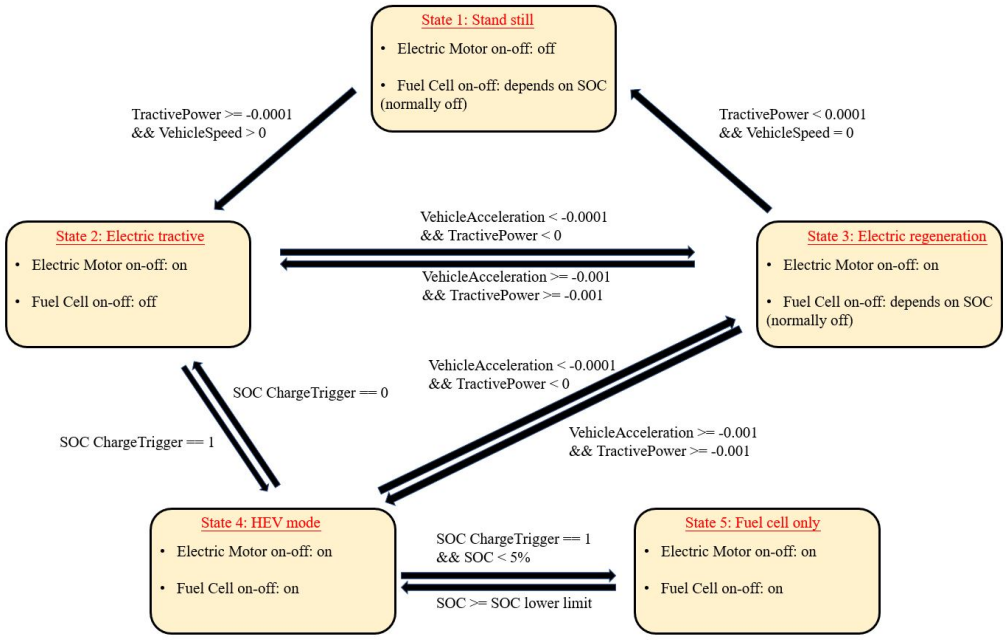

Figure 3.21: The Finite State Machine control logic for FC-PHEV

One can find the mode shifting control logic in Figure 3.21 above. Based on the comparison of inputs with the transition conditions, the FSM decides in which state the vehicle should run. The text in between the states represents the transition conditions based on which the states keep changing. State outputs like different driving modes and electric modes will be sent out to other control models like battery management system model (BMS) or hardware models like the electric motor model and battery model after the execution of each state.

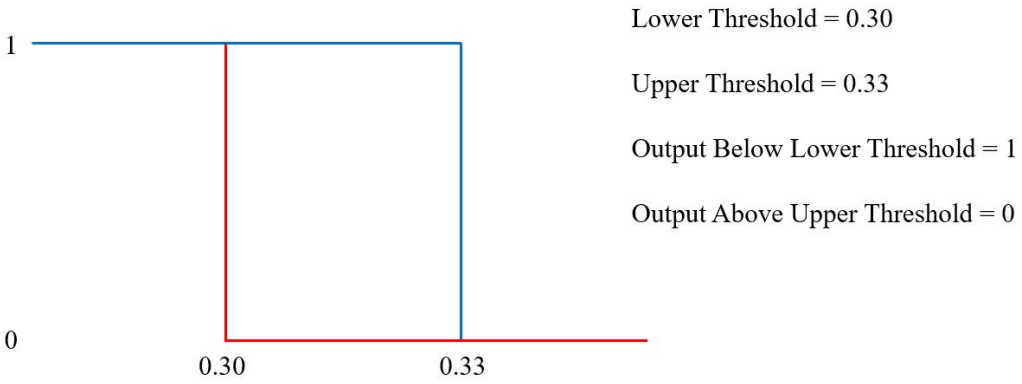

Figure 3.22: The hysteresis controller for SOC Charging Trigger for Fuel Cell-PHEV

Figure 3.22 presents how the SOC Charge Trigger switches between on and off depends on the battery SOC level. It is controlled by a hysteresis controller, which switches from one value to another at a specific threshold, and then switches another

value at a second threshold. The lower threshold is set to be 0.30, and the upper threshold is 0.33. If the battery SOC level is below the lower threshold, then the charging trigger is switched on, and the fuel cell system starts to charge the battery as follow the control strategy presented in Figure 3.23 below as described in the last section until it reaches the lower threshold.

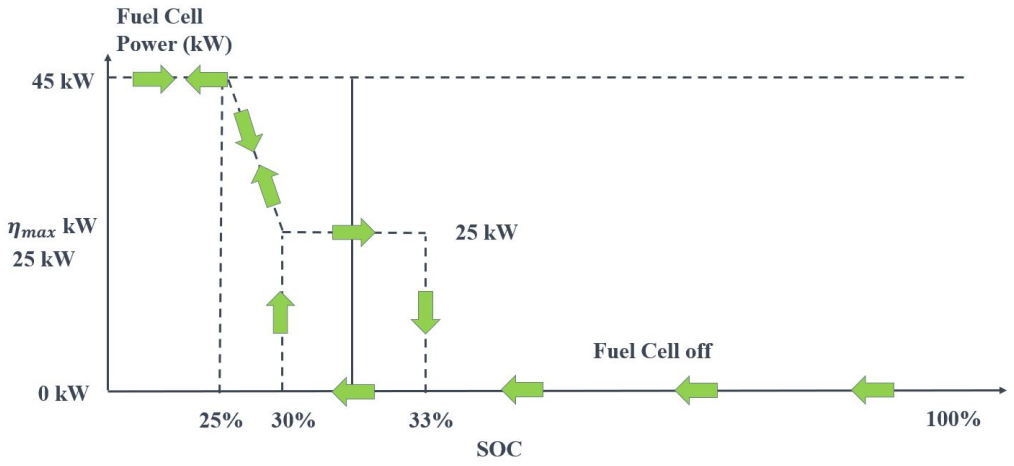

Figure 3.23: One more complex and more realistic CDCS control strategy for the Fuel Cell-PHEV

3.5.2.2 State Selection Controller for FC-HEV Model

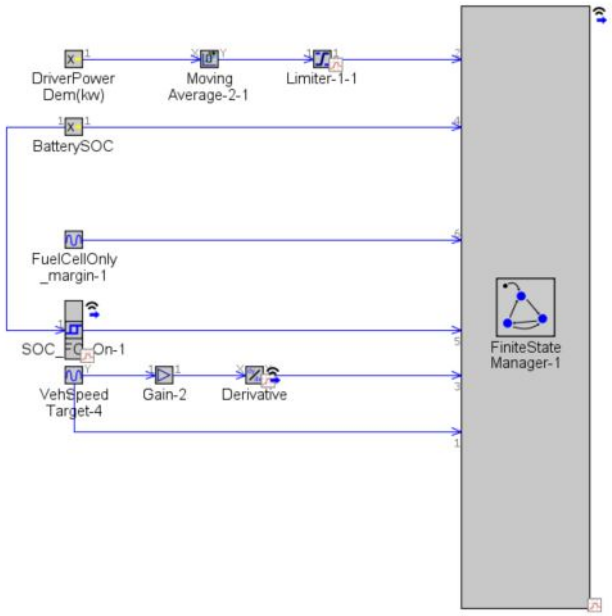

Figure 3.24: The State Selection Controller for FC-HEV Model in GT-Suite

The input signals in the Finite State Machine (FSM) do not change much compared with Fuel Cell-PHEV model. However the logical statements upon the conditions being satisfied for the mode shifting change a lot based on different power request from the wheel, the battery SOC level, the fuel cell optimal operating region, etc.

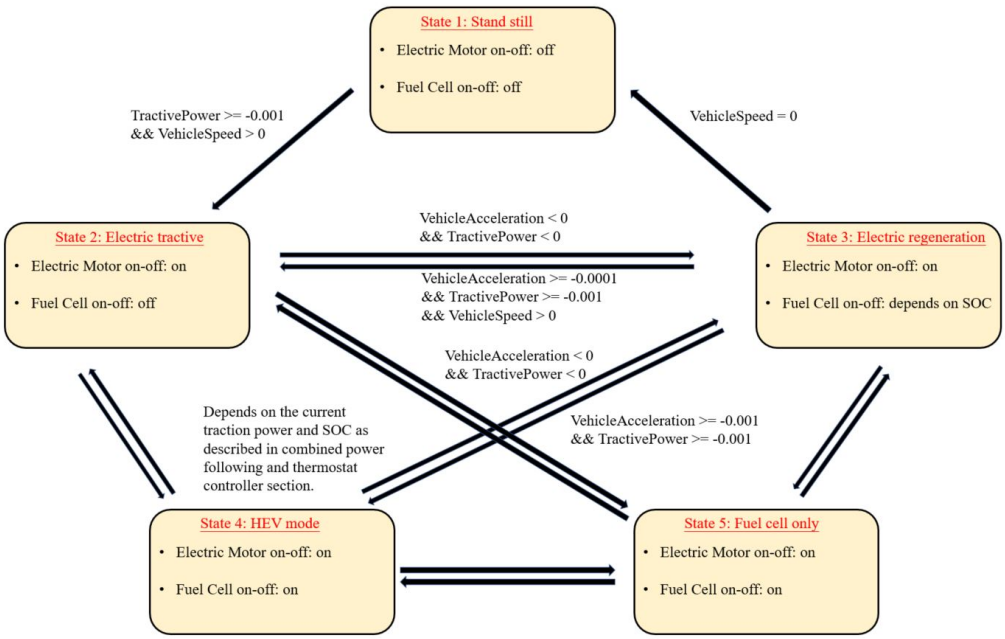

Figure 3.25: The Finite State Machine control logic for FC-HEV

One can find the mode shifting control logic for Fuel Cell-HEV in Figure 3.25 above. Based on the comparison of inputs with the transition conditions, the FSM decides in which state the vehicle should run. The text in between the states represents the transition conditions based on which the states keep changing.

3.5.3 PEM Fuel Cell System Model

The fuel cell is a kind of energy converter which converts chemical energy into electrical energy. In other words, a fuel cell is a device which provides a place for chemical reaction and outputs the energy produced by the chemical reaction. Proton exchange membrane(PEM) fuel cell is one of the most common fuel cells which has a full application on vehicles recently.

A completed PEM fuel cell system consists of PEM fuel cell stack and auxiliary system. The stack is where the chemical reaction takes place and it outputs electrical power to the external circuit, which is like the cylinder in the combustion engine. Moreover, the auxiliary system is to make sure the chemical reaction taking place in stacks is processing stable and adequate. Usually, it consists of H_2/O_2(air) supplying system, water management system and heat management system.

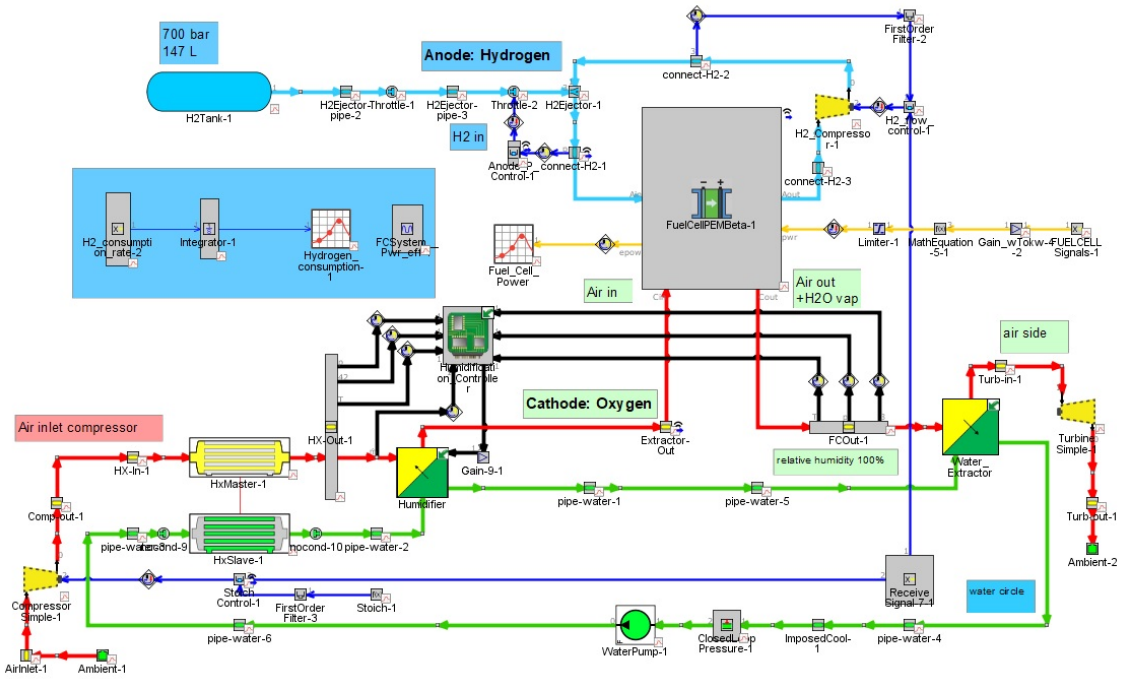

Figure 3.26: PEM fuel cell system model in GT-Suite

In GT-Suite, the new fuel-cell-PEM-Beta template is introduced to model the fuel cell stack since it models the flow, mass transfer, heat transfer, and electric power generation, which is one step closer to the real condition. Hydrogen is removed from the anode pipe, oxygen is removed from the cathode pipe, and water vapor is added to the cathode pipe at a rate based on electron production from the chemical reaction needed to match the current being produced. The internal losses generate heat that is transferred to the thermal mass of the fuel cell. The heat is then transferred to the anode and cathode fluid as well as the ambient environment or external cooling system.

As shown in Figure 3.26, it is the simplified completed PEM fuel cell system model.

3.5.3.1 PEM Fuel Cell Stack

Similar to the battery, for the electrochemical reaction, there are also anode and cathode in the fuel cell stack where hydrogen and oxygen are the reactants fed into anode and cathode respectively. The reaction is shown as follows, and the reaction enthalpy $\Delta H < 0$, which means the reaction will produce heat.

$$H_2 + \frac{1}{2}O_2 \rightarrow H_2O \qquad \Delta_r H < 0 \tag{3.13}$$

The main feature of the PEM fuel cell is that there is a proton exchange membrane between anode and cathode. The general structure of the PEM fuel cell is shown in Figure 3.27 and an example of fuel cell stack which used in Honda clarity as Figure

3.28 and 3.29.

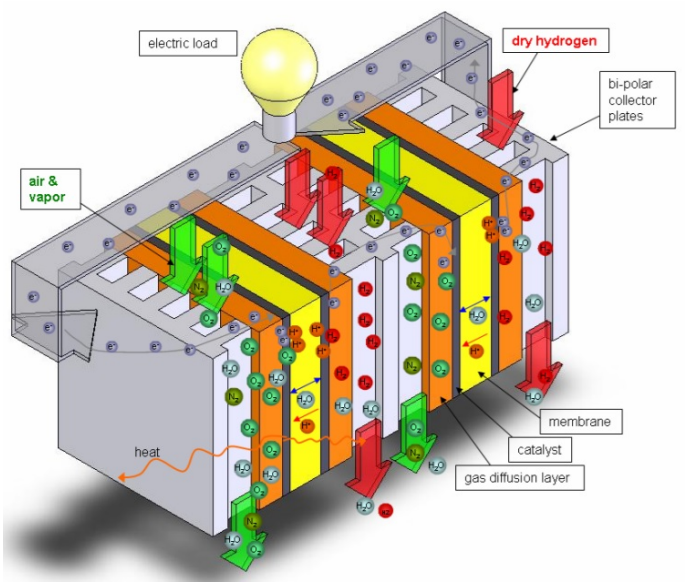

Figure 3.27: PEM fuel cell stack structure example [43]

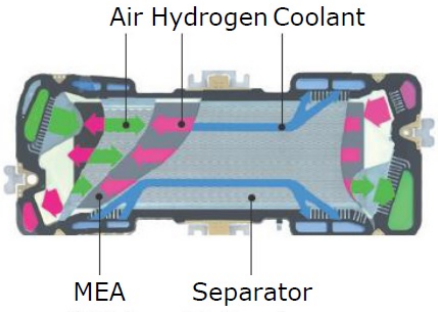

Figure 3.28: Honda clarity PEM fuel cell stack 1

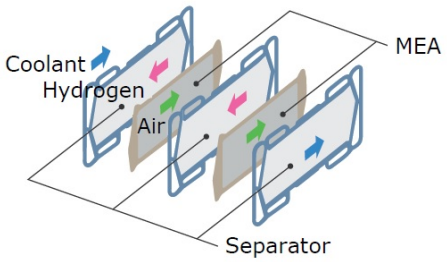

Figure 3.29: Honda clarity PEM fuel cell stack 2

The available energy for the external circuit is the Gibbs free energy difference between products and reactants. The Gibbs free energy difference for reaction 3.13 can be defined as follows,

$$\Delta G = G(products) - G(reactants) = G(H_2O) - G(H_2) - G(O_2) \tag{3.14}$$

Depending on the phases of the water product, the Gibbs free energy is also different. In standard condition (25°C, 100 kPa), the value of gaseous and liquid water product are -228.57 kJ/mol(LHV) and -237.13 kJ/mol(HHV) respectively.

Theoretically, the open circuit voltage(OCV) is defined as equation 3.15 under standard condition, where F is the Faraday constant (96485.33289 C/mol) and n is the number of electrons. In this chemical reaction n=2, since it delivered two H^+ for one H_2 molecule in the reaction.

$$E^0 = \frac{\Delta G}{nF} \tag{3.15}$$

In real condition, the OCV is also affected by the temperature and pressure which can be estimated by Nernst equation 3.16 in which T is the current temperature of fuel cell stack(°C), R represents universal gas constant(8.3145 J/mol $\cdot$ K) [44] moreover, P is the partial pressure.

$$E = E^0 + \frac{RT}{2F} ln(\frac{P_{H_2} {P_{O_2}}^{\frac{1}{2}}}{P_{H_2O}}) \tag{3.16}$$

Besides, there are three losses within the cell, which are Activation losses, Ohmic losses, and Concentration losses(mass transport losses). Therefore the terminal voltage(fuel cell voltage) which is available for the external circuit is shown in calculation 3.17.

$$V = E - V_{act} - V_{ohm} - V_{conc} \tag{3.17}$$

Activation losses, which are defined by the Tafel equation, is shown as follows. In which α is the charge transfer coefficient, i is current density and i_0 is exchange current density.

$$V_{act} = \frac{RT}{2\alpha F} ln(\frac{i}{i_0}) \tag{3.18}$$

Ohmic losses, i represents the fuel cell current density, and R is the resistance.

$$V_{ohm} = i \cdot R \tag{3.19}$$

Concentration losses or mass transport losses, C is the concentration loss coefficient, and i_1 is limiting current density.

$$V_{conc} = -C \cdot ln(1 - \frac{i}{i_1}) \tag{3.20}$$

All the coefficients can be pre-designed to define a specified fuel cell operating map which called polarization curve. An example is shown as Figure 3.30.

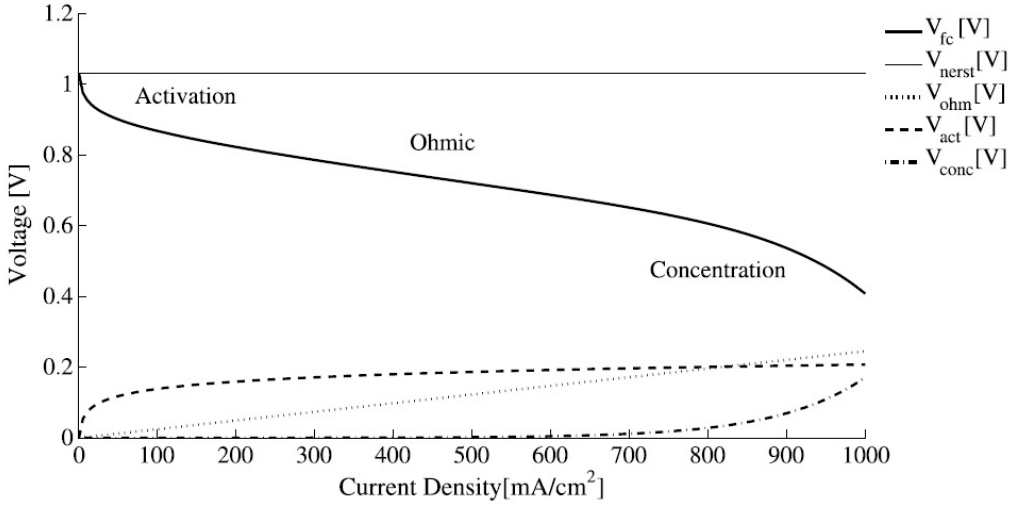

Figure 3.30: Example polarization curve [43]

As shown in Figure 3.31, it is the real measurements of single cell polarization curve which got from supplier A. To specify the fuel cell stack, this polarization curve has been inserted into the fuel cell stack template in the GT-Suite.

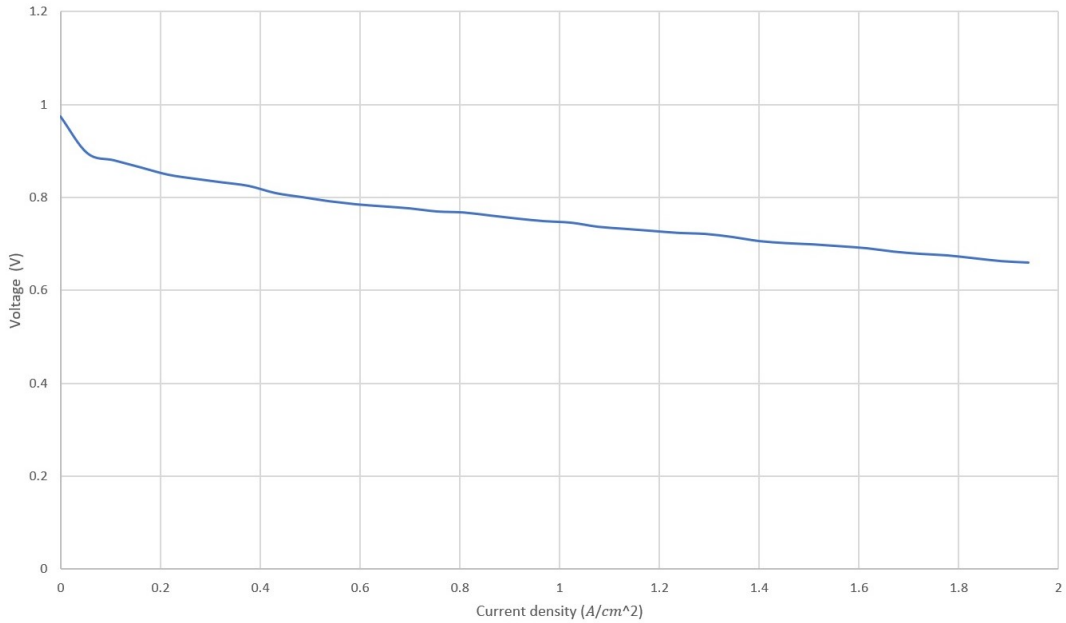

Figure 3.31: Specified polarization curve

3.5.3.2 Supplying System

The supplying system contents anode supplying subsystem and cathode supplying subsystem. In reactants supplying system, compressors or turbines are needed to adjust the hydrogen and air mass flow to feed the reactants into fuel cell stacks for achieving the required chemical reaction rate.

The hydrogen supplying system is in a closed loop for increasing the system efficiency, since the hydrogen consumed by the stack may not be completed and the outlet of the anode side can be used continuously for the future reaction as well. The fuel(hydrogen) is stored in a compressed hydrogen tank under pressure of 70Mpa usually for vehicle applications, and after that, the fuel will travel through a series of throttles decreased to the proper pressure. The decompressed hydrogen will then be injected into each anode channels of the stack.

To mimic the whole mass flow process, the hydrogen mass flow rate for the stack needs to be calculated to estimate the amount of hydrogen needs to be injected into the stack. The hydrogen mass flow rate(gram per second) can be estimated by Equation 3.21, where n_{H_2} represents the molar flow rate of hydrogen and M_{H_2} is the molar weight of hydrogen (equal to 2).

$$m_{H_2} = n_{H_2} \cdot M_{H_2} \ [g/s] \tag{3.21}$$

To estimate the hydrogen molar mass consumption rate, equation 3.22 is defined. In which I is the current of the stack and N is the number of cells. Again, the 2 times F is because of 2 moles of exchange electrons per molar hydrogen within the reaction.

$$n_{H_2} = \frac{I \cdot N}{2F} \ [mol/s] \tag{3.22}$$

Besides, depending on the system design, a new quantity called stoichiometry λ (usually higher than 1) is taking into consideration and is defined by the reactant molar ratio between feeding and consumption.

$$\lambda = \frac{n_{feed}}{n_{consumed}} \tag{3.23}$$

Therefore, combining all the equations (3.21 to 3.23) the final estimation of hydrogen mass consumption rate is calculated as,

$$m_{H_2} = \lambda_{anode} \cdot M_{H_2} \frac{I \cdot N}{2F} \ [g/s] \tag{3.24}$$

Based on this, a controller can be designed. The controller of the supplying system in the model is simply a PID controller which is fair enough to simulate. Eq. 3.24 calculates the input value of the controller which considered as the targeting value and the output signal is sending to the hydrogen compressor which used to adjust the hydrogen mass flow.

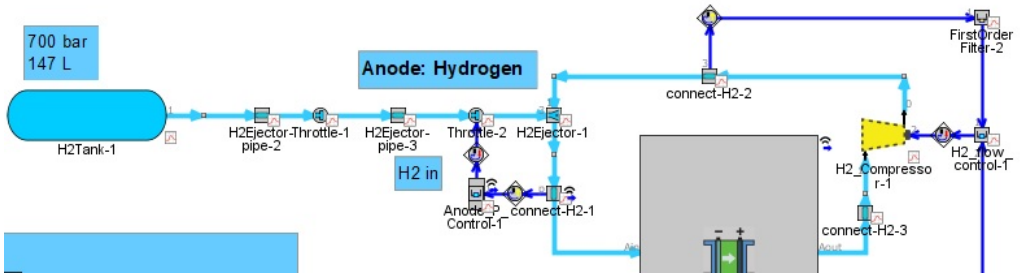

Figure 3.32: Anode reactants supplying system model in GT-Suite

As mentioned before, the stoichiometry λ usually is higher than 1, which means the amount of feeding reactant is always higher than the one of consumed reactants. Therefore, to increase the system efficiency and to avoid the waste of hydrogen, the anode mass flow is in a closed-loop. In Figure 3.32 the light blue line represents the hydrogen mass flow the output of anode flows back to the inlet. The Mazarin blue lines represent the signal read for the controller, one is for the compressor controlling to adjust the mass flow rate, and the other one is for the throttle to adjust the anode pressure.

Similar to the anode mass flow system, the cathode mass flow system is also designed based on Equation 3.21 to 3.24 with few differences. There are four molar exchange electrons for per molar O_2, and the cathode injection is not pure O_2. Therefore the calculation of cathode mass flow rate should be as Equation 3.25, where x_{O_2} is the percentage of oxygen in the air.

$$m_{air} = \lambda_{cathode} \cdot M_{air} \frac{I \cdot N}{4F \cdot x_{O_2}} \ [g/s] \tag{3.25}$$

As shown in Figure 3.33, the red lines are the air mass flow path. The air comes from ambient and flows into the stack in a specific flow rate, which adjusted by the cathode compressor. The blue lines represent the control signal for the compressor controller, which is a PID controller as well, Equation 3.25 calculates the targeting value, and the input signal of the compressor is the requested power. The products of the cathode will finally be removed into ambient through a turbine.

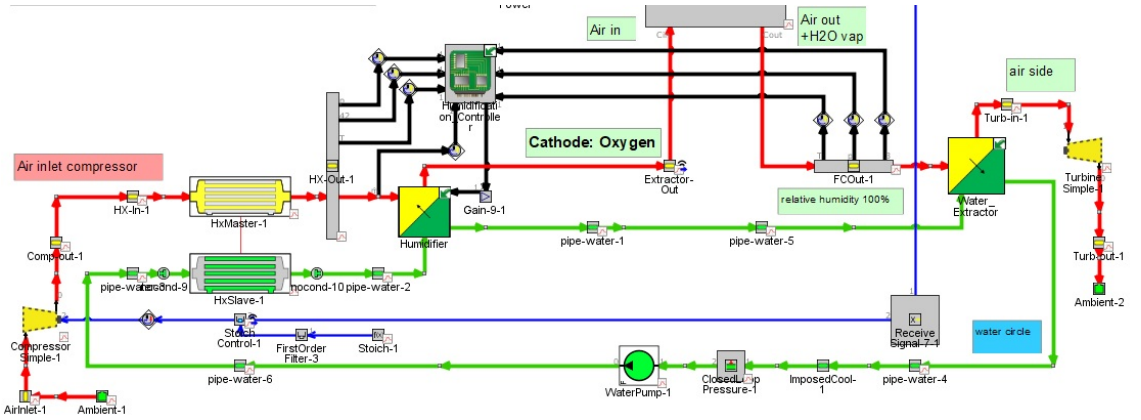

Figure 3.33: Cathode reactants supplying system model in GT-Suite

3.5.3.3 Water Management System

According to chemical function 3.13, the only product is water. It is also essential to know that water content of the proton exchange membrane will affect its performance a lot, including protonic conductivity, water transport properties, gas permeability, mechanical resistance, and dimensional stability [45]. Therefore, to increase the system efficiency, the water product could be reused for humidifying the membrane of the stack and proper water management is needed to achieve it.

As shown in Figure 3.34, the cathode output air flow through a water extractor which separating the water from the cathode output air and injecting the water into the water circulation loop used for humidifier and heat exchange device. Figure 3.35 and 3.36 show the structure of humidifier and extractor, which injected water from water circulation and extracted water from stack outputs, respectively.

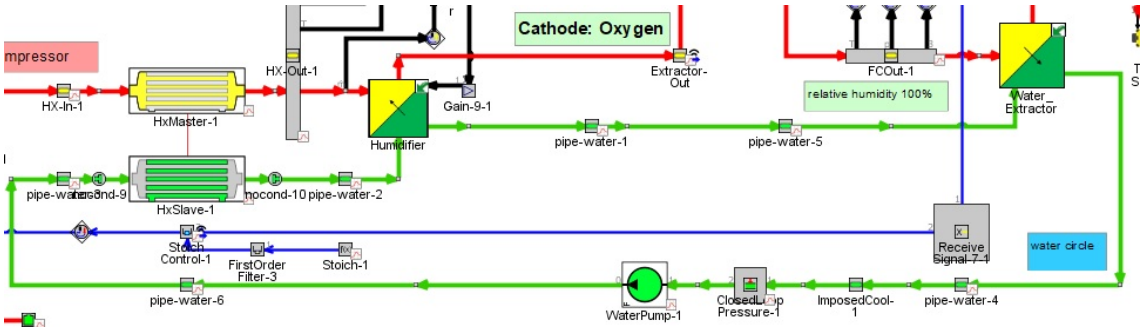

Figure 3.34: Water flow path in GT-Suite

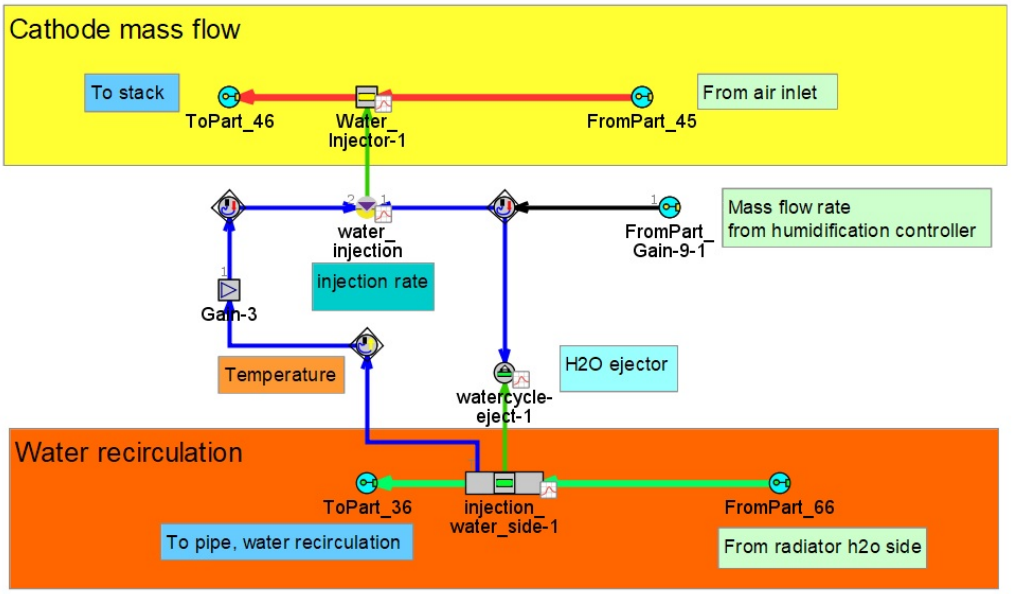

Figure 3.35: Humidifier in GT-Suite

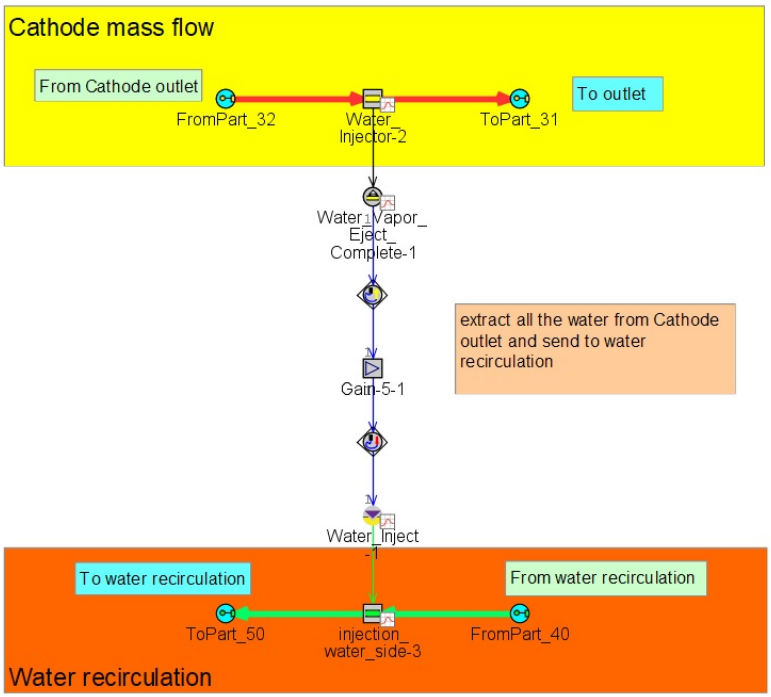

Figure 3.36: Water extractor in GT-Suite

The humidifier controller is modeled as Figure 3.38, the principles which the controller is based on is explained as follow. Starting from ideal gas law (Equation 3.26) which explains the relationship between pressure P and temperature T. In the equation V is the volume of gas, n means the molar of gas and R is the universal gas constant.

$$P \cdot V = n \cdot R \cdot T \tag{3.26}$$

Relationship between mass and molar is expressed as Equation 3.27, n is the number of molars and M is the molar weight.

$$m = n \cdot M \tag{3.27}$$

The specific humidity is defined as the mass ratio between vapor and dry air, which can be expressed as Equation 3.28, m_v and m_a are the mass of vapor and dry air respectively.

$$\omega = \frac{m_v}{m_a} \tag{3.28}$$

Summarizing the Equations 3.26 to 3.28, the further calculation of specific humidity is

$$\omega = 0.62198 \cdot \frac{P_v}{P - P_v} \tag{3.29}$$

and it is used in the humidifier controller design.

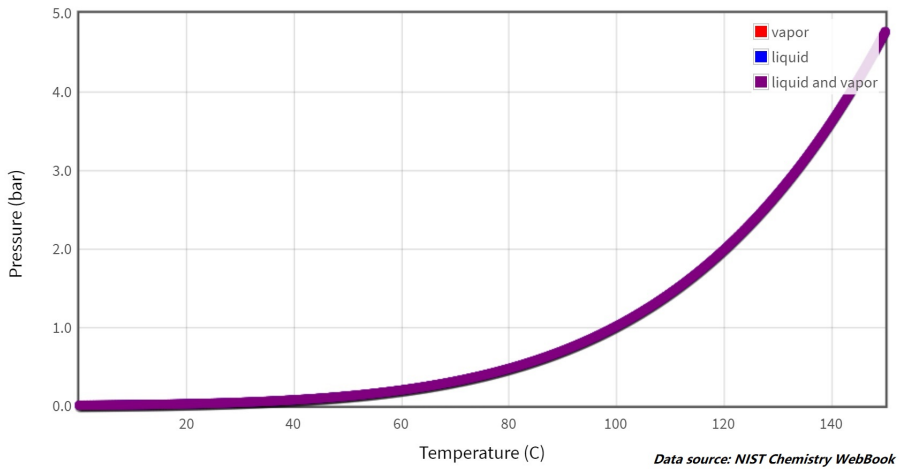

Figure 3.37: Saturation properties of water[46]

The humidifier controller model in GT-Suite is shown in Figure 3.38 which calculated the water amounts for injected into the cathode mass flow to keep the membrane in the stack under a proper humidity. The curve in Figure 3.37 shows the numerical relation of water between pressure and temperature. It has been inserted into the model as a look-up table to read the saturated pressure.

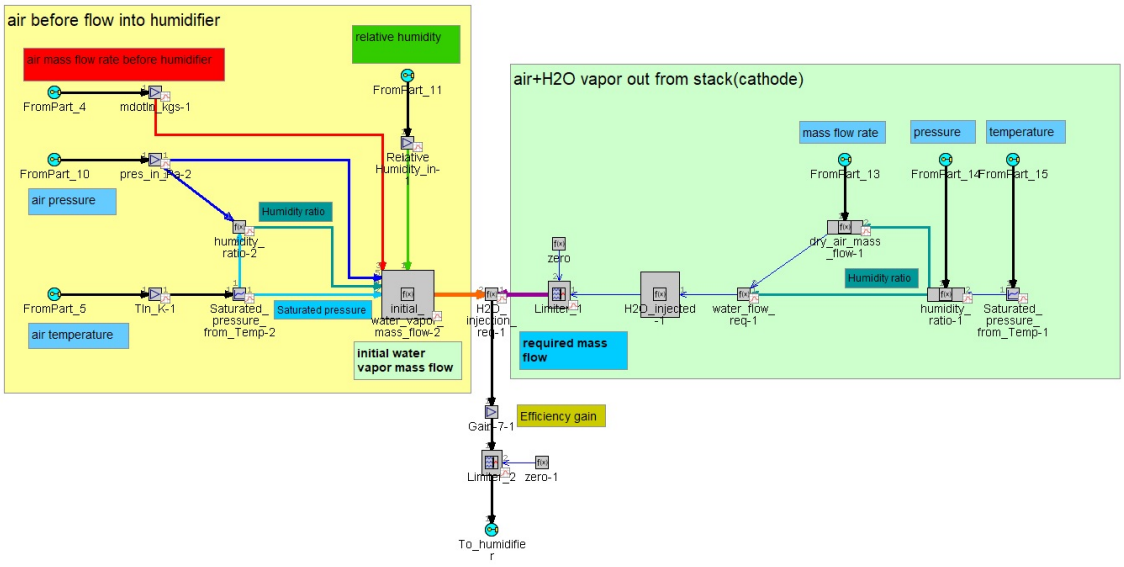

Figure 3.38: Humidifier controller in GT-Suite

3.5.4 Boost Converter Model

The DC-DC converter model is modeled in a straightforward way, which is a map-based DC-DC system level template. The 'DC-DConverter' template is used to model a simple map-based (efficiency map) DC-DC Converter. The component works with efficiency and an output power request (power on the DC-DC Converter's electrical output port). A positive output power request will source power to the output and sink power from the input; whereas, a negative output power request will sink power from the output and source power to the input.

The connection of the DC-DC converter is shown in Figure 3.41, which in the project model has been linked between the fuel cell system and DC link. Figure 3.39 is the efficiency map which inserted into the DC-DC converter, the X-axis represents the output power of the converter, and the Y-axis is the converter output voltage.

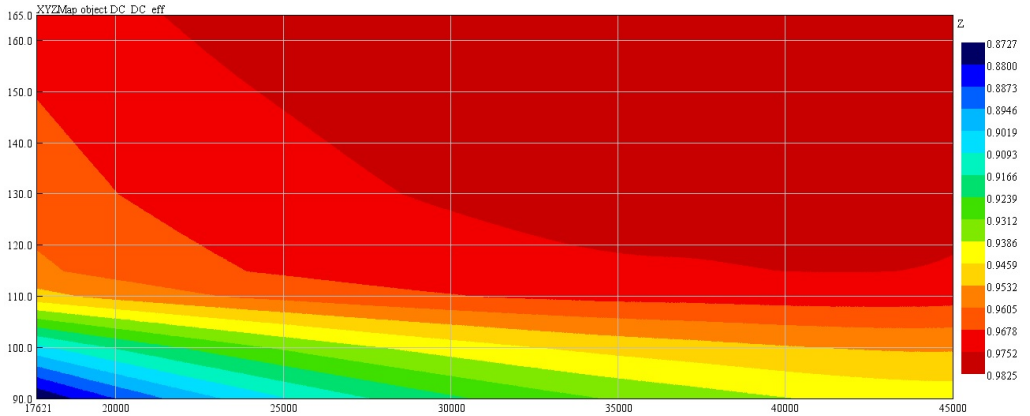

Figure 3.39: DC-DC converter efficiency map

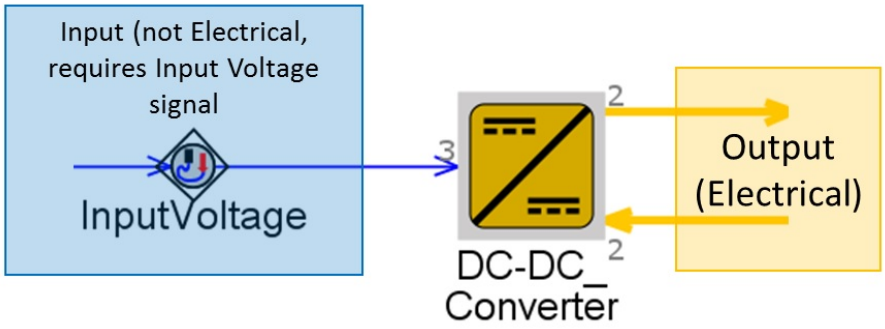

Figure 3.40: DC-DC converter required connection in GT-Suite

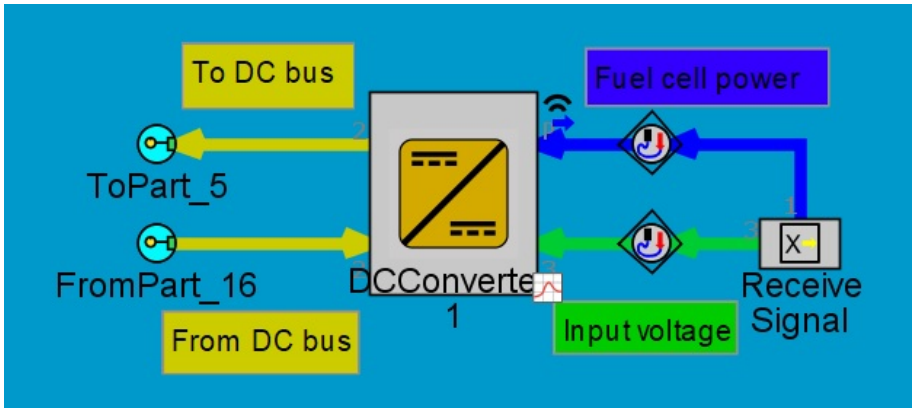

Figure 3.41: DC-DC converter connection

3.5.5 Electric Motor Model

Similar to the DC-DC converter model, the electric motor has been modeled most easily since this project requiring a system-level propulsion system modeling.

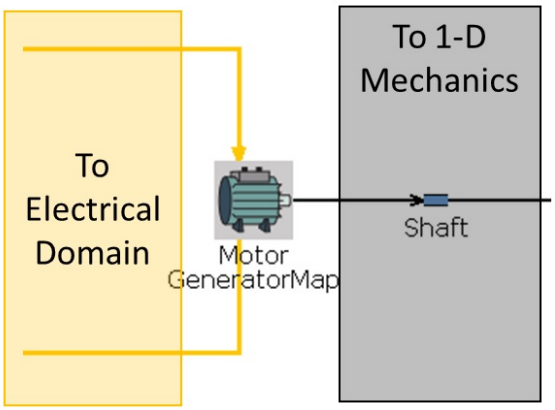

Figure 3.42: Electric motor required connection in GT-Suite

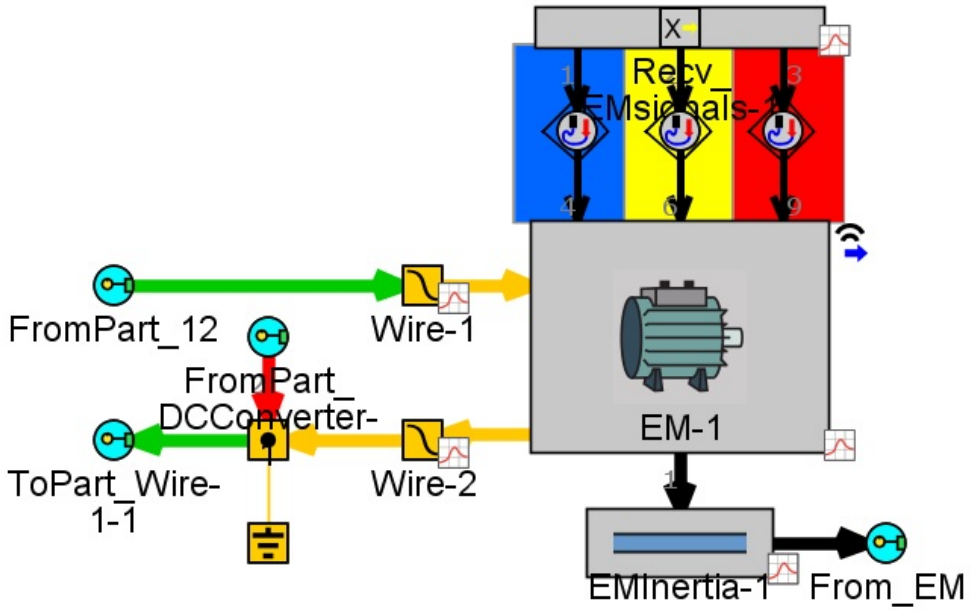

Figure 3.43: Electric motor model in GT-Suite

As shown in Figure 3.43, the modeling is implemented by the map-based motor template and connected to the shaft through mechanical connections (red lines).

3.5.6 Battery Model

Battery modeling using the electrochemical equation provides an in-depth insight into the physical and chemical process occurring inside the battery. It provides information on battery charging, discharging, the transient behavior of the battery as a function of factors such as temperature and discharge rate.

A simple way of modeling the battery is by equivalent circuit based modeling (ECM) as shown in Figure 3.44, Where V_{oc} is the open circuit voltage of the battery, R_0 represents the internal resistance of the battery present in the electrodes, separator, and bulk of the electrolyte. Further, the RC-link represents the added impedance offered in the circuit due to the polarization effect [47].

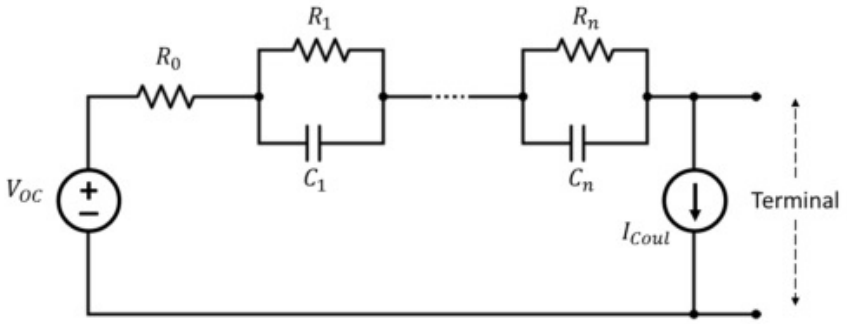

Figure 3.44: Equivalent circuit of simple battery model

State of Charge(SOC) is an essential characteristic of battery which is known as the usable capacity. In other words, SOC describes the percentage of the remaining usable energy in the battery, and it can be calculated as follows,

$$SOC(t) = SOC_{initial} - \frac{\int_t^{t_0} I(\tau)d\tau}{Q_{tot}} \tag{3.30}$$

where $SOC_{initial}$ is the initial SOC and Q_{tot} is the total charge capacity of the battery in (Ah).

The relationship between the state of charge and energy and the relationship between cells and battery pack will be introduced,

$$E_{cell} = I_{cell} \cdot V_{SOC} \tag{3.31}$$

Where, E_{cell} is the energy per cell, I_{cell} corresponds to the current flowing through each cell and V_{VOC} is the voltage per cell depending on the SOC level of the battery. Further, the number of cells in series can be calculated as

$$n_{cell} = \frac{E_{bat}}{E_{cell}} \tag{3.32}$$

Where, E_{bat} is the energy storage capacity of the battery and n_{cell} is the total number of cells in the battery. Additionally, the number of cells in series can be expressed as,

$$n_{series} = \frac{V_{oc}}{V_{SOC=100}} \tag{3.33}$$

where, V_{oc} is the open circuit voltage and $V_{SOC=100}$ is the per cell voltage at 100 percent SOC level. Lastly, in order to calculate the number of cells in parallel and current capacity of the battery it can be found as

$$Ah_{bat} = \frac{E_{bat}}{V_{oc}} \tag{3.34}$$

$$n_{parallel} = \frac{Ah_{bat}}{Ah_{cell}} \tag{3.35}$$

where $n_{parallel}$ is the number of cells in parallel and Ah_{bat} denotes the current capacity of the battery.

The following table introduced the parameters of the battery which used in the GT-Suite model for PHEV and HEV.

Table 3.8: Battery data for PHEV

Parameter	Value
Open Circuit Voltage at 100% SOC, V_{oc}	$372.9[V]$
Cell Current Capacity, Ah_{cell}	$30[Ah]$
Cell Voltage at 100% SOC, $V_{SOC=100}$	$4.1434[V]$
Cell Voltage at 50% SOC (Nominal Voltage), $V_{SOC=50}$	$3.649[V]$
Cell Voltage at 0% SOC, $V_{SOC=0}$	$2.9457[V]$
Number of cells in series, n_s	90
Number of cells in parallel, n_p	1
Battery Capacity, E_{bat}	$9.852[kWh]$

Table 3.9: Battery data for HEV

Parameter	Value
Open Circuit Voltage at 100% SOC, V_{oc}	$294.26[V]$
Cell Current Capacity, Ah_{cell}	$6.9[Ah]$
Cell Voltage at 100% SOC, $V_{SOC=100}$	$4.087[V]$
Cell Voltage at 50% SOC (Nominal Voltage), $V_{SOC=50}$	$3.67[V]$
Cell Voltage at 0% SOC, $V_{SOC=0}$	$2.728[V]$
Number of cells in series, n_s	72
Number of cells in parallel, n_p	1
Battery Energy Capacity, E_{bat}	$1.823[kWh]$

Figure 3.45 and 3.46 is the cell voltage curve for PHEV and HEV used in the battery template.

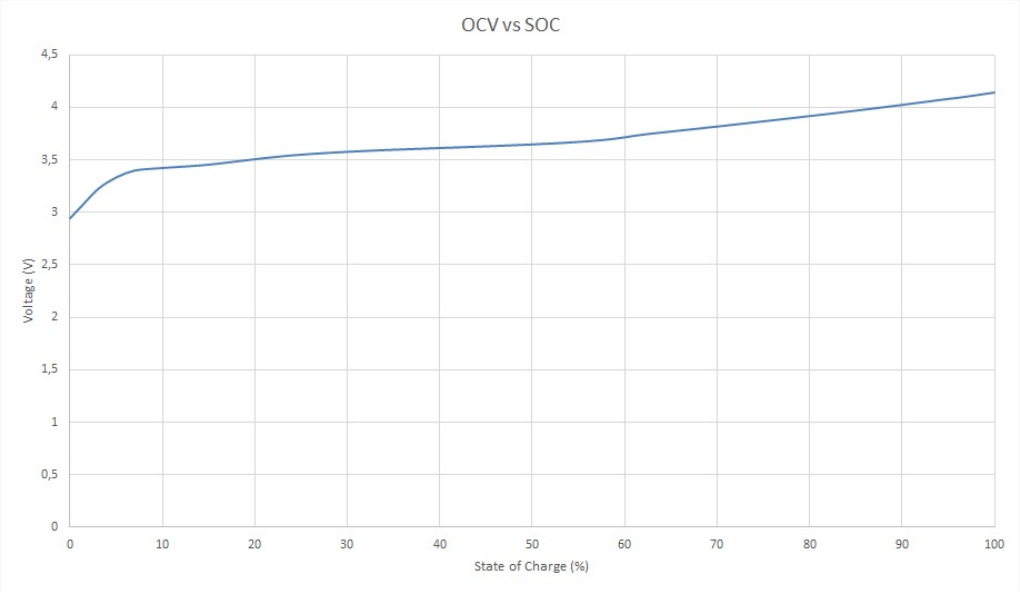

Figure 3.45: PHEV battery cell U-I curve

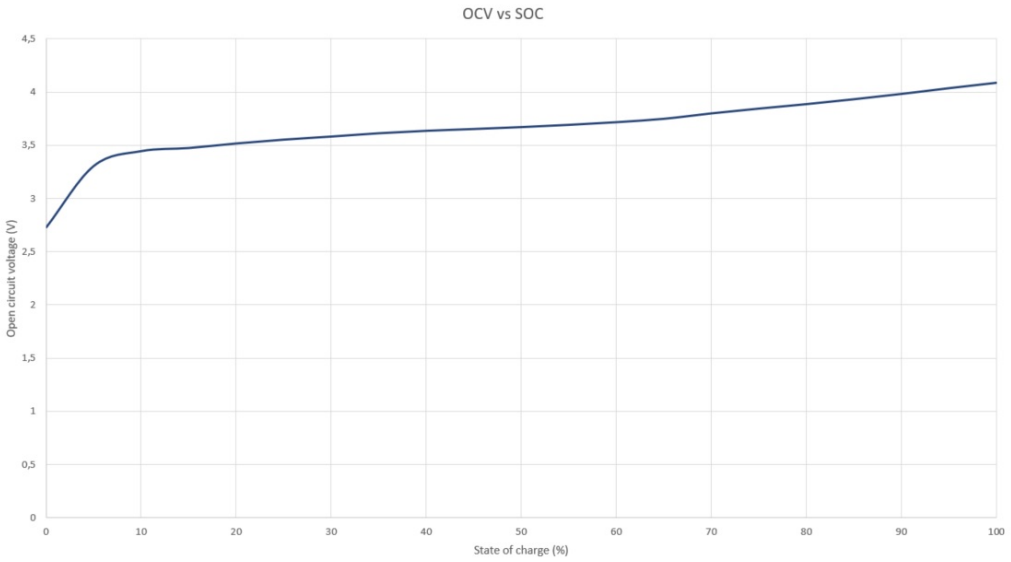

Figure 3.46: HEV battery cell U-I curve

In GT-Suite, many templates can be used directly and simplify the model building. The final battery model of this project implemented by battery template is shown in Figure 3.47. The yellow, red, and black lines represent the electrical connections connected to different components. The blue lines are the signals received from BMS.

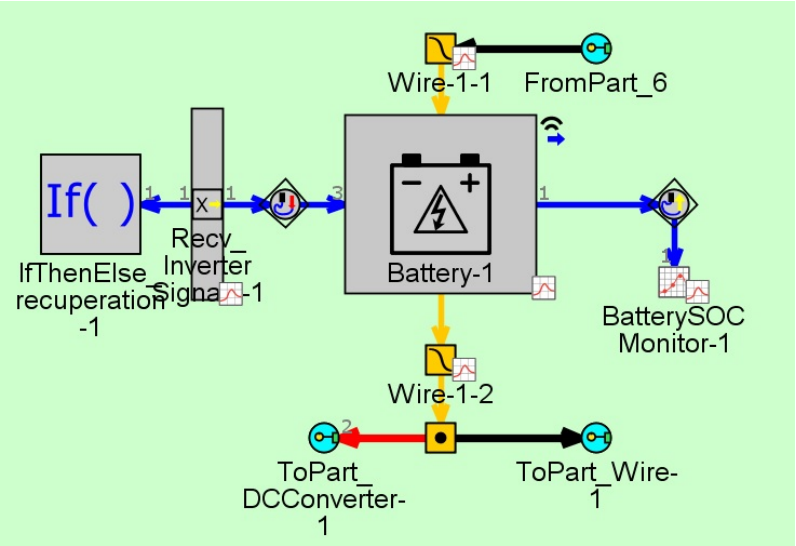

Figure 3.47: Battery model in GT-Suite

3.5.7 Battery Management System Model

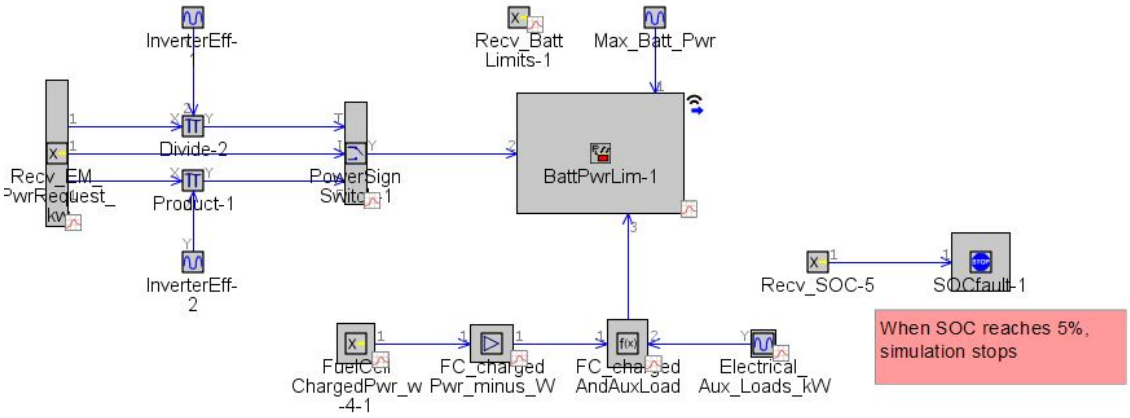

Figure 3.48: The Battery Management System Model in GT-Suite

In the Battery Management System Model, one function is to calculate how much traction power is requested from the battery and how much regenerative braking power is charged to the battery with the electric motor. The inverter efficiency is also considered by implementing an inverter block, as shown in Figure 3.48. When discharging, the power request will be divided by the inverter efficiency, which means more power is needed from the battery in reality. When charging, the power will multiply with the inverter efficiency, which means less power can be charged and stored in reality. The discharge and charge power of the electric machine is limited according to the maximum available peak power of the battery, which is 65 kW for the PHEV battery and 50 kW for the HEV battery.

Another function is to calculate how much power will be charged from fuel cell to battery when the fuel cell is turned on. Auxiliary loads are also considered and send to the controller. There is also a battery diagnostic block, which will stop the simulation when the battery SOC reaches 5%.

3.5.8 Electric Motor Control Unit Model

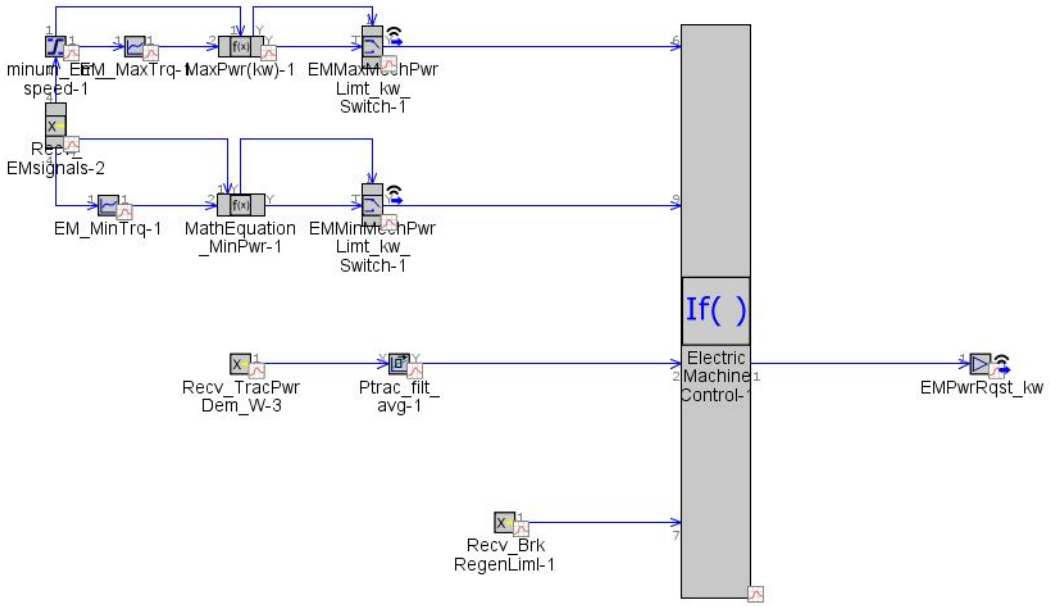

Figure 3.49: The Electric Motor Control Unit Model in GT-Suite

The main function for Electric Machine Control Unit is to calculate the traction power and regenerative braking power request at current vehicle speed and send those signals to the Electric Motor Model. The maximum and minimum electric motor power limit at current speed can be calculated based on the electric motor speed-torque curves which are shown in Figure 3.50, to make sure the current power demand does not exceed the electric motor power limit. If the vehicle is in standstill mode, then there will be no power send to Electric Motor Model.

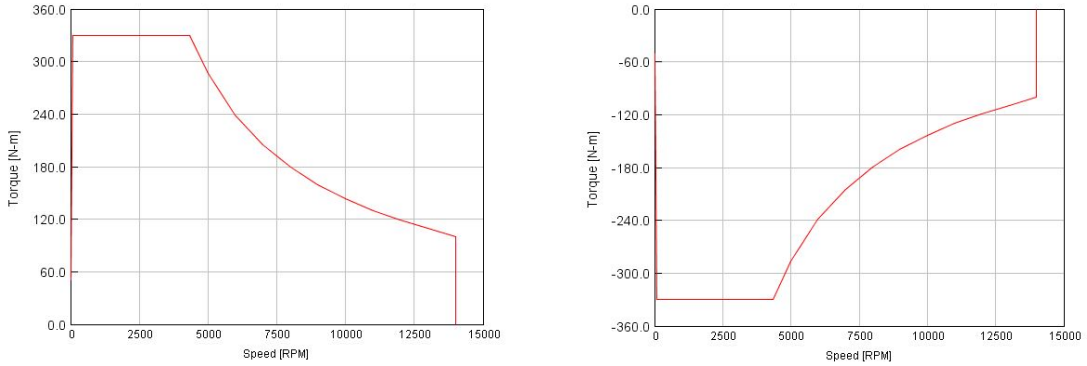

(a) The electric motor maximum torque line

(b) The electric motor minimum torque line

Figure 3.50: The electric motor torque line in GT-Suite

3.5.9 Fuel Cell Control Unit Model

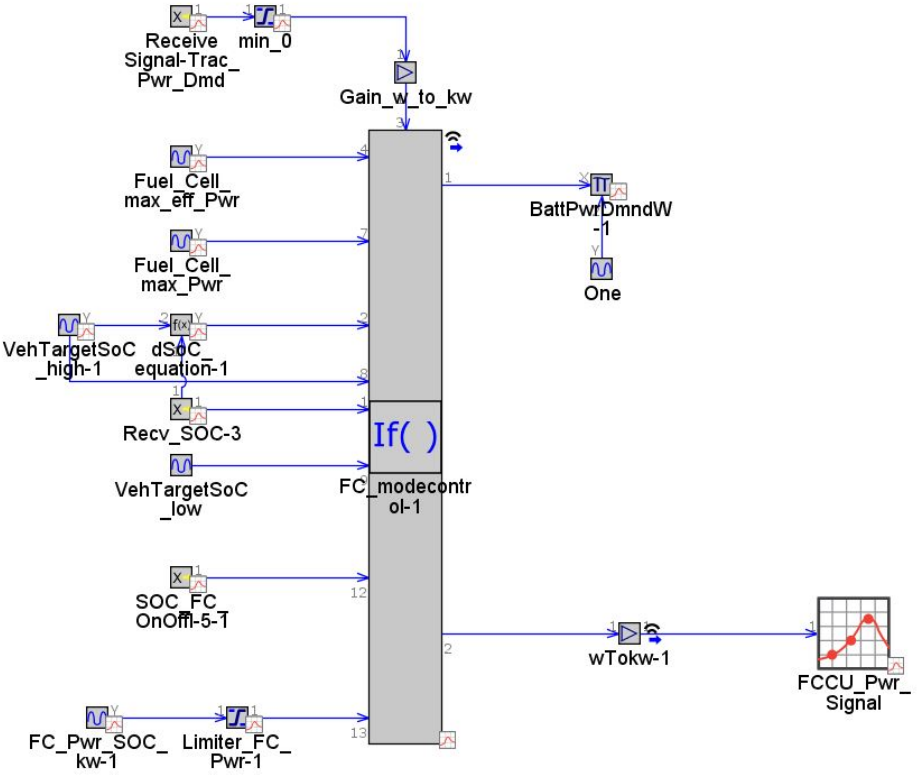

Figure 3.51: The Fuel Cell Control Unit Model in GT-Suite

The main function for the Fuel Cell Control Unit Model is to determine how much power should be used to charge the battery if in charging mode and how much power should come from the fuel cell to charge the battery or meet the traction power demand. Also, the fuel cell charging power will change following the battery

SOC level both in Fuel Cell-PHEV and Fuel Cell-HEV. So that the fuel cell stack system can run as efficiently as possible.

When in charge sustaining mode, which means the fuel cell will be switched on to charge the battery, there are two possible options:

1. Stop Fuel Cell charging when regenerative braking, because of the high battery I^2R losses in more significant power.

2. Continue Fuel Cell charging when regenerative braking to avoid the Fuel Cell System frequently turning on-and-off in order to extend the Fuel Cell working life.

3.5.10 Braking Control Unit Model

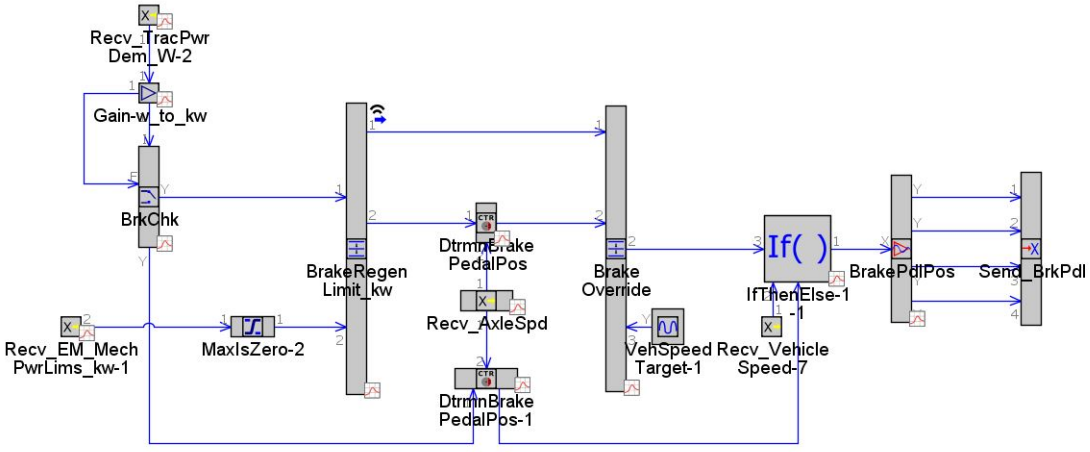

Figure 3.52: The brake controller model in GT-Suite

In the brake controller model, it mainly has two brake pedal situations. One is called 'HEV Brake Pedal' situation; another one is called 'Friction Brake Pedal' situation. In 'HEV Brake Pedal' situation, as can be seen in Table 3.10 it calculates the brake power request during driving and determines the split between frictional and regenerative braking. If the braking power request exceeds the maximum available regenerative braking power, the difference will be accommodated via the friction brake, and those signals will be sent into the four brakes in each wheel. 'Friction Brake Pedal' situation, which is shown in Table 3.11 will occur until the vehicle slows to a certain speed when regeneration will cease, and the friction brakes assume 100% of the braking request.

Table 3.10: Brake Controller for HEV Brake Pedal situation.

Description	Conditions	Regenerative Braking power demand (kW)	Mechanical Braking power demand (kW)
Limited Regeneration	Brake Power Request<=Maximum available regenerative braking power	Brake Power Request	0
Full Regeneration	Brake Power Request>Maximum available regenerative braking power	Maximum available regenerative braking power	Brake Power Request-Maximum available regenerative braking power

Table 3.11: Brake Controller for Friction Brake Pedal situation.

Situation	Actions	Conditions
Friction Brake Pedal	If	Vehicle Speed<5 km/h
HEV Brake Pedal	If	Vehicle Speed>=5 km/h

Another function in this model is brake override: an active vehicle safety feature to work as a fail-safe measure. When working in the driving cycle, if the vehicle speed reaches 0 km/h, then the brake pedal position is set to 100% to make sure the vehicle stop.

3.6 Daily driving distance analysis

One of the main reasons why EVs have some obstacles to entry into the market is range anxiety, because of the relatively short driving range for EVs compared with traditional fossil fuel vehicle.

From a report by Deloitte [48], 80% of the U.S. participants of the survey want a range of 100 miles or more from an electric car. Around 60% of them want to be able to drive at least 200 miles before a recharge, and 37% expects a range of 300 miles or more [7].

It is essential to find what is the daily driving range in order to decide how large the battery size should be, especially for EVs and PHEVs. Assuming that these kinds of cars only can charge at home during the night.

According to the 2009 National Household Travel Survey from U.S.Department of Transportation Federal Highway Administration, the average driving distance for a driver is 49 km in weekday and 40 km in the weekend. The average commuting distance is 19.5 km. The average daily miles of travel per person also shows a different picture of gender difference. It shows that women have traditionally traveled fewer miles per day than men, regardless of age. The average daily driving distance was 45 miles and 36 miles for men and women respectively in 2001 and 41.5 miles and 32 miles for men and women respectively in 2009 [49].

In ample driving range for everyday deeds by Nissan Motor Corporation. In European countries, 90% of the people drive less than 120 km per day On average. In the USA, 90% of the people drive less than 135 km per day On average [47] [50].

Based on The Swedish Car Movement Data Project, the results show that 90% of the cars travel less than around 70 km per day on average [51].

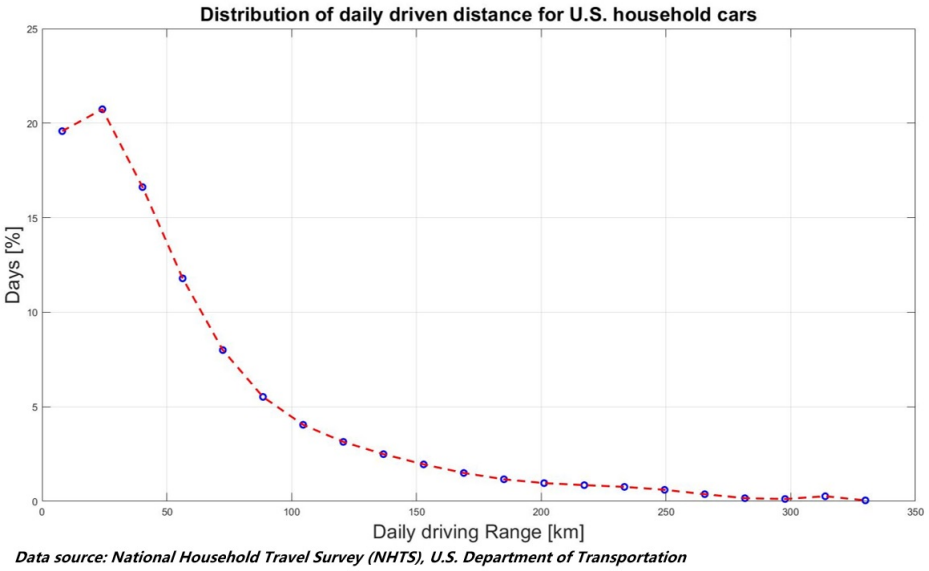

Figure 3.53: Distribution of the daily driven distance for U.S.household cars

Based on the 2009 National Household Travel Survey from U.S.Department of Transportation Federal Highway Administration, the distribution of the daily driven distance for U.S.household cars can be seen in Figure 3.53 above. About 93.9% of all driving days have daily driving range below 150 km. About 86.3% of all driving days have daily driving range below 100 km. About 68.7% of all driving days have daily driving range below 50 km.

3.7 Cost model for determining energy capacity of battery for PHEV

Nowadays, the hydrogen refilling network is not yet as convenient as fossil fuel refilling network, and it still needs an enormous scale of investment and long term to construct. Therefore, a proper topological structure like PHEV may be an excellent choice to satisfy all the requirements including competitive driving range, zero emissions and better practicality in the early days of the hydrogen network.

Battery size determination is an essential task for PHEV design, to achieve that a mathematical model is introduced. If the daily driving distribution is, for example, shown as Figure 3.54 and the pure electric range has been set as X km. The integration of the shadow part should be covered by electricity, and the rest part will be covered by Hydrogen. In Figure 3.55, we can get the cost of using Hydrogen or electricity corresponding to X km pure electric range. To get the total cost corresponding to the energy capacity of the battery, all the cost should be added

which is shown as Figure 3.56 and there should be an optimal pure electric range corresponding to the minimum TCO which can be used to define the battery size.

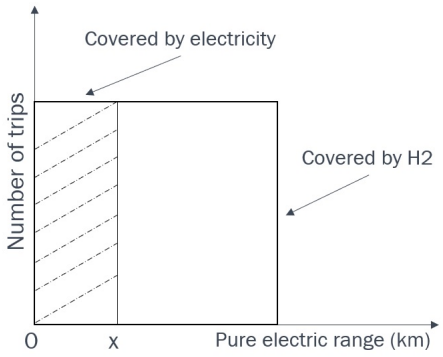

Figure 3.54: Daily driving distribution example

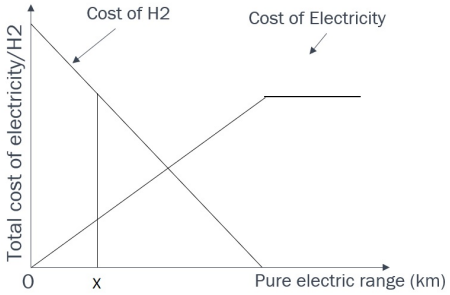

Figure 3.55: Cost of using Hydrogen/electricity

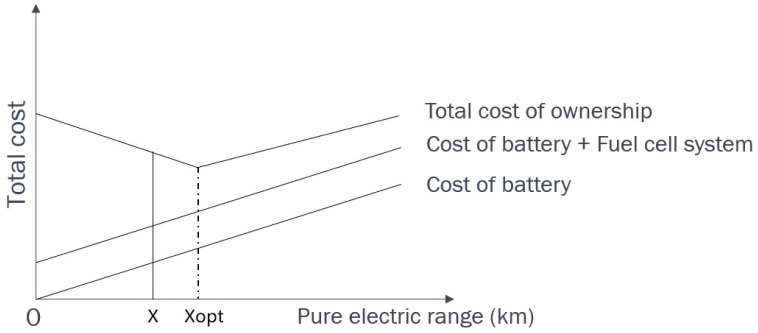

Figure 3.56: Total cost

An example calculation for determining the proper energy capacity of the battery is presented. In the U.S. market, the daily driving distribution is shown in Figure 3.53, which is in percentage. According to the data available from *Statista*©[52] about 'U.S. vehicles - projected average age 2017-2019' which is 11.8 years, roughly 4307days. By assuming different percentages of the life length the scenarios can be simulated, for instance, 60%, 70% or 80% of the total lifespan the vehicle were used as shown in Figure 3.57.
The parameters, for instance, needed for calculation are shown in Table 3.12.

Table 3.12: Parameters for example calculation

A:Vehicle energy consumption(kwh/km)	G:Fuel cell system efficiency	F:Battery efficiency	H:Battery SOC window
0.19	0.5	0.9	0.1-0.9
B:Battery cost($/kwh)	C:Hydrogen tank cost($/kwh)	D:Hydrogen cost($/kg)	E:Electricity cost($/kwh)
190	19	13.9	0.13

Theoretically, the energy density of compressed hydrogen in 700 bar which used for most of fuel cell vehicles is 39.405 kWh/kg. This value can be used for calculating the usage amount of hydrogen, corresponding to x km as equation 3.36, in which x

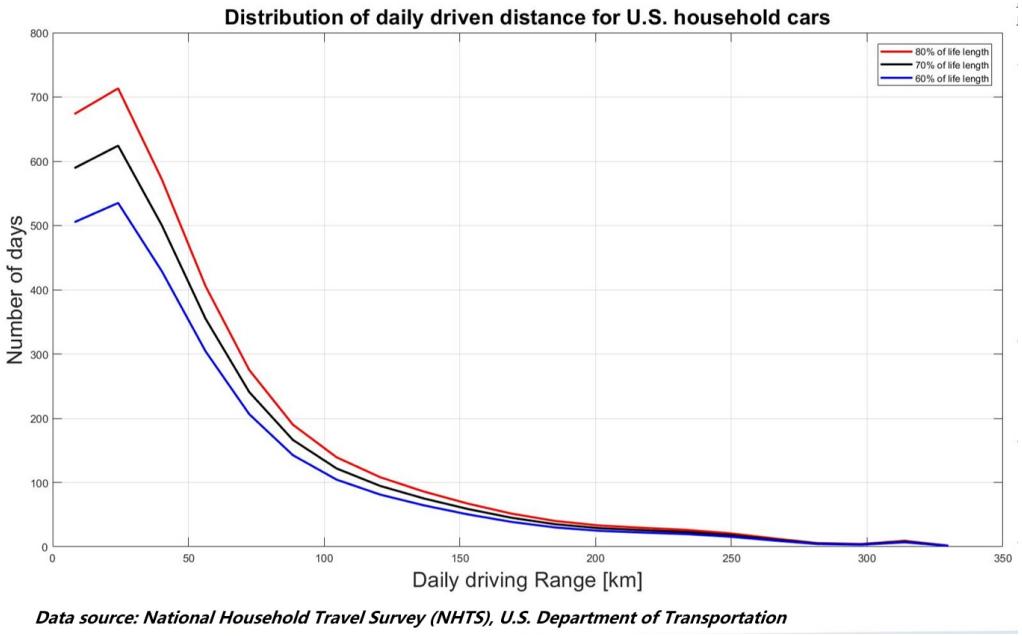

Figure 3.57: Distribution of the daily driven distance for U.S.household cars in number of days

is the pure electric range and $f(x)$ is the number of days corresponding to x based on Figure 3.57.

$$H_2\ cost = \int_x^{\infty} \frac{D \cdot A}{39.405 \cdot G} \cdot x \cdot f(x) dx \tag{3.36}$$

The cost of using electricity can be also calculated if the pure electric range is x,

$$Electricity\ cost = \int_0^{x} \frac{E \cdot A}{F} \cdot x \cdot f(x) dx \tag{3.37}$$

The cost for battery and hydrogen tank per kilometre can be calculated according to equation 3.38 and 3.39, respectively.

$$Battery\ cost = \frac{A \cdot B}{H} \cdot x \tag{3.38}$$

$$H_2\ tank\ cost = \frac{A}{C \cdot G} \cdot x \tag{3.39}$$

Additionally, the total cost, which contents the cost of using hydrogen/electricity and the cost of battery/hydrogen tank, can be concluded as function 3.40.

$$Total\ cost = (\frac{A \cdot B}{H} + \frac{A}{C \cdot G}) \cdot x + \frac{A \cdot E}{F} \cdot \int_0^{x} x \cdot f(x) dx + \frac{A \cdot D}{39.405 \cdot G} \cdot \int_x^{\infty} \cdot x \cdot f(x) dx \tag{3.40}$$

By inserting the value from Table 3.12, a new function can be presented as 3.41 and the optimal value of x corresponding to the minimum total cost for scenario 60%, 70% and 80% life length driving can be calculated, which are 55 km, 60 km and 65 km respectively.

$$Total\ cost = 45.145 \cdot x + 0.0274 \cdot \int_0^x x \cdot f(x)dx + 0.134 \cdot \int_x^\infty x \cdot f(x)dx \tag{3.41}$$

The final step for determining the battery energy capacity can be done by multiplying with vehicle energy consumption (A), divided by the battery SOC window (H), which got 13.05 kWh, 14.22 kWh and 15.48 kWh respectively for scenario 60%, 70% and 80% of lifespan.

4

Results and discussion

In this chapter, the results from simulations of both Fuel Cell-PHEV and Fuel Cell-HEV will be analyzed and discussed. The Worldwide Harmonized Light Vehicles Test Cycle (WLTC) Class 3 driving cycle is used to evaluate the propulsion system models and the control strategies to ensure the functioning in each time step.

Initially, some simulation results for components and control unit models which are shared by both Fuel Cell-PHEV and Fuel Cell-HEV are described and studied together. For example, the Driver Model, the Electric Motor Control Unit Model, and the Brake Control Unit Model. Then, simulation results for unique components or control unit models for Fuel Cell-PHEV and Fuel Cell-HEV will be analyzed and discussed separately. For example, the State Selection Controller Model, the Fuel Cell Control Unit Model and the Fuel Cell Stack System Model. Finally, the conclusion will be made depending on the obtained results.

4.1 Driver Model

Firstly, driving performance from Driver Model is studied. As is shown in Figure 4.1 below, the red line is the target vehicle speed and the blue line is the actual vehicle speed. Two lines are overlapping, which means both the Fuel Cell-HEV and Fuel Cell-PHEV propulsion system model follow each driving conditions like acceleration, deceleration, and standstill during the WLTC Class 3 driving cycle well.

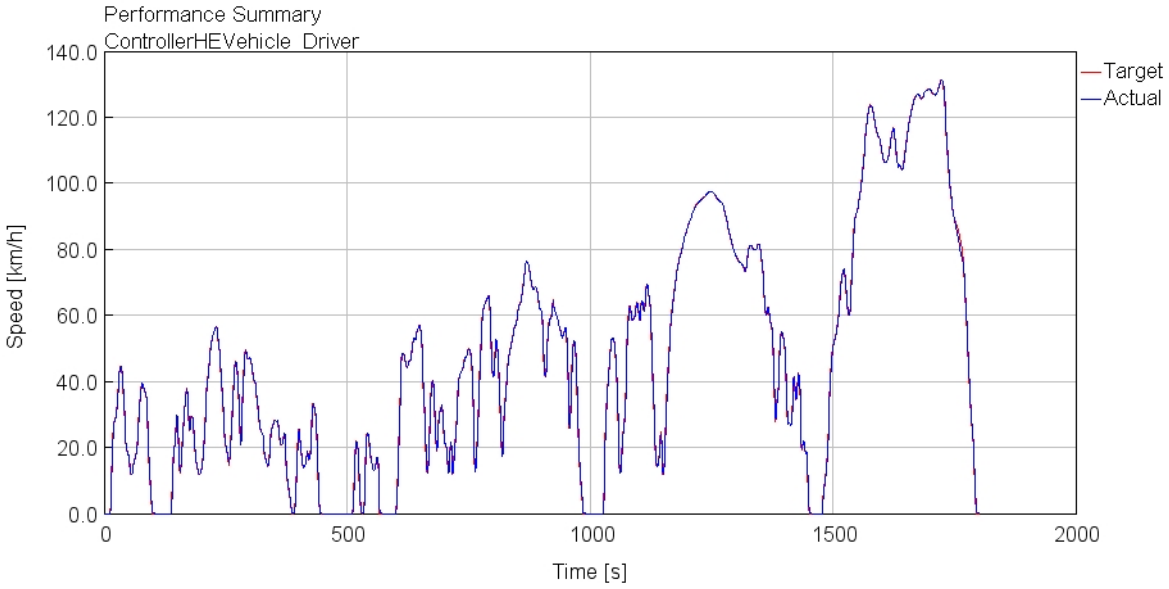

Figure 4.1: Fuel Cell-HEV and PHEV driving performance during WLTC driving cycle

4.2 Electric Motor Control Unit Model

The primary function for Electric Machine Control Unit is to calculate the traction power and regenerative braking power request at current vehicle speed and send those signals to the Electric Motor Model. The positive and negative electric motor power request and torque request can be seen in Figure 4.2 and Figure 4.3 below. For the simulation driving cycle, the maximum power request is 51.7 kW and the negative power will be sent to Brake Controller Model for regenerative braking. If the vehicle is standstill, then there will be no power send to Electric Motor Model.

4.3 Braking Control Unit Model

The brake power request from the wheel is presented in Figure 4.4. The braking power request does not exceed the maximum available regenerative braking power, which is the maximum charging power of the electric motor at current speed. Therefore, all the braking power energy during deceleration will be collected.

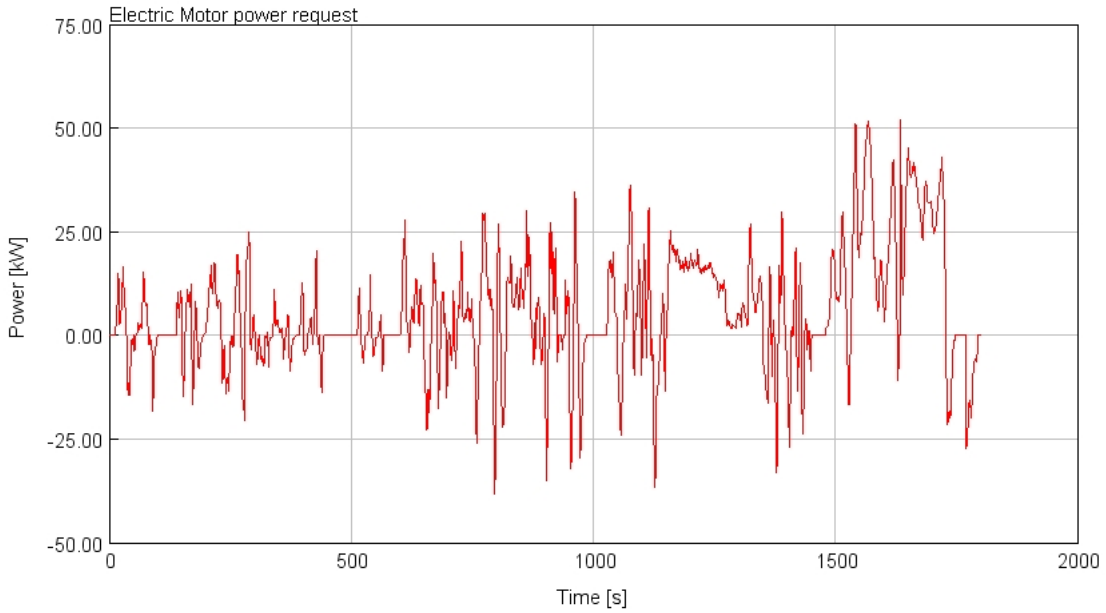

Figure 4.2: Electric motor power request

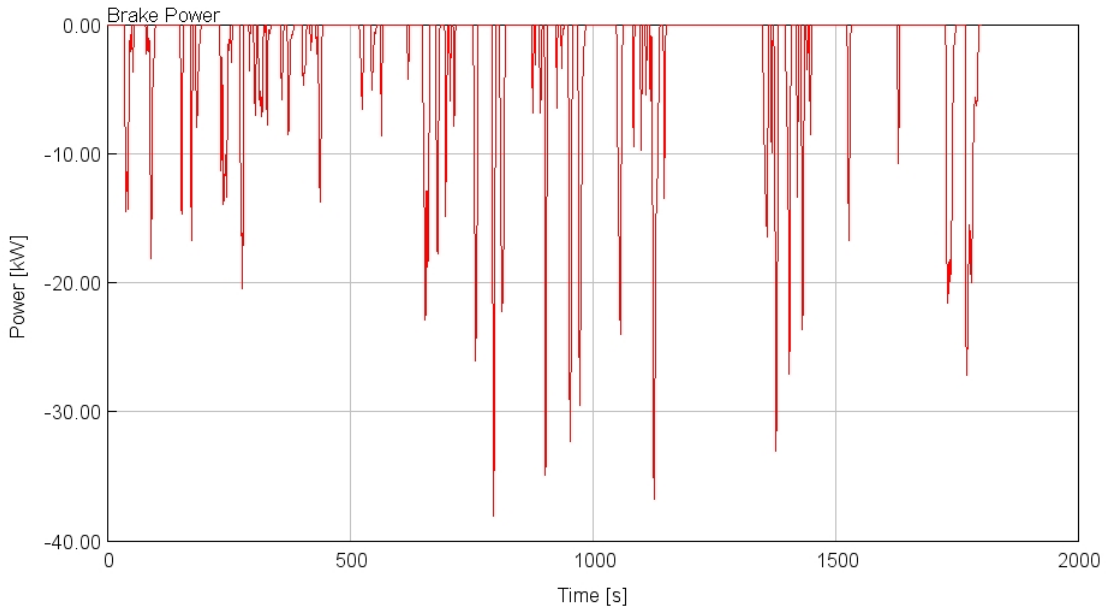

Figure 4.4: Brake power request

Figure 4.5 presents the result for the fail-safe measure, where the brake pedal position for friction brake is set to 100% to make sure the vehicle stop when the vehicle speed reaches 0 km/h .

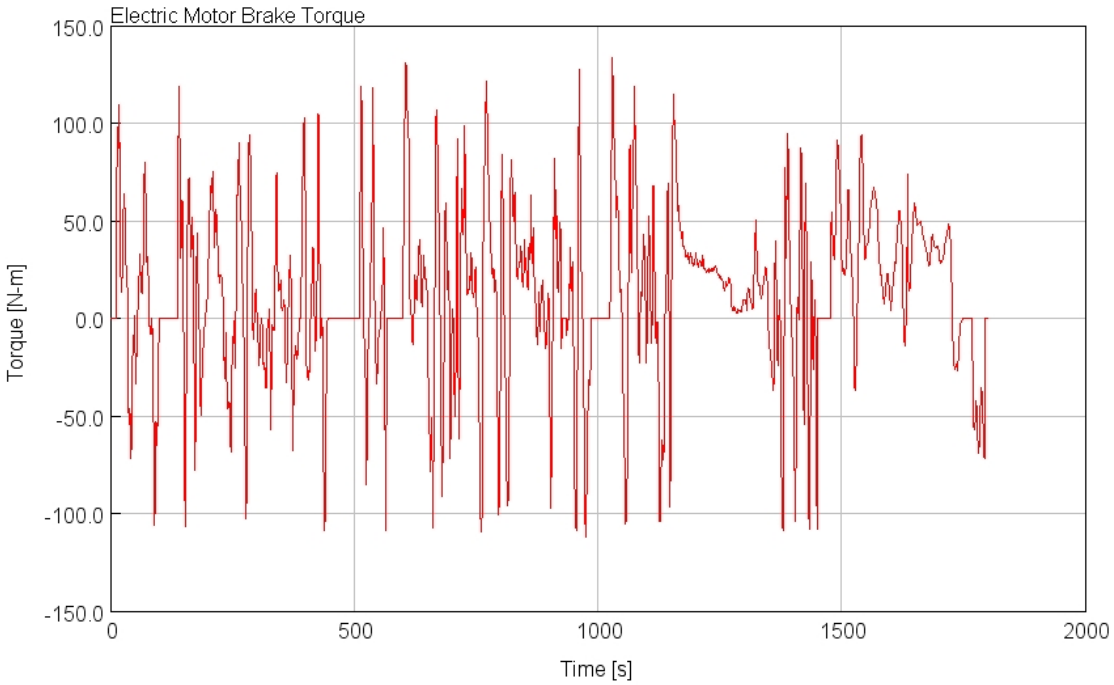

Figure 4.3: Electric motor brake torque request

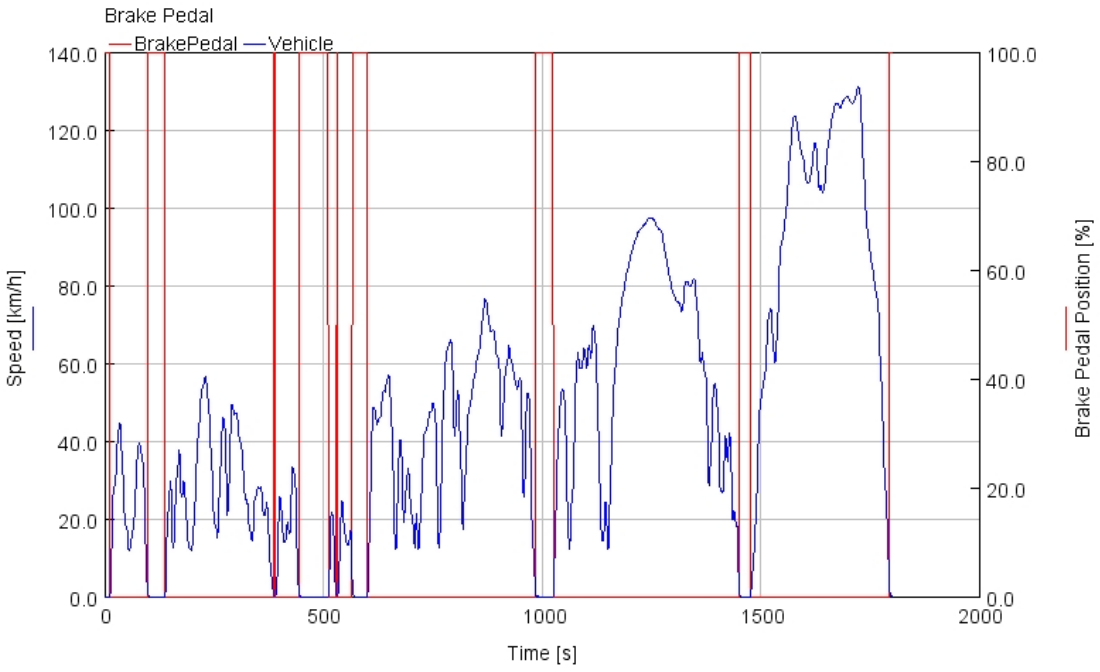

Figure 4.5: Brake pedal position when vehicle stop

4.4 Fuel cell stack simulation

Figure 4.6 and 4.7 illustrate the fitting condition of the polarization curve in the fuel cell stack model for HEV and PHEV, in which the dots represent the measurement data from supplier A and the solid lines represent the auto fitting curve within the fuel cell stack model. From the result, the curve fits quite well for both HEV and PHEV.

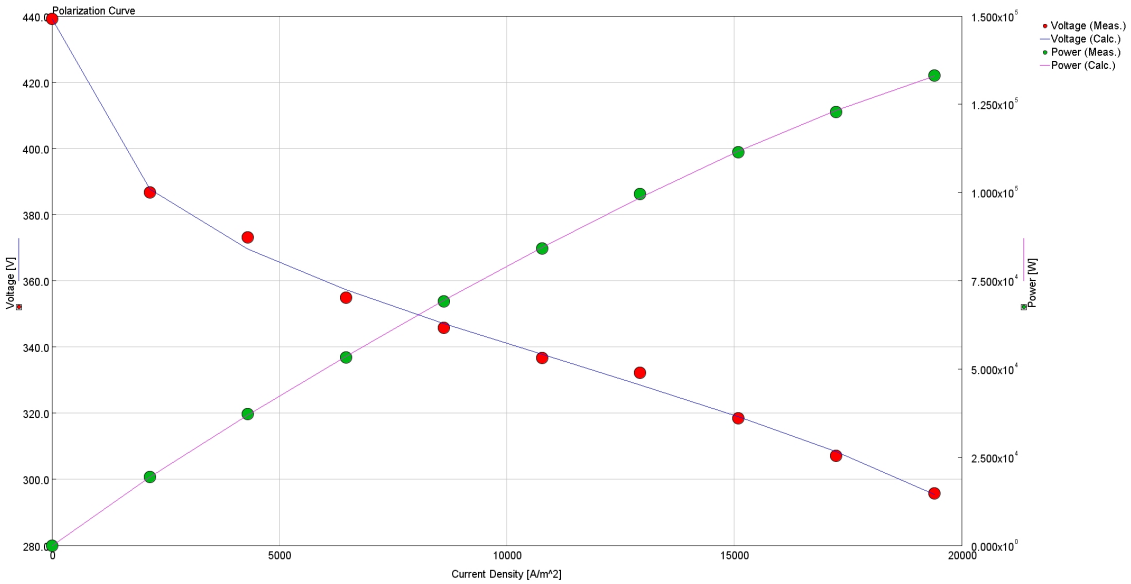

Figure 4.6: Polarization curve fitting for HEV fuel cell

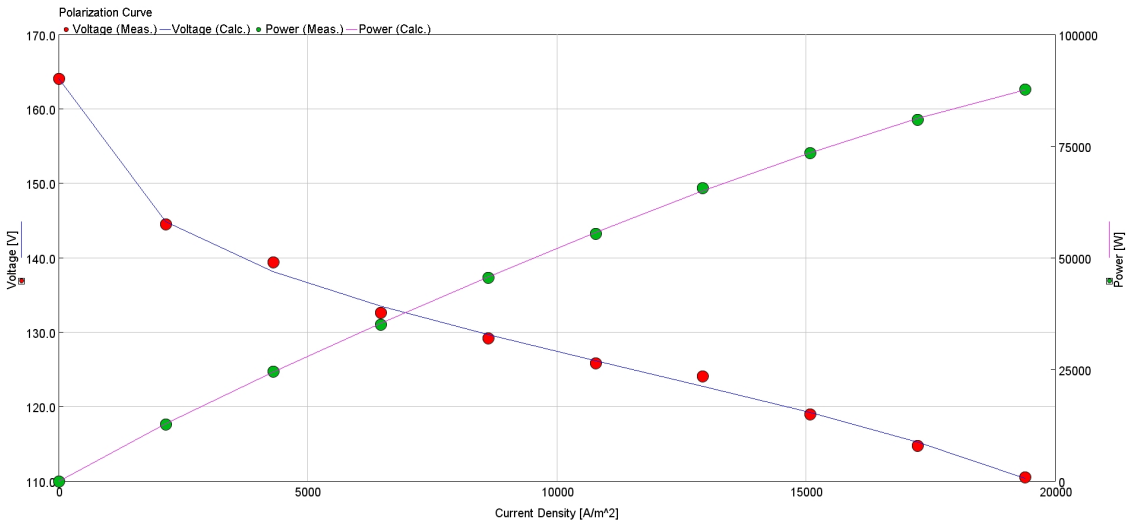

Figure 4.7: Polarization curve fitting for PHEV fuel cell

The performance of the FC stack in this project model is shown in Figure 4.8 and Figure 4.9 for HEV and PHEV respectively. In general, the fuel cell stack can follow the power request quite well but with few problems, for instance, the response

time delay of the fuel cell system was not simulated accurately. That is because the compressor used in the model is an ideal simple compressor model, and it can act according to the signal from its PID controller with no delay. Meanwhile, the PID controller has been adjusted to operate fast. Therefore the power output of the fuel cell stack follows the request nearly without lagging time. In the real condition, the compressor is connected to a motor through mechanical connection and the lagging time of the motor is the main factor which caused the fuel cell system power-output delay. To mimic the time delay a detailed motor model is needed for the future working.

Compared to FC-HEV, the fuel cell stack of PHEV followed the power request better. This is because the fuel cell stack in FC-PHEV works in a more simple condition without many dynamic changes compared to HEV, and the transient load power is mainly covered by battery. However, in FC-HEV the fuel cell stack is considered as the primary power source of the vehicle and the transient load power is handled by both fuel cell stack and battery which lead to frequent dynamic changes for the fuel cell stack.

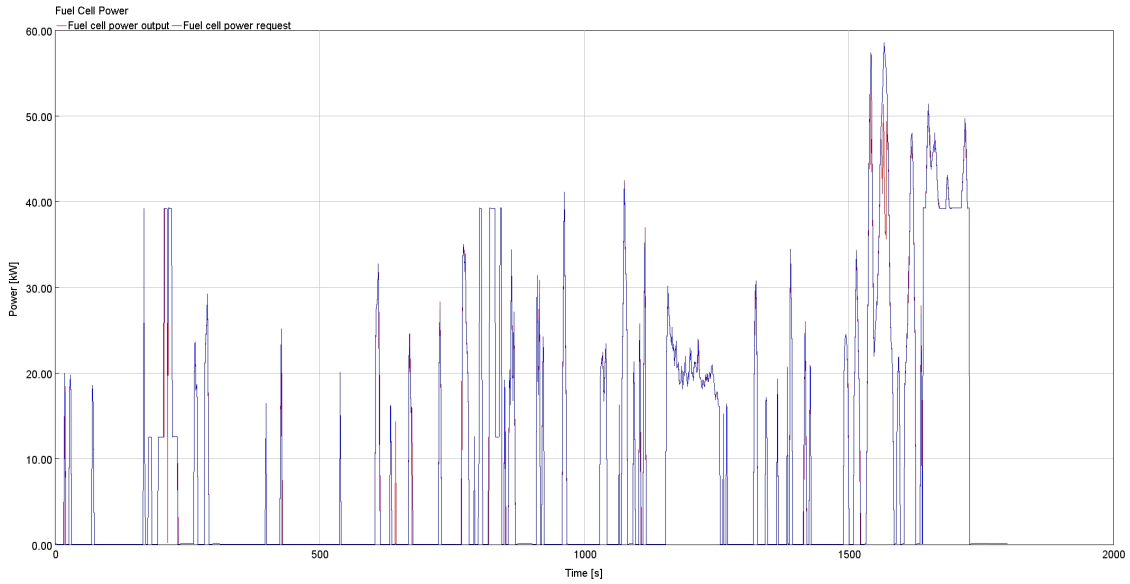

Figure 4.8: HEV FC performance in WLTC driving cycle

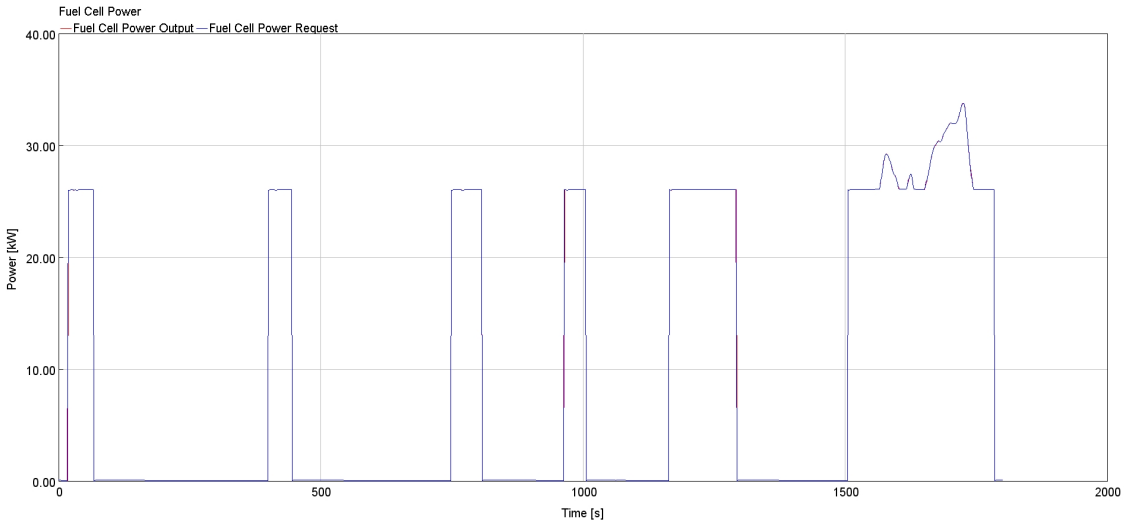

Figure 4.9: PHEV FC performance in WLTC driving cycle

Figure 4.10 and Figure 4.11 illustrate the voltage and current dynamics of fuel cell stack for HEV and PHEV under WLTC driving cycle. In general, the stack power output mainly follows the current output, and its output power increases when the current increases and the current increment will lead to the voltage drop of the stack. Figure 3.30 can explain this.

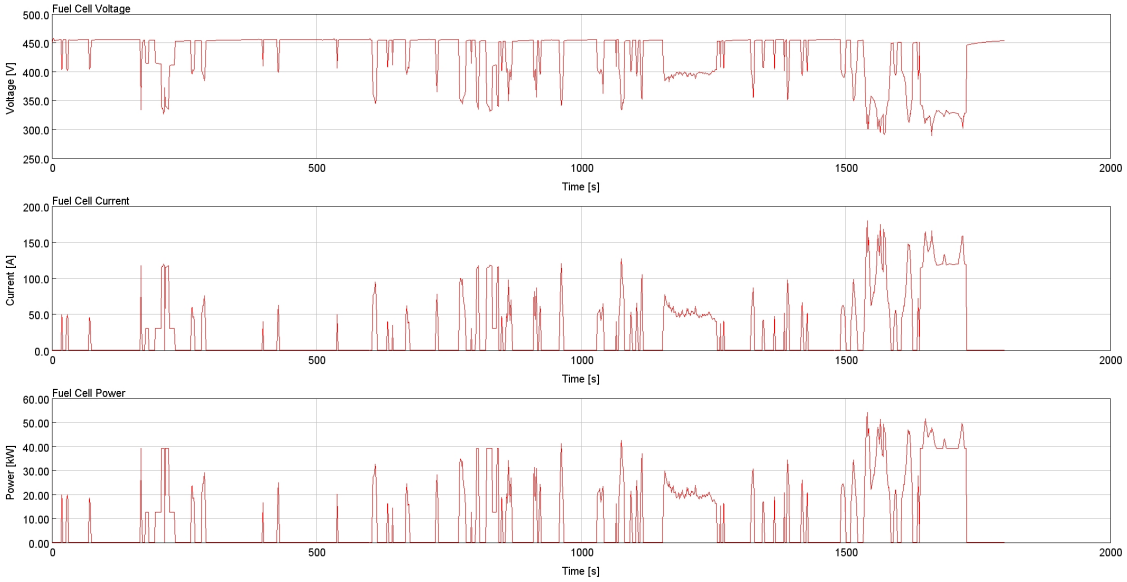

Figure 4.10: HEV FC voltage and current dynamics in WLTC driving cycle

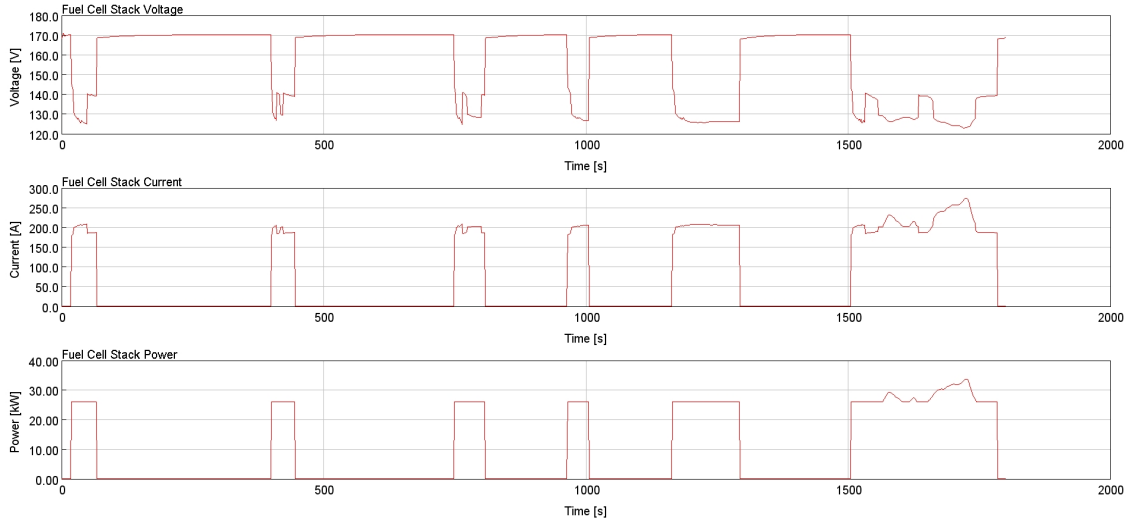

Figure 4.11: PHEV FC voltage and current dynamics in WLTC driving cycle

4.5 Fuel Cell-PHEV

As was noted in Fuel Cell Vehicle Modeling and Simulation Chapter before. For this Fuel Cell-PHEV, the maximum power for the fuel cell stack is 45 kW, the battery size is 9.2 kWh with the maximum power of 65 kW. The results for the main system models and energy management strategies are presented below.

4.5.1 Battery SOC level

The battery usable SOC window for this Fuel Cell-PHEV is from 20% to 95%. Two cases are studied with different initial battery SOC level. The first case simulates the situation that the customer drives the Fuel Cell-PHEV with some energy obtained from a plug-in source, where the initial battery SOC is 50%. The vehicle hydrogen consumption is 0.54 kg/100km in WLTC driving cycle, and the battery SOC trajectory is presented in Figure 4.12 below. The small fluctuation in the SOC trajectory is due to the absorbed regenerative power when the vehicle decelerates.

From report [40], which analyze the behavior of more than 12 000 XC90 T8 Plug-in hybrid customers worldwide. The average customer spends more time driving in sustain mode than in depletion mode. In addition, 56% of the time is spent driving with a battery SOC below 35% (the combustion engine can be used to charge the battery up to a SOC of 33%). The result could indicate that there are many customers that do not plug-in their vehicles which then increases the amount of time in the lowest SOC-interval [40].

The second case simulates that the driver starts driving the Fuel Cell-PHEV in lower SOC value, where the initial battery SOC is 30.2%. So that the vehicle quickly jumps into charge sustaining mode as is presented in Figure 4.13 below. The battery SOC

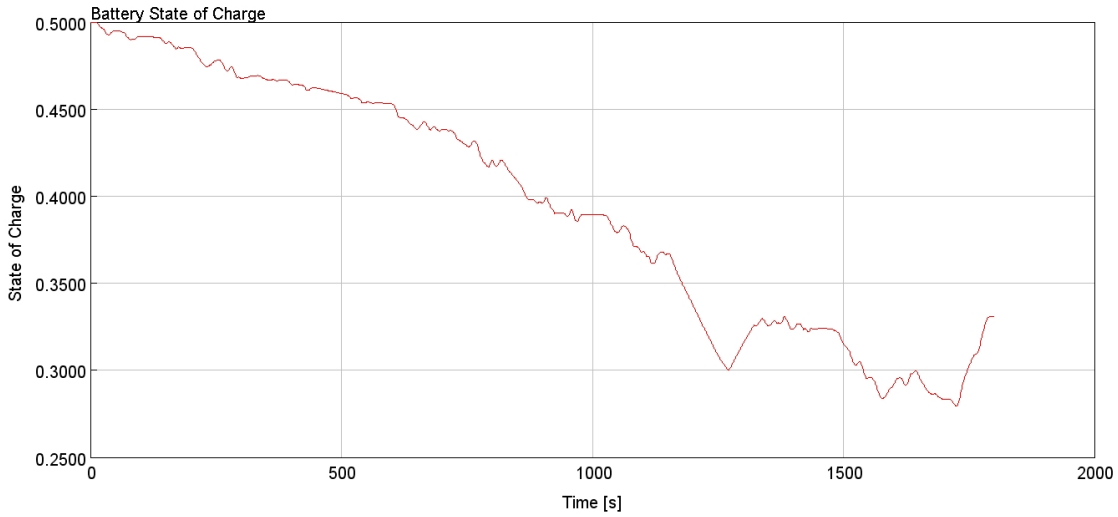

Figure 4.12: Case 1: The initial SOC value is 50%, WLTC driving cycle.

increases quickly at the end of the driving cycle. The reason is that the SOC is lower than the lower limit of charging trigger 30%, and the SOC difference reaches 2%. So that fuel cell charging power will be larger than the power which has maximum efficiency. The vehicle hydrogen consumption is 0.95 kg/100km in the second case in the WLTC driving cycle.

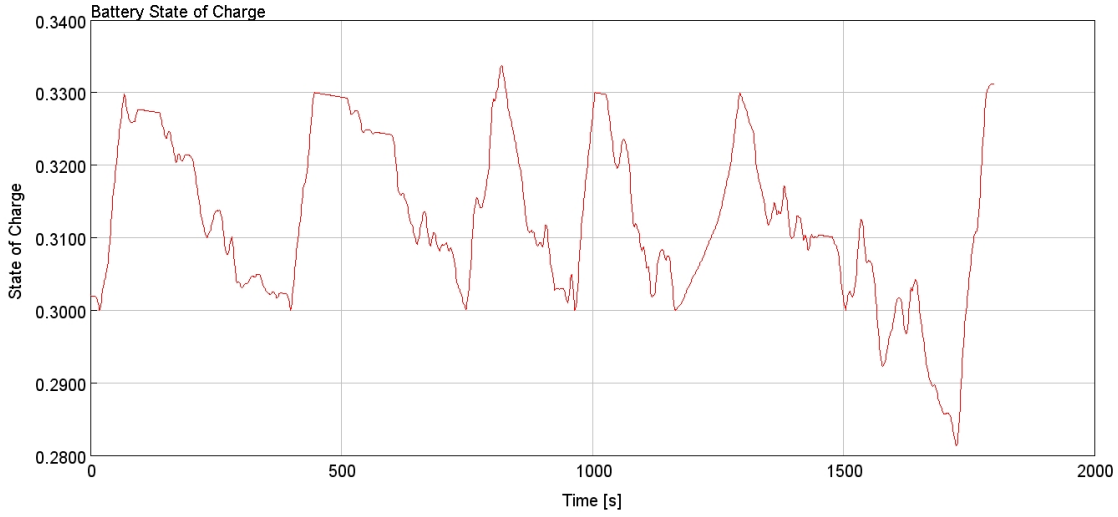

Figure 4.13: Case 2: The initial SOC value is 30.2%, WLTC driving cycle.

NEDC driving cycle, which is another official cycle, is also used to simulate the second case. The SOC trajectory is presented in Figure 4.14 below. The vehicle hydrogen consumption is 0.92 kg/100km in the second case in the NEDC driving cycle.

The result could indicate that vehicle hydrogen consumption depends on the driving condition or the driving cycles a lot. Compared with the NEDC driving cycle, hydrogen consumption has increased by 3.4% in the WLTC driving cycle With the

same initial battery SOC level and control strategy. The reason could be the higher average and maximum speed and accelerations in the WLTC driving cycle.

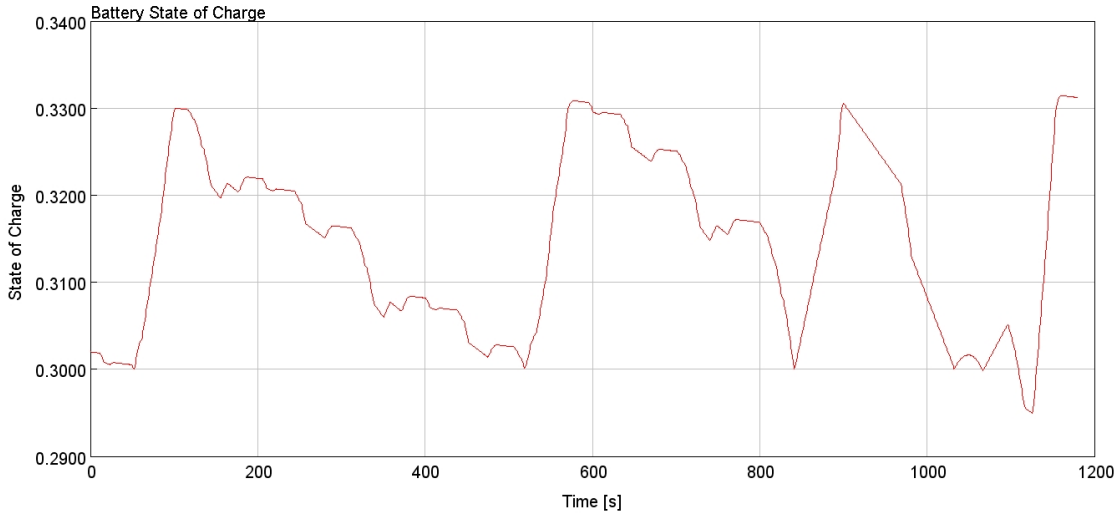

Figure 4.14: Case 2: The initial SOC value is 30.2%, NEDC driving cycle.

4.5.2 State Selection Controller Model

4.5.2.1 The Fuel Cell charging On-Off trigger

As shown in Figure 4.15, the operation of the vehicle in the WLTC driving cycle is analyzed as follows. At time 0, the battery SOC is 30.2%. After 16.97 s the SOC reaches the lower limit of the hysteresis controller and the system enters the charging mode in which the fuel cell starts to charge the battery. After 67.88 s, the SOC reaches the upper limit 33%, and the On-Off trigger for charging is off at that time step, which indicates the hysteresis controller follows the strategy well. Subsequent similar situations will not be described. The fuel cell system charging power will be analyzed in the Fuel Cell Control Unit section.

4.5.2.2 The Driving Mode and Electric Mode

To assess the functionality of the State Selection Controller for the Fuel Cell-PHEV, the Driving Mode and Electric Mode are analyzed. Figure 4.16 shows the dynamic response of the mode changes depending on the current vehicle speed, the traction power, vehicle acceleration, and the battery SOC level.

By observing the simulation results, the only difference between the Driving Mode and the Electric Mode is that the Electric Mode splits the electric driving mode into the more specific electric-tractive and electric-regeneration mode. At time 0, the Fuel Cell-PHEV is standstill the battery SOC is 30.2%, and the fuel cell stack remains idle. The Electric Mode is 0, which is standstill mode. After 10.91 s the vehicle starts to drive and the Electric Mode turns to 1, which is electric-tractive mode.

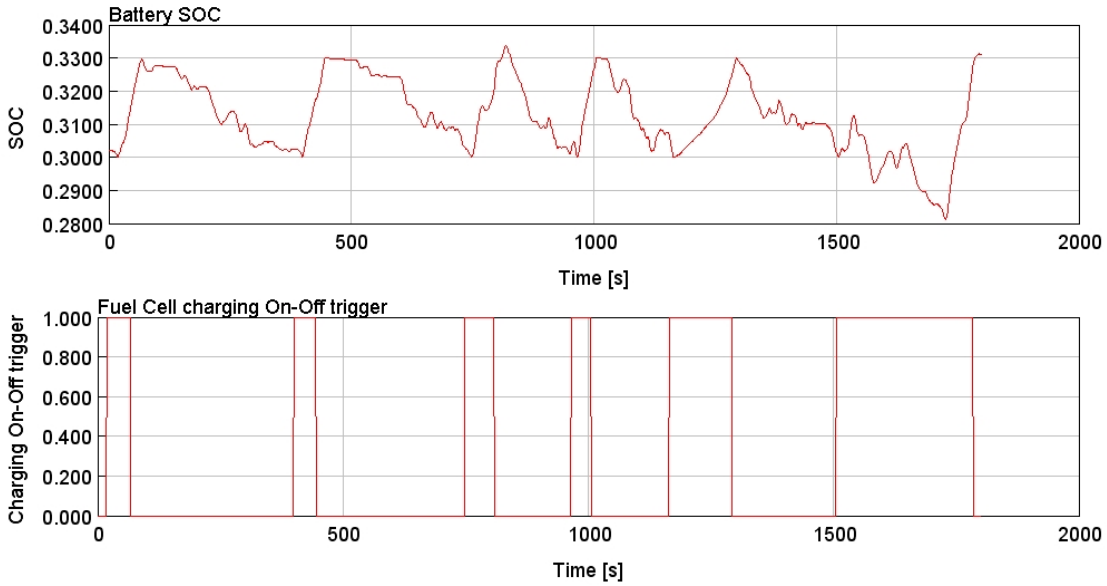

Figure 4.15: The Fuel Cell-PHEV charging On-Off trigger

At 16.97 s, the battery SOC reaches the lower limit, and the Electric Mode turns to 3, which is HEV-charging mode. At that time, the fuel cell starts to charge the battery and the SOC curve starts to go up. At the time period of 35.16 s to 55.76 s, the vehicle decelerates and the Electric Mode enters to 2, which is electric-regeneration mode. The battery will absorb the braking power while the HEV charging mode and the slope of the SOC curve become larger. At time of 66.67 s, the battery SOC reaches the upper limit and the range extender fuel cell system will be switched off, at the same time the Electric Mode switches from 3 HEV charging mode to 1 electric-tractive mode till 78.79 s.

Similar mode selection results also validated on the NEDC cycle in Figure 4.17. However, the modes shifting less than that in the WLTC driving cycle due to the more constant speed in the NEDC cycle. The simulation results from Figure 4.16 and Figure 4.17 indicate that the State Selection Controller function well and the Driving Mode and Electric Mode run in the right mode depends on the current vehicle speed, the traction power, vehicle acceleration, and the battery SOC level.

4.5.3 Fuel Cell Control Unit Model

The simulation result of the vehicle speed and power distribution for the Fuel Cell-PHEV is shown in Figure 4.18. During the test, all the traction power demand by the electric motor does not exceed the maximum battery power limitation, which is 65 kW. Therefore all the traction power will be provided by the battery if the SOC level is above the lower SOC threshold. When the vehicle decelerates, the battery will absorb the braking power. As presented in the battery power and fuel cell system power figure, the negative power means charging, it is clear to see that the fuel cell system will continue charging when regenerative braking to avoid the

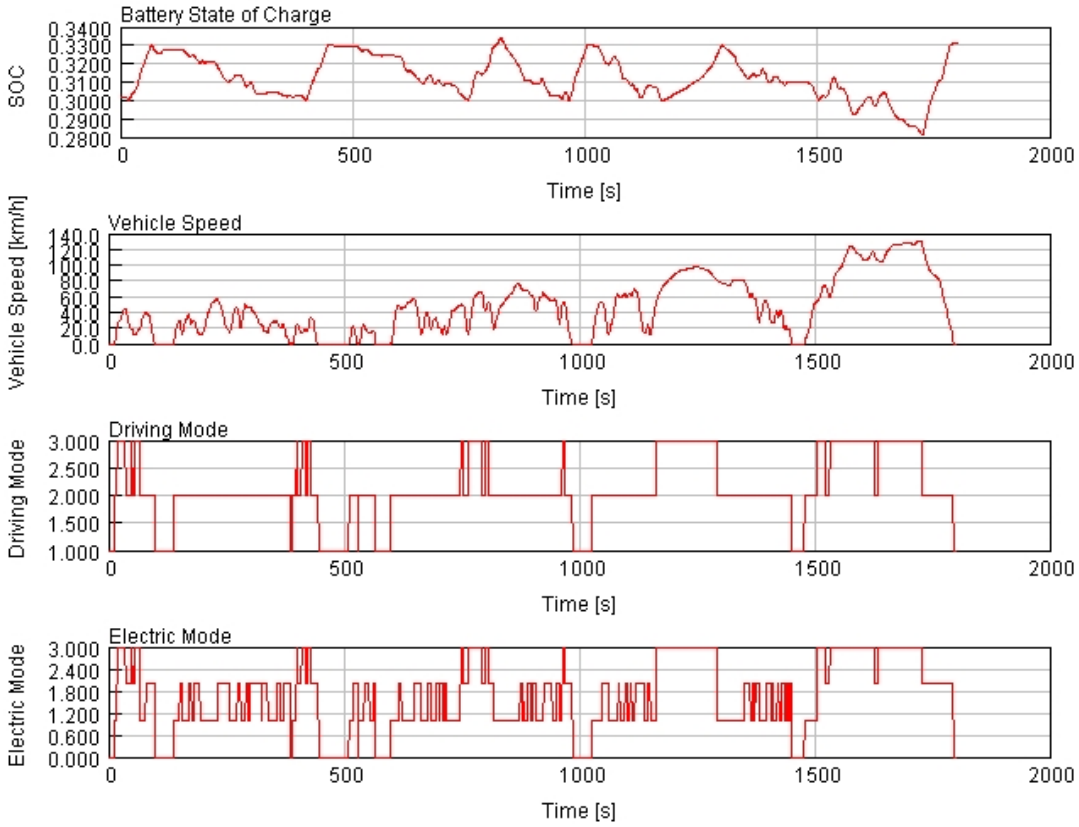

Figure 4.16: The Driving Mode and Electric Mode in State Selection Controller with WLTC driving cycle for the Fuel Cell-PHEV in case two.

fuel cell system frequently turning on-and-off in order to slow down the degradation of the fuel cell to extend the working life.

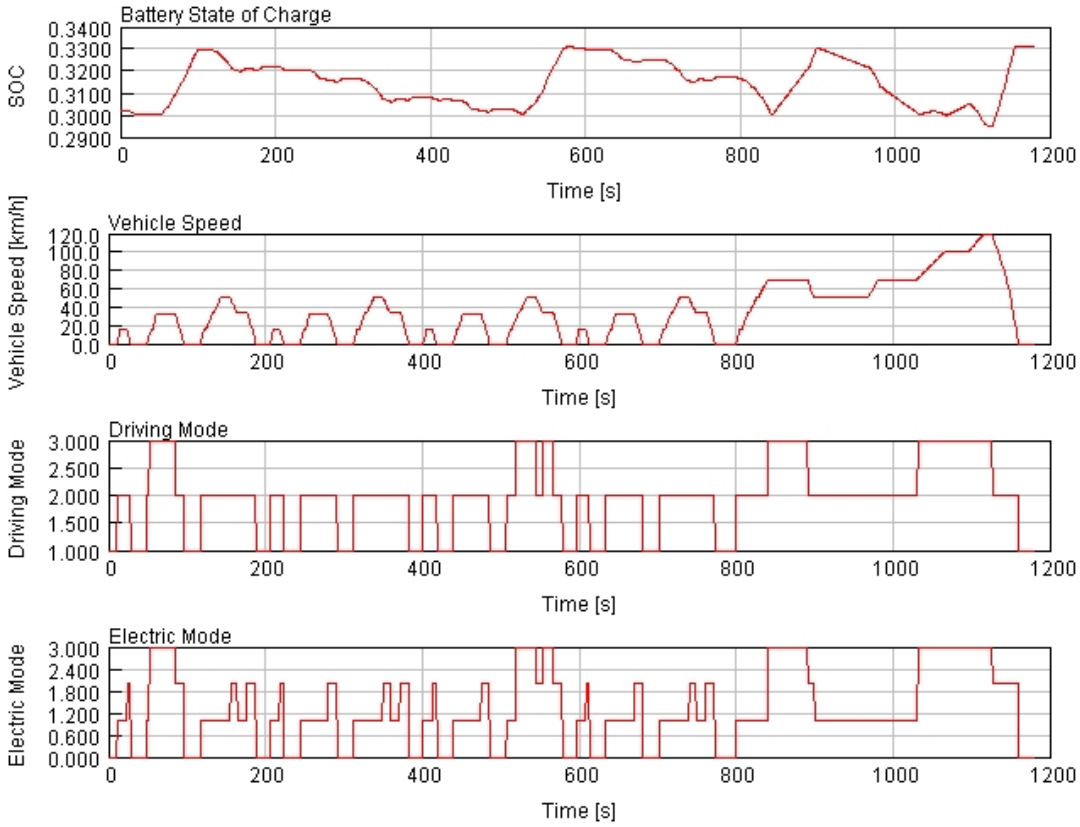

Figure 4.17: The Driving Mode and Electric Mode in State Selection Controller with NEDC driving cycle for the Fuel Cell-PHEV in case two.

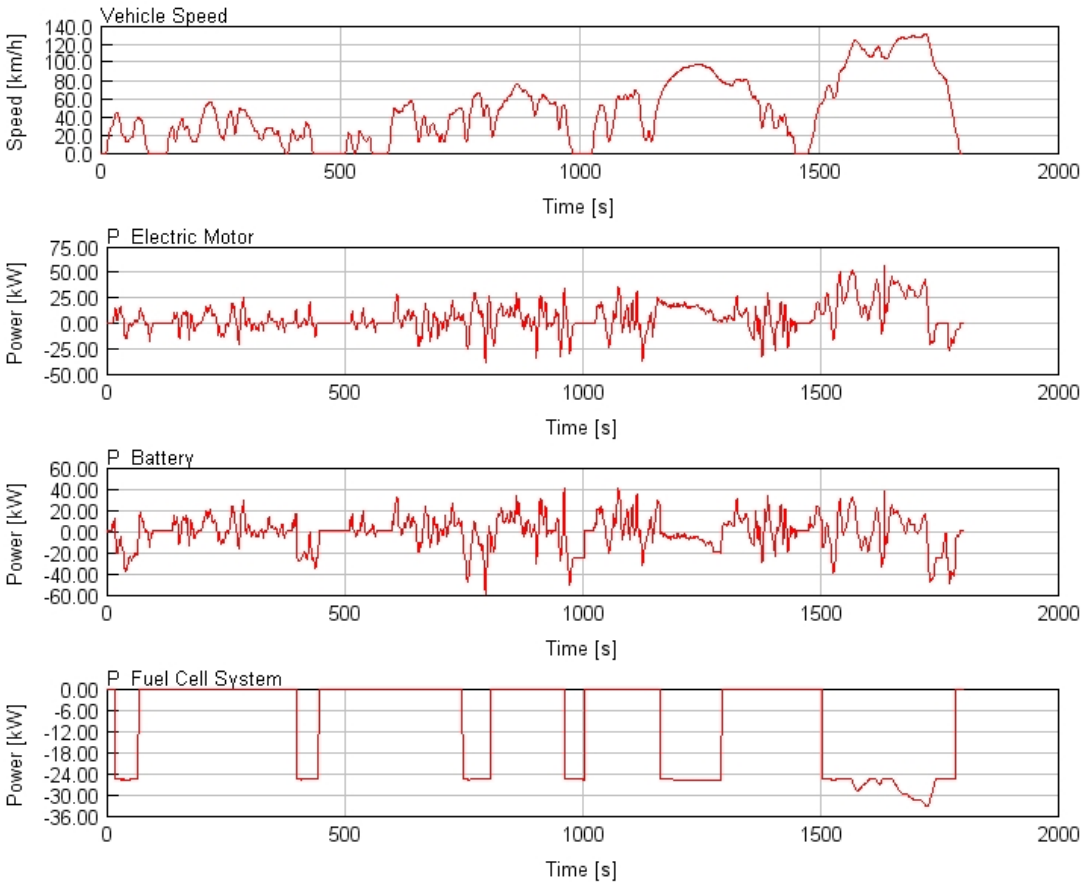

Figure 4.18: Vehicle speed and power distribution for Fuel Cell-PHEV.

More detailed battery power and fuel cell distribution results can be found in Figure 4.19. The red line represents battery power and the blue line represents fuel cell system power. The power request is provided primarily by the battery, and the fuel cell works as an auxiliary power source or as a range extender. For example at the time from 16.97 s to 67.88 s, the fuel cell starts working as a range extender and charges the battery at its most efficient operating point, which is 25 kW. During the same time period, the vehicle is decelerating, so that part of the negative charging power for the battery is smaller than -25 kW. At the time from 1164.9 s to 1290.9 s, the fuel cell starts working as a range extender again, and the negative charging power for the battery is from -2.2 kW to -19.9 kW. That is because part of the fuel cell power will be used as traction power; the rest will flow to charge the battery. At the time from 1652.1 s to 1749.1 s, the fuel cell operates away from the most efficient point, and the power varies from 25 kW to 33.2 kW. The reason is the low SOC level and the extra high speed at the end of the WLTC cycle as shown in Figure 4.18.

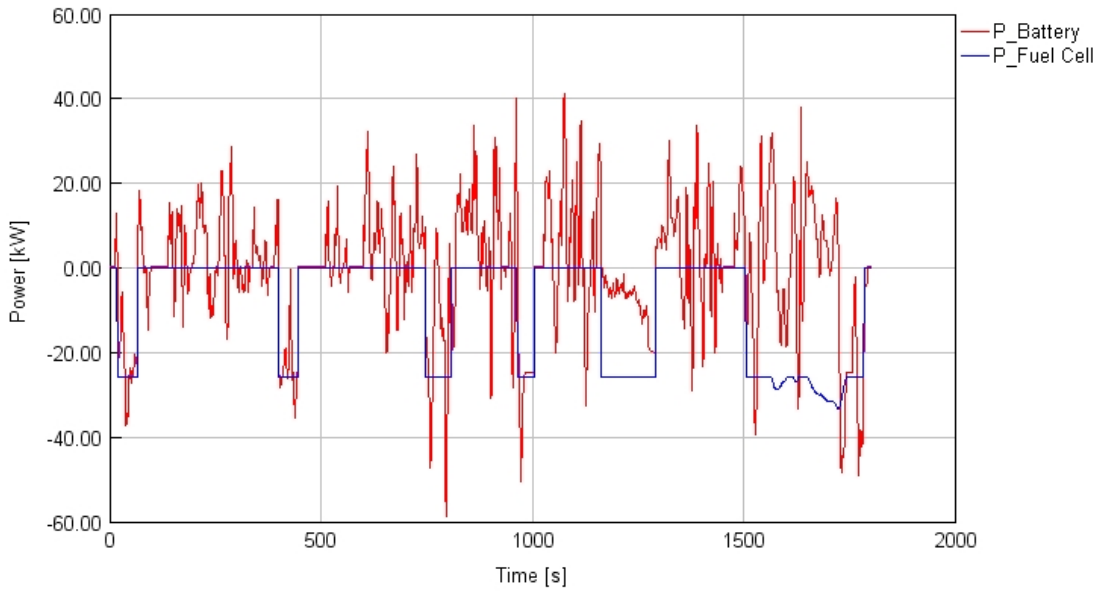

Figure 4.19: Battery power and fuel cell stack power for the Fuel Cell-PHEV.

4.6 Fuel Cell-HEV

As was noted in Fuel Cell Vehicle Modeling and Simulation Chapter before, for this Fuel Cell-HEV, the PEM fuel cell system works as the main power source and the battery works as an auxiliary power source to handle transient conditions. The maximum power for the fuel cell stack is 100 kW, the battery size is 1.8 kWh with the maximum power of 50 kW. The results for the main system models and energy management strategies are presented below.

4.6.1 Battery SOC level

The battery SOC window for this Fuel Cell-HEV is from 30% to 70%, which leaves some margin for start-up and regenerative braking. The battery SOC trajectory is presented in Figure 4.20 below. Due to the smaller battery size compared with the PHEV battery, the SOC drops down and goes up quickly. The initial SOC is 70%, and at the end of the driving cycle, the SOC reaches almost the same value as initial. The vehicle hydrogen consumption is 0.82 kg/100km in WLTC driving cycle.

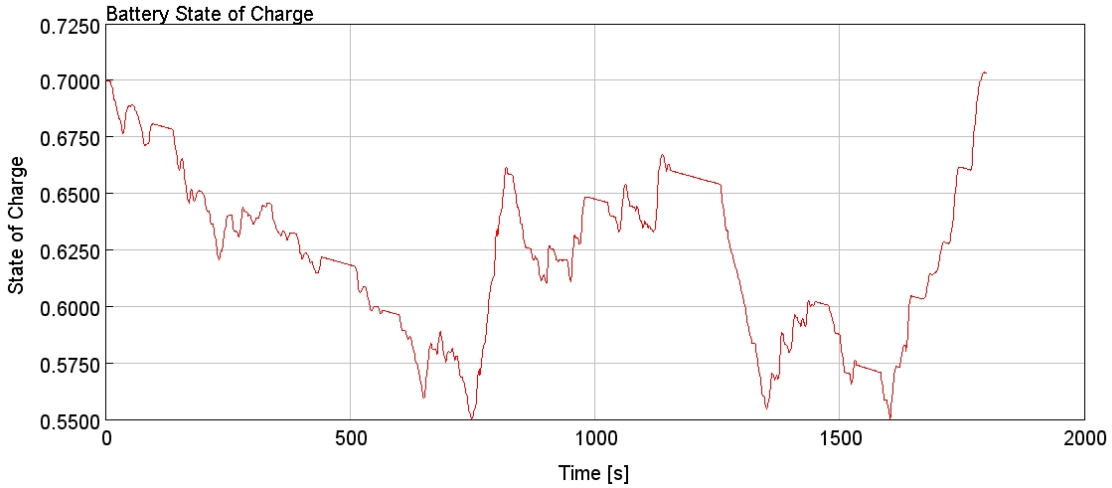

Figure 4.20: The initial SOC value is 70%, WLTC driving cycle.

The NEDC driving cycle is also used to simulate the Fuel Cell-HEV. The SOC trajectory is presented in Figure 4.21 below. As shown in the figure, the SOC level increases quickly and goes beyond 70% and goes into the margin area leaving for unexpected large regenerative braking at the end, therefore, all the braking energy can be collected. The vehicle hydrogen consumption is 0.72 kg/100km in the NEDC driving cycle. The hydrogen consumption in NEDC driving cycle reduces 12.2% compared with WLTC driving cycle due to the lower average speed and maximum speed.

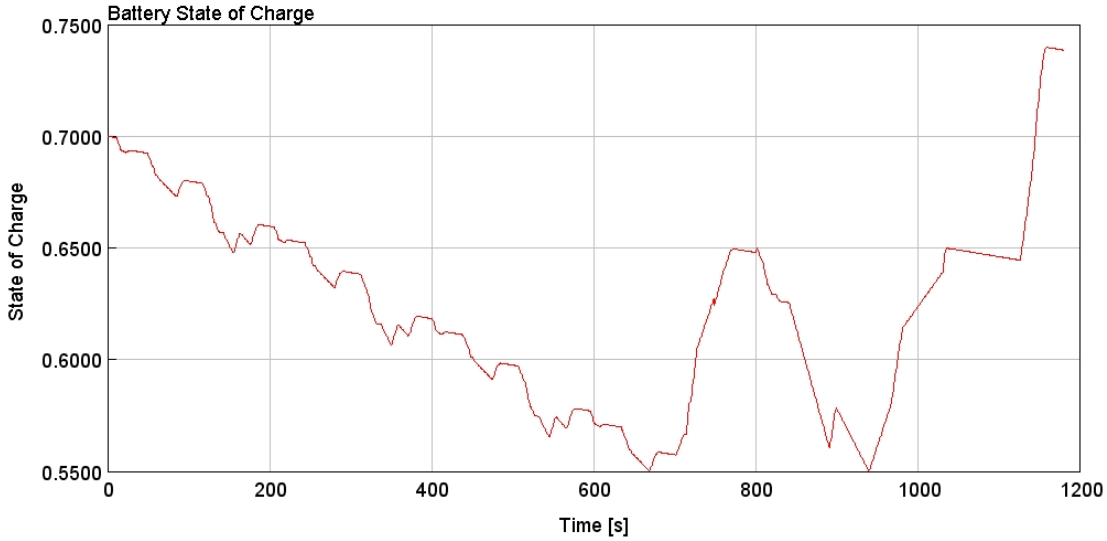

Figure 4.21: The initial SOC value is 70%, NEDC driving cycle.

4.6.2 State Selection Controller Model

4.6.2.1 The Fuel Cell charging On-Off trigger

As presented in Figure 4.22, the operation of the vehicle in the WLTC driving cycle is analyzed as follows. At time 0, the initial battery SOC is 70%. After 745.46 s the SOC reaches the lower boundary and the Fuel Cell System starts charging the battery until 814.55 s. The same situation also happens from 1601.22 s to 1736.97 s.

In Figure 4.23 below, the fuel cell power output can be studied. When the fuel cell active charging trigger is on, as shown from 745.46 s to 814.55 s and 1601.22 s to 1736.97 s. The fuel cell system power output line is nearly flat, which is one of the optimal operating points 38 kW as noted in the Fuel Cell-HEV control strategy chapter. The rest fuel cell power output is due to the vehicle running in the fuel cell-only mode, which follows the control strategy well.

4.6.2.2 The Driving Mode and Electric Mode

To assess the functionality of the State Selection Controller for the Fuel Cell-HEV, the Driving Mode and Electric Mode are analyzed. Figure 4.24 shows the dynamic response of the mode changes depending on the current vehicle speed, the traction power, vehicle acceleration, and the battery SOC level.

By observing the simulation results, compared with the results in Fuel Cell-PHEV, the chance running in Electric Mode 4 increase dramatically, which is the fuel cell-only mode, because the fuel cell works as the main power source in Fuel Cell-HEV. When the vehicle speed is 0: from 0 s to 10.91 s, 100.61 s to 136.97 s, 387.88 s to 390.31 s, 446.07 s to 510.31 s, 567.28 s to 600.01 s, 987.88 s to 1023.04 s and 1453.34

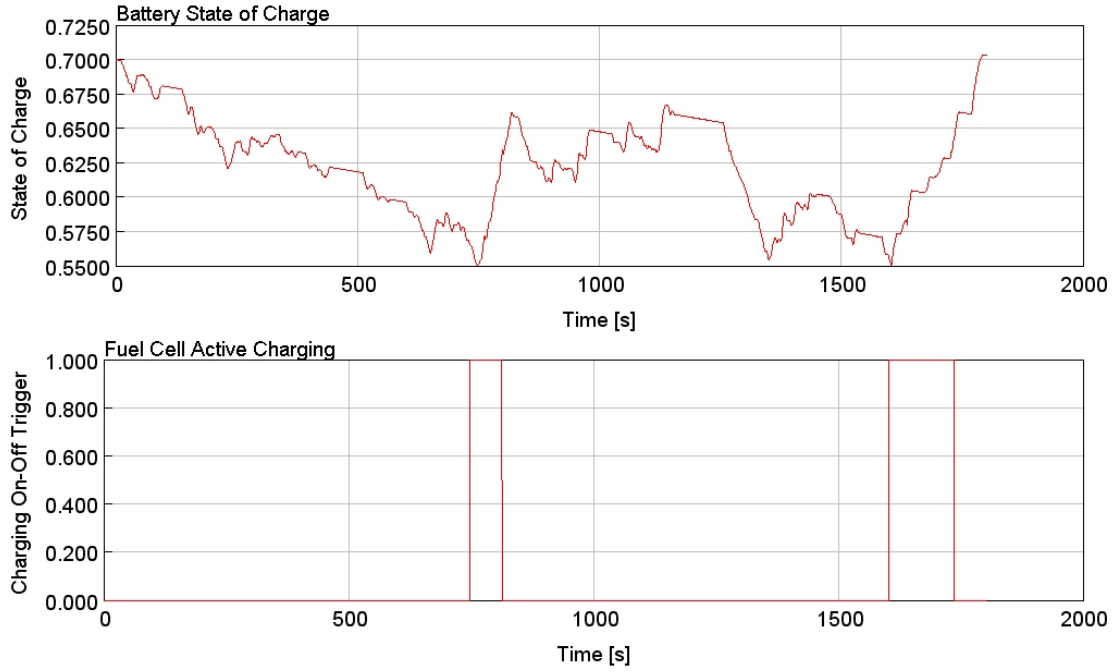

Figure 4.22: The Fuel Cell-HEV active charging On-Off trigger.

s to 1475.16 s the vehicle is in standstill mode which is Driving Mode 1 or Electric Mode 0. In the time period from 745.46 s to 808.49 s and from 1603.64 s to 1727.28 s the vehicle runs in HEV mode which is Electric Mode 3. During this mode, both the fuel cell system and the battery are working. Either the fuel cell is charging the battery, or the battery is assisting the fuel cell, therefore, the fuel cell stack can run on the optimal operating points. When vehicle starting or the traction power is low, the vehicle will run in battery-electric mode, which is Electric Mode 1. When the vehicle decelerates for example from 77.58 s to 100.61 s, the vehicle will run in Electric Mode 2.

Similar mode selection results have also been validated on the NEDC cycle in Figure 4.25. However, the modes shifting occurs less than in the WLTC driving cycle due to the more constant speed in the NEDC cycle. The vehicle will run less time on Electric Mode 4, which is fuel cell-only mode. However, it will run more time on Electric Mode 1, which is battery-electric mode. Because of the lower power demand compared with the WLTC cycle. After the SOC level reaches the lower limit, the Electric Mode shifts to 3 immediately as shown from 940.03 s to 1034.57 s.

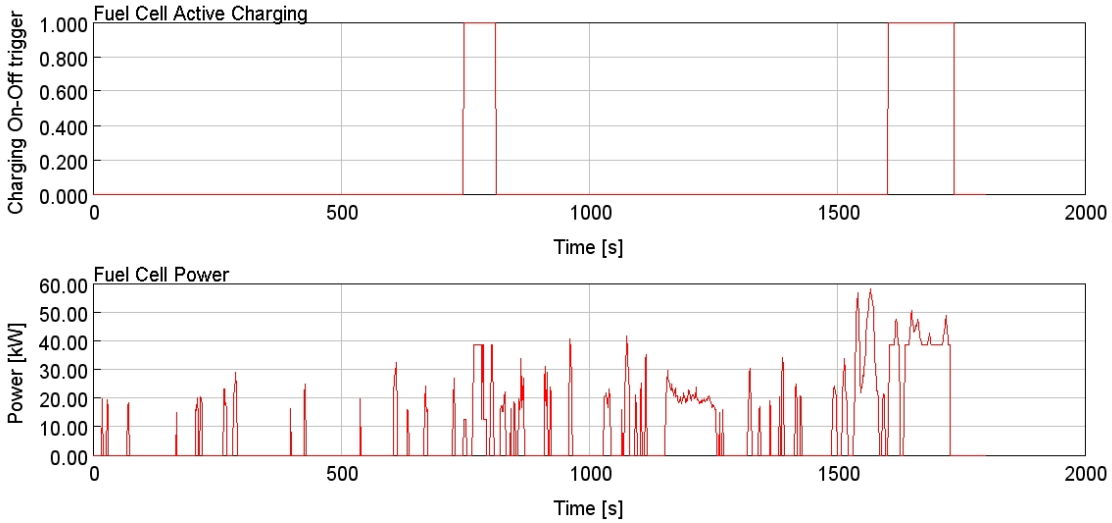

Figure 4.23: The Fuel Cell power output for the Fuel Cell-HEV.

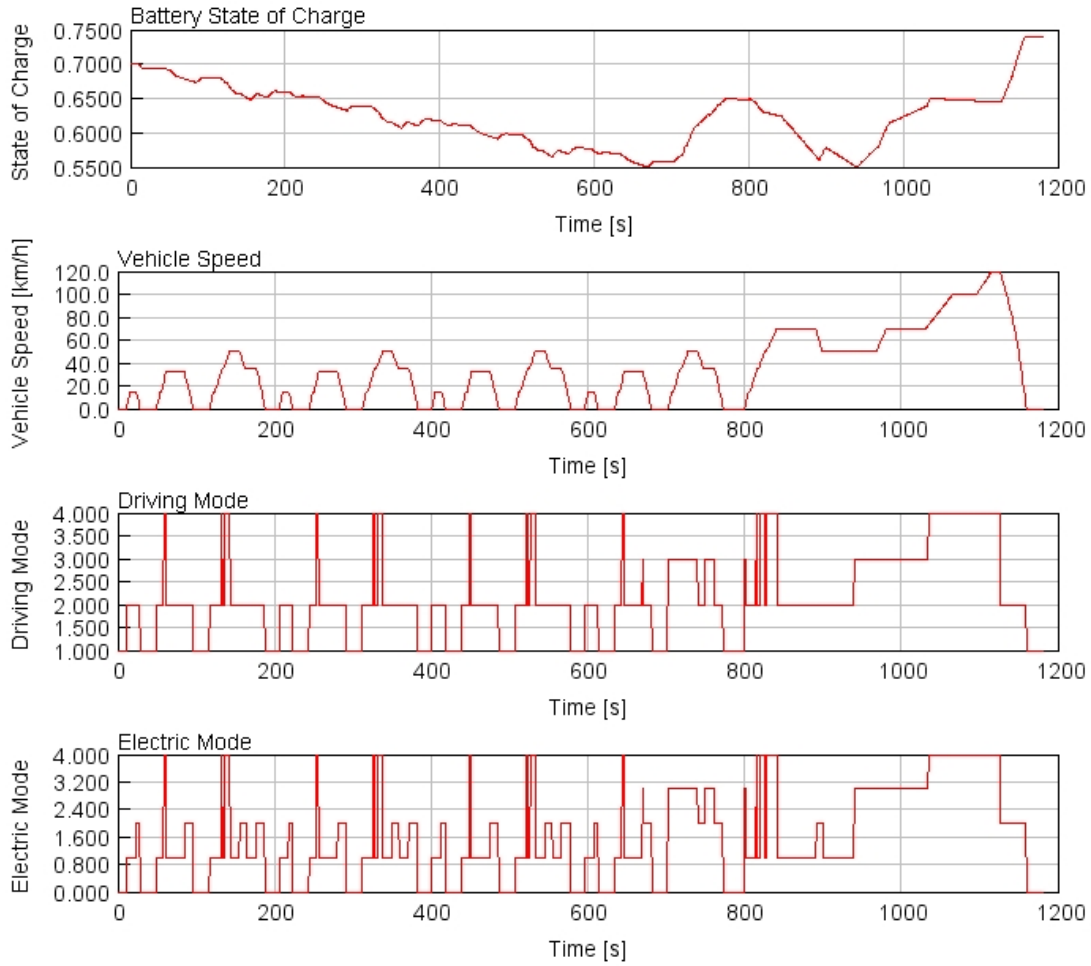

Figure 4.25: The Driving Mode and Electric Mode in State Selection Controller with NEDC driving cycle for the Fuel Cell-HEV.

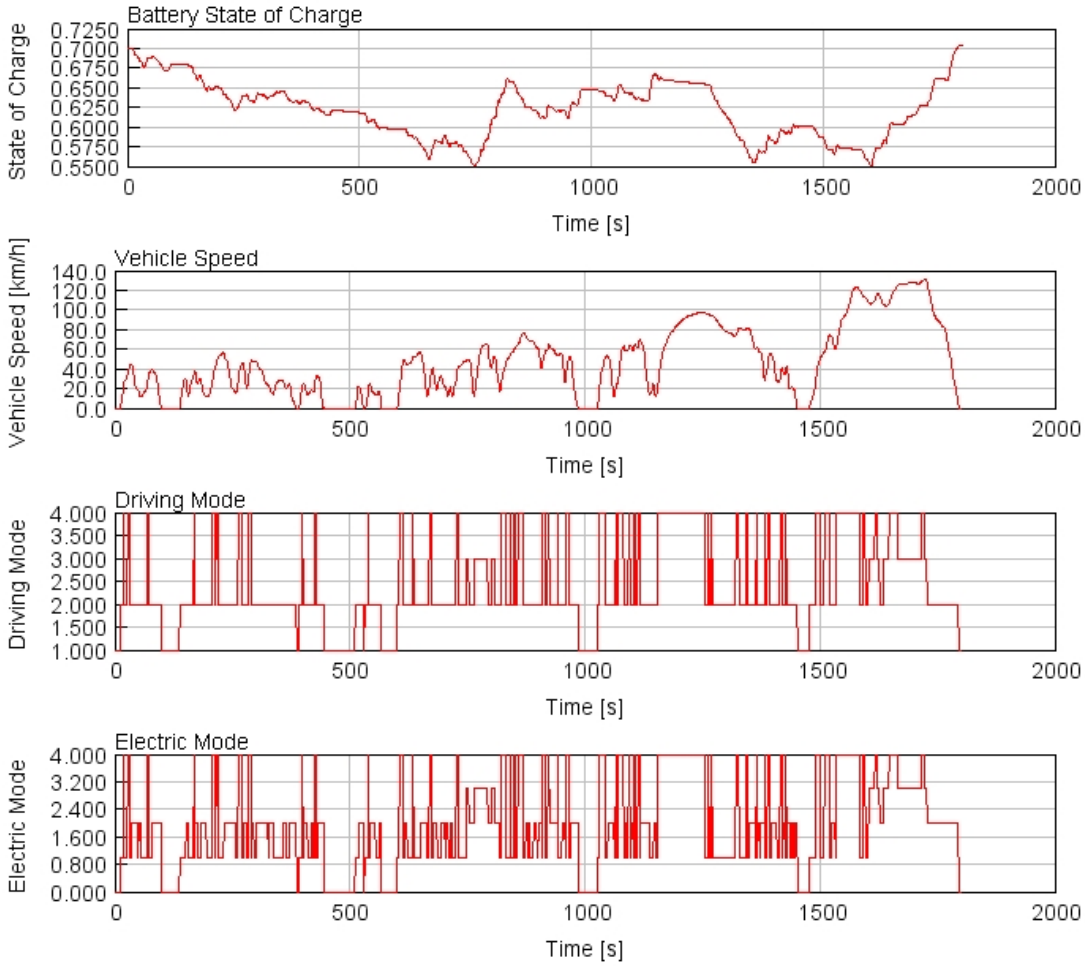

Figure 4.24: The Driving Mode and Electric Mode in State Selection Controller with WLTC driving cycle for the Fuel Cell-HEV.

4.6.3 Fuel Cell Control Unit Model

The simulation result of the vehicle speed and power distribution for the Fuel Cell-HEV is shown in Figure 4.26. During the test, as shown in the battery power line, the positive battery traction power is lower compared with that for the Fuel Cell-PHEV. All the battery traction power is around 10 kW, which mainly for vehicle starting and when in low-speed driving. If the power demand beyond a certain level, then the fuel cell will cover the rest of the power request. When the battery power is negative, most of them concentrate in the region from 0 kW to 20 kW due to the regenerative braking and fuel cell charging.

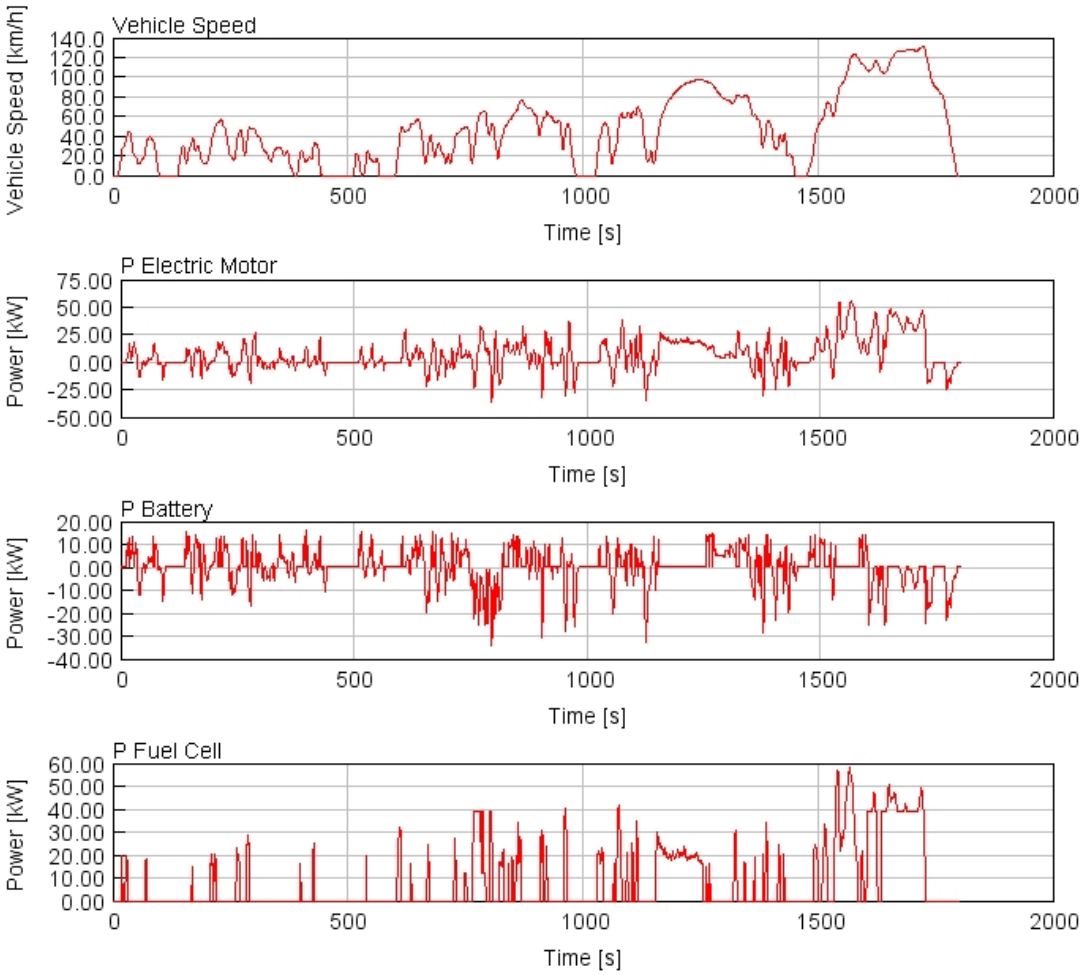

Figure 4.26: Vehicle speed and power distribution for Fuel Cell-HEV.

More detailed battery power and fuel cell distribution results can be found in Figure 4.27. When the traction power is lower than 12 kW, and the battery SOC is higher than a certain level, the battery will provide all the traction power, and the fuel cell will remain idle. For example, from 0 s to 16.97 s, the vehicle starts driving and the power demand is low at that time. Therefore the battery will cover all the power request. However after 16.97 s, the fuel cell system will cover all the traction power and meanwhile, the battery SOC is detected to see whether the fuel cell should run in one optimal operating point and part of the power flows to charge the battery or provide exactly the power requested from the wheel. As shown from 753.94 s to 808.49 s, the fuel cell system runs either at low optimal point 12 kW or medium optimal operating point 38 kW. At that time the battery power is negative which means it is being charged. From 1153.94 s to 1253.34 s, the vehicle is driven by fuel cell only. The power from the fuel cell stack perfectly follows the power changes requested by the wheel. The battery only provides 0.4 kW, which is set as auxiliary power for the AC or the car display system.

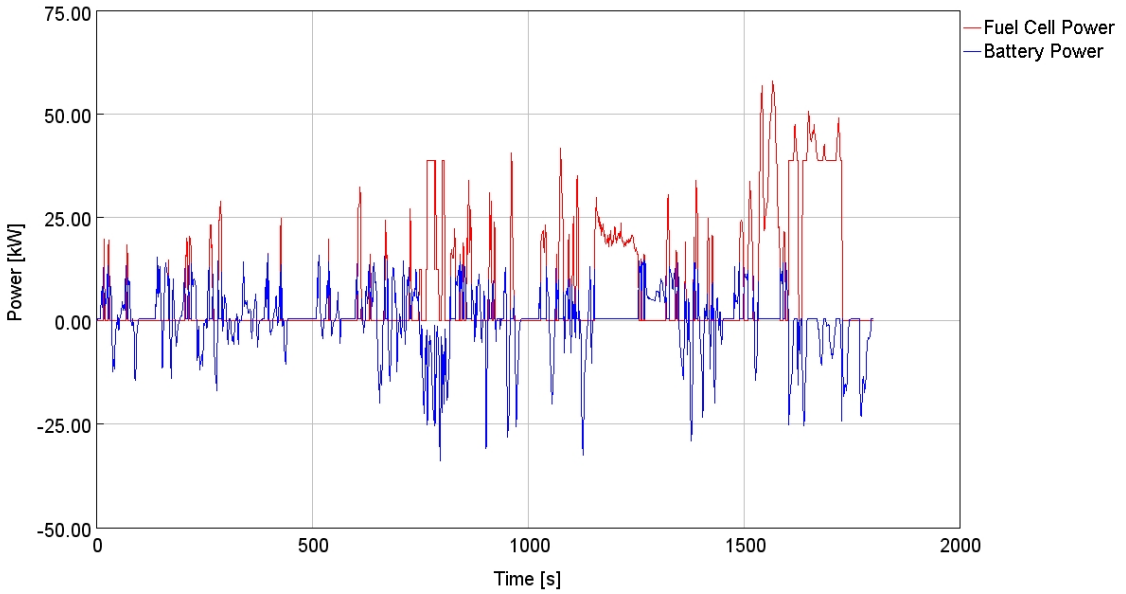

Figure 4.27: Battery power and fuel cell stack power for the Fuel Cell-HEV in WLTC cycle.

Similar results have also validated on the NEDC cycle shown in Figure 4.28 below. However, in the NEDC driving cycle, the vehicle can run more in battery traction mode compared with that in the WLTC cycle as shown from initial to 648.41 s, which simulates the city driving.

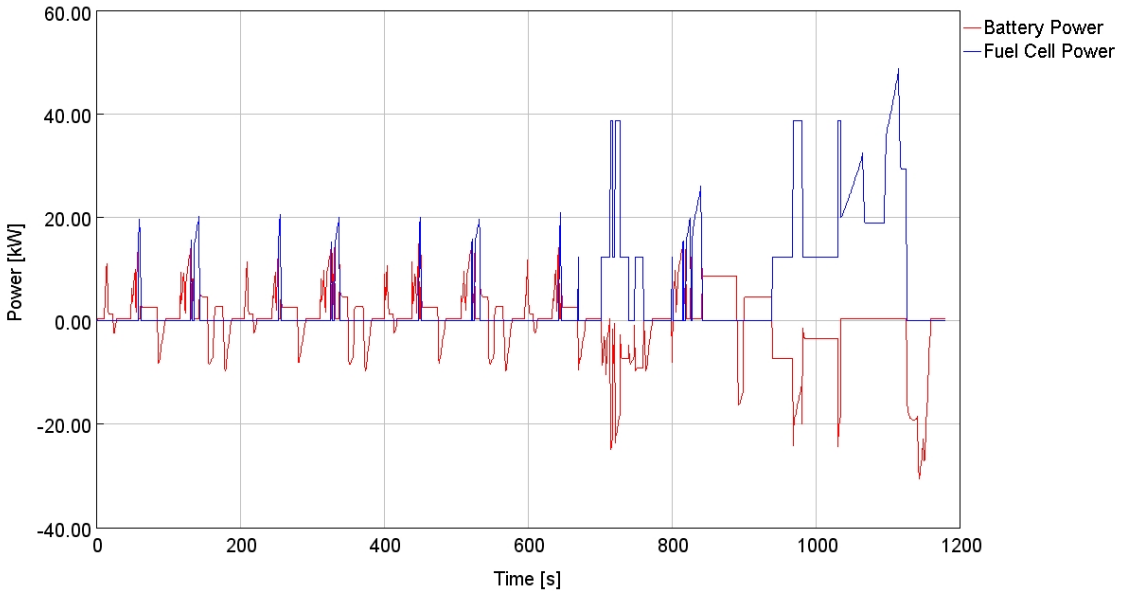

Figure 4.28: Battery power and fuel cell stack power for the Fuel Cell-HEV in NEDC cycle.

4.7 Hydrogen Consumption Comparison

In this section, both the Fuel Cell-HEV and Fuel Cell-PHEV with their energy management control strategies are tested under specific driving conditions, and the hydrogen consumption is compared.

Longer driving cycles are used as presented in Figure 4.29 below:

The first figure shows running WLTC 5 times consecutively, which lasts for 9000 seconds with a total distance of 116.33 km. The second figure shows running NEDC 5 times consecutively, which lasts for 5900 seconds with a total distance of 55.12 km.

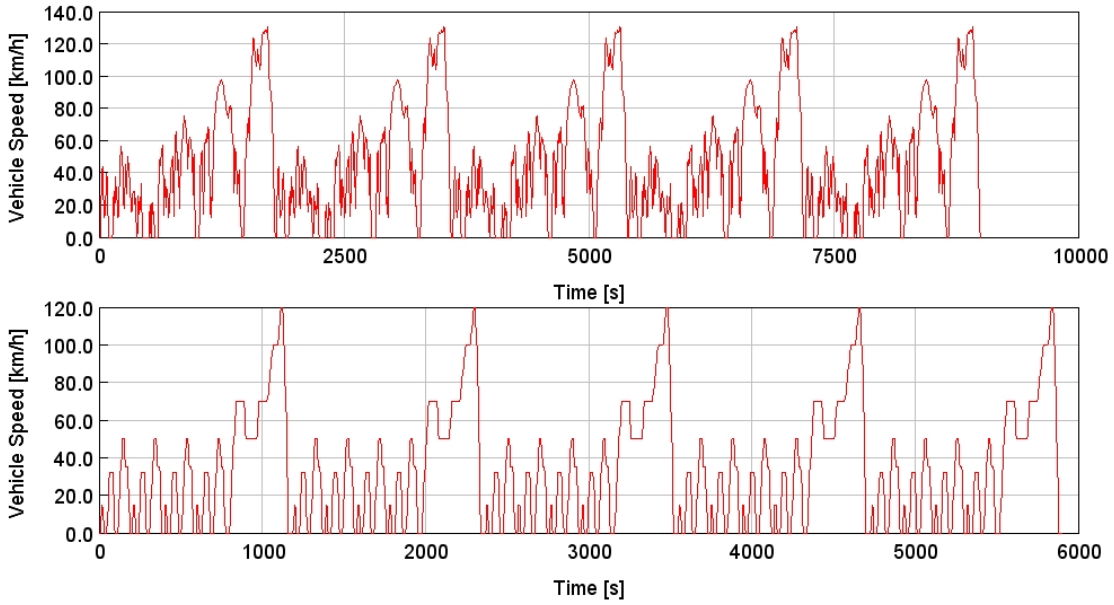

Figure 4.29: Running WLTC and NEDC 5 times consecutively.

4.8 Hydrogen Consumption for the Fuel Cell-PHEV

Firstly, the initial value of the battery SOC for the Fuel Cell-PHEV is set to be 95%, which is the upper limit of the usable SOC window.

The hydrogen consumption for the Fuel Cell-PHEV running WLTC 5 times consecutively is 0.61 kg/100 km, and the battery SOC trajectory is shown in Figure 4.30 below.

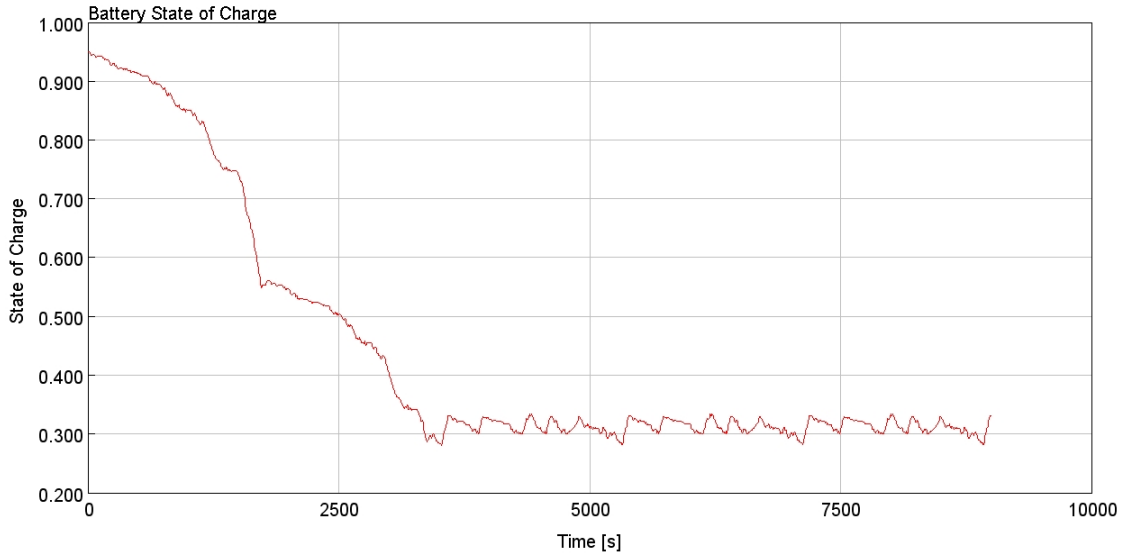

Figure 4.30: Battery SOC trajectory for the Fuel Cell-PHEV driving WLTC 5 times consecutively with initial SOC 95%.

The hydrogen consumption for the Fuel Cell-PHEV running NEDC 5 times consecutively is 0.18 kg/100 km and the battery SOC trajectory is shown in Figure 4.31 below.

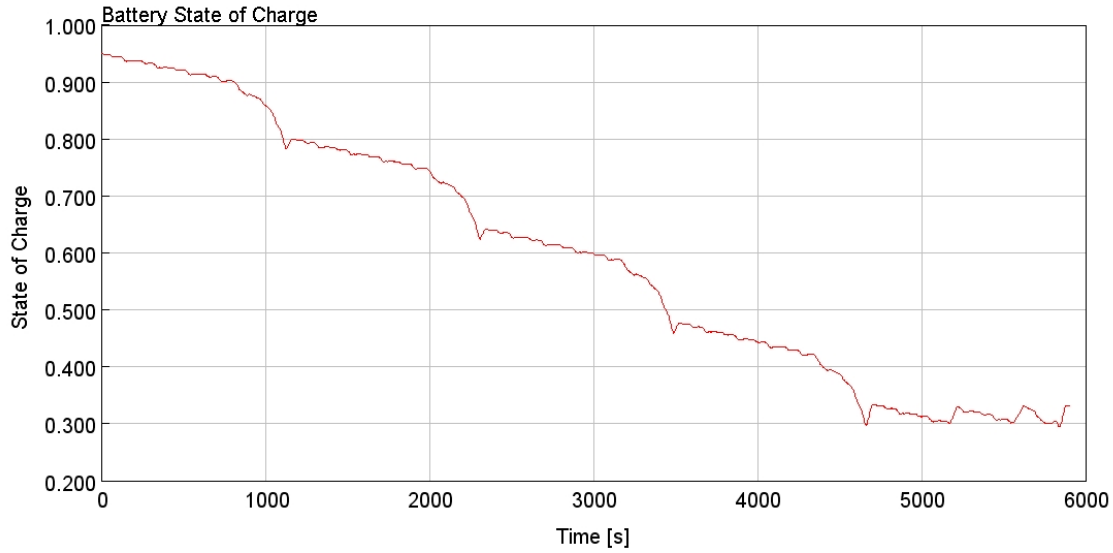

Figure 4.31: Battery SOC trajectory for the Fuel Cell-PHEV driving NEDC 5 times consecutively with initial SOC 95%.

However, if the charge sustaining mode is kept from the beginning of the driving cycle, and the SOC value at the end of the cycle is almost the same with the value at the beginning, which is SOC neutral. The hydrogen consumption for running WLTC 5 times consecutively will increase to 0.89 kg/100 km, which increases 45.9% compared with the hydrogen consumption when the battery is fully charged. The

battery SOC trajectory is plotted in Figure 4.32 below.

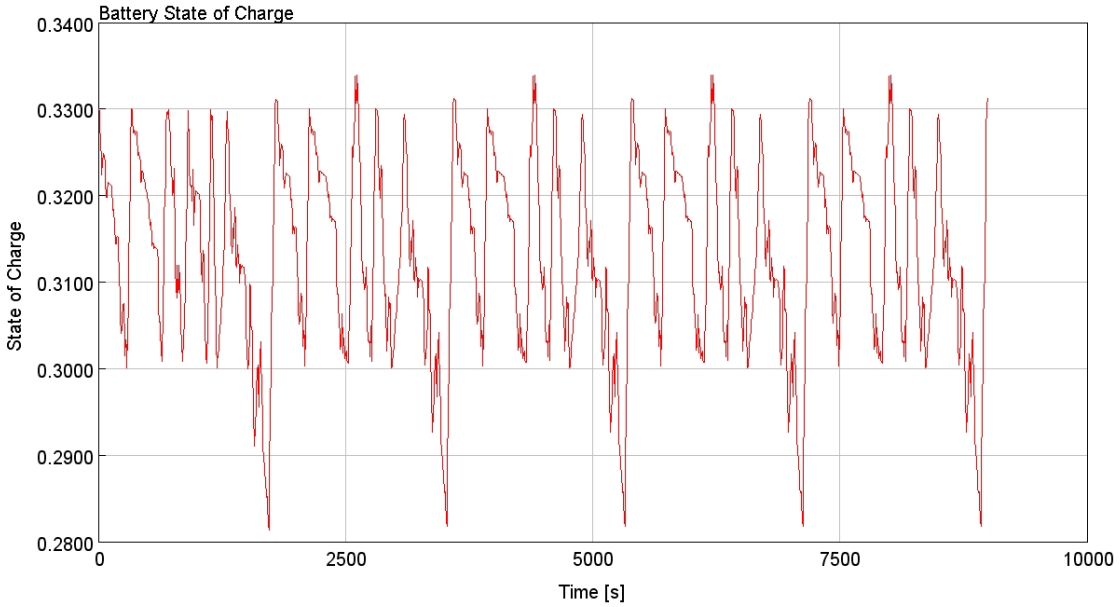

Figure 4.32: Battery SOC trajectory for the Fuel Cell-PHEV driving WLTC 5 times consecutively with initial SOC 33%.

Similarly, the hydrogen consumption for running NEDC 5 times consecutively will increase to 0.78 kg/100 km and the battery SOC trajectory is plotted in Figure 4.33 below.

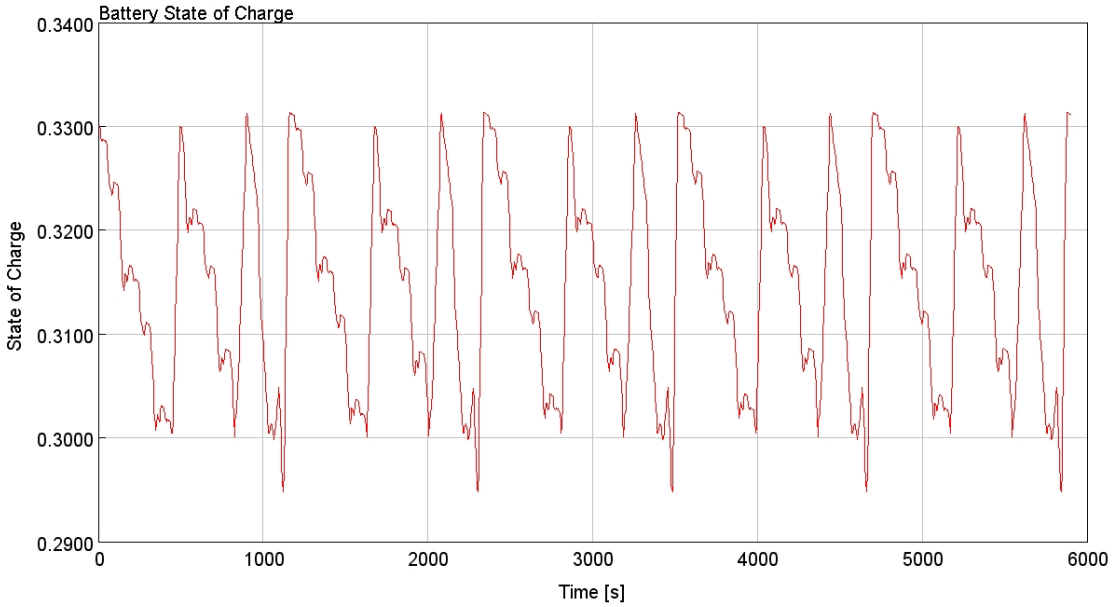

Figure 4.33: Battery SOC trajectory for the Fuel Cell-PHEV driving NEDC 5 times consecutively with initial SOC 33%.

The current procedure for the determination of fuel consumption specifically for PHEVs in Europe is described in the United Nations Economic Commission for Europe (UN-ECE) Regulation R101 [53].

As presented above a PHEV can drive in two operating modes, which are Charge-Depleting (CD) mode and charge-sustaining (CS) mode. There is no discrete point in time when the vehicle decides to transition from CD to CS mode, but the test procedure provides for a calculation to estimate that point. The PHEV test procedure measures separate fuel and electricity consumption values for both of these operation modes and combines them into one weighted average fuel consumption for the final test result [53].

Combining the results for CD and CS mode, a weighted fuel consumption result, C, can be calculated according to the following formula:

$$C = \frac{D_e * C_1 + D_{av} * C_2}{D_e + D_{av}} \tag{4.1}$$

Where:
C = fuel consumption in liters per 100 kilometers,
C_1 = fuel consumption in liters per 100 kilometers in CD mode,
C_2 = fuel consumption in liters per 100 kilometers in CS mode,
D_e = electric range of the vehicle, and
D_{av} = 25 km (average distance driven in CS mode, assumed by UN-ECE R101).

For the C_1, the hydrogen consumption in CD mode is 0 kg/100 km. For the C_2, the hydrogen consumption in CS mode is 0.89 kg/100 km for WLTC and 0.78 kg/100 km for NEDC as shown above. For the D_e, as shown in Figure 4.30 and Figure 4.31, the battery SOC will reach the lower boundary after 3364 seconds and 4664 seconds for the WLTC and NEDC respectively. Corresponding to 39.7 km for the WLTC and 43.4 km for the NEDC. Which means the electric range D_e in WLTC is 39.7 km and in NEDC is 43.4 km. D_{av} is the weighting factor for the current CS test, which is 25 km.

So that the Fuel Cell-PHEV combined hydrogen consumption can be calculated as:

$$C_{WLTC} = \frac{39.7 * 0 + 25 * 0.89}{39.7 + 25} = 0.34 \tag{4.2}$$

and for NEDC,

$$C_{NEDC} = \frac{43.4 * 0 + 25 * 0.78}{43.4 + 25} = 0.29 \tag{4.3}$$

In Table 4.1, one can see the hydrogen consumption for the modeled Fuel Cell-PHEV in different driving cycles and scenarios. With the same driving cycle, for

example running WLTC 5 times consecutively, the hydrogen consumption will increase 45.9% from 0.61 kg/100 km to 0.89 kg/100 km if the initial battery SOC changes from 95% to 33%. With the same initial battery SOC, for example, 33%, the hydrogen consumption will decrease 12.4% from 0.89 kg/100 km to 0.78 kg/100 km if the driving cycle changes from running WLTC 5 times consecutively to running 5 times consecutively. The result indicates that for the Fuel Cell-PHEV, the hydrogen consumption is largely determined by the initial battery SOC level and the driving conditions have less impact on hydrogen consumption.

Table 4.1: The Hydrogen consumption for the Fuel Cell-PHEV in different driving cycles and scenarios.

Vehicle Model	Hydrogen Consumption
Fuel Cell-PHEV (WLTC 5 times, initial SOC 95%)	0.61 kg/100 km
Fuel Cell-PHEV (WLTC 5 times, initial SOC 33%)	0.89 kg/100 km
Fuel Cell-PHEV (NEDC 5 times, initial SOC 95%)	0.18 kg/100 km
Fuel Cell-PHEV (NEDC 5 times, initial SOC 33%)	0.78 kg/100 km

In Table 4.2, one can see the hydrogen consumption for the modeled Fuel Cell-PHEV classified by mode according to Regulation R101.

Table 4.2: The hydrogen consumption for the Fuel Cell-PHEV classified by mode according to Regulation R101.

	Range in CD-mode	Hydrogen Consumption in CD-mode	Hydrogen Consumption in CS-mode	Combined Hydrogen Consumption
NEDC	43.4 km	0 kg/100 km	0.78 kg/100 km	0.29 kg/100 km
WLTC	39.7 km	0 kg/100 km	0.89 kg/100 km	0.34 kg/100 km

According to [25] as shown in the Table 4.3 below, the (combined) hydrogen consumption for Mercedes-Benz GLC F-CELL, which is also a Fuel Cell-PHEV (with a 13.8 kWh storage battery) is 0.34 kg/100 km. From the data source, it mentions that the combined hydrogen consumption was provisional and was determined by the technical service for the certification process in accordance with the WLTP test method and correlated into NEDC figures. The certificate of conformity with official figures is not yet available. Differences between the stated figures and the official figures are possible.

For the reference Fuel Cell-PHEV on the market, the initial SOC, the combined driving cycles used and the driving conditions are unknown. Therefore, the hydrogen consumption cannot be compared. However, it can be listed as a reference and give the reader a general idea about the hydrogen consumption for Fuel Cell-PHEV.

Table 4.3: The Hydrogen consumption for the reference Fuel Cell-PHEV on the market [25]

Vehicle Model	Hydrogen Consumption
Mercedes-Benz GLC F-CELL (Plug-in)	0.34 kg/100 km (Combined)

4.9 Hydrogen Consumption for the Fuel Cell-HEV

The initial value of the battery SOC for the Fuel Cell-HEV is set to be 70%.

The hydrogen consumption for the Fuel Cell-HEV running WLTC 5 times consecutively is 0.82 kg/100 km, and the battery SOC trajectory is shown in Figure 4.34 below.

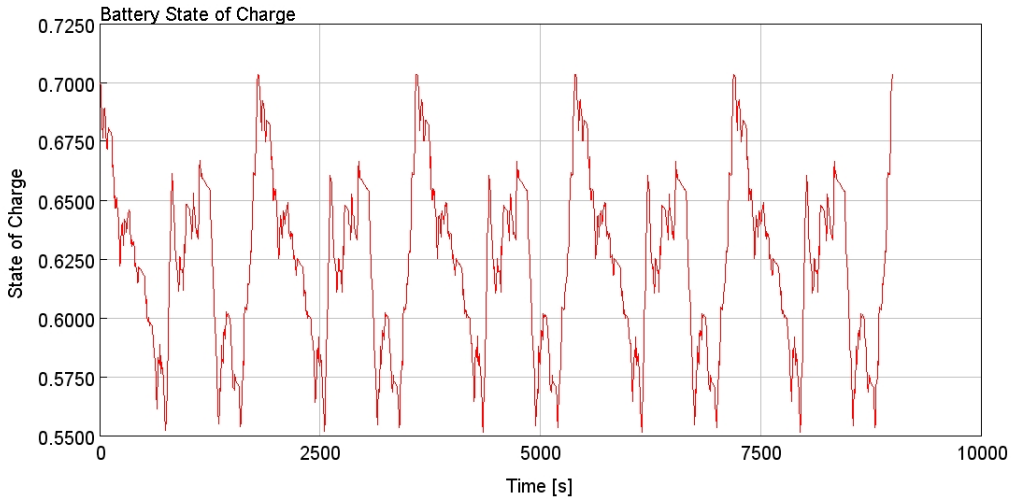

Figure 4.34: Battery SOC for the Fuel Cell-HEV driving WLTC 5 times consecutively with initial SOC 70%.

The hydrogen consumption for the Fuel Cell-HEV running NEDC 5 times consecutively is 0.68 kg/100 km and the battery SOC trajectory is shown in Figure 4.35 below.

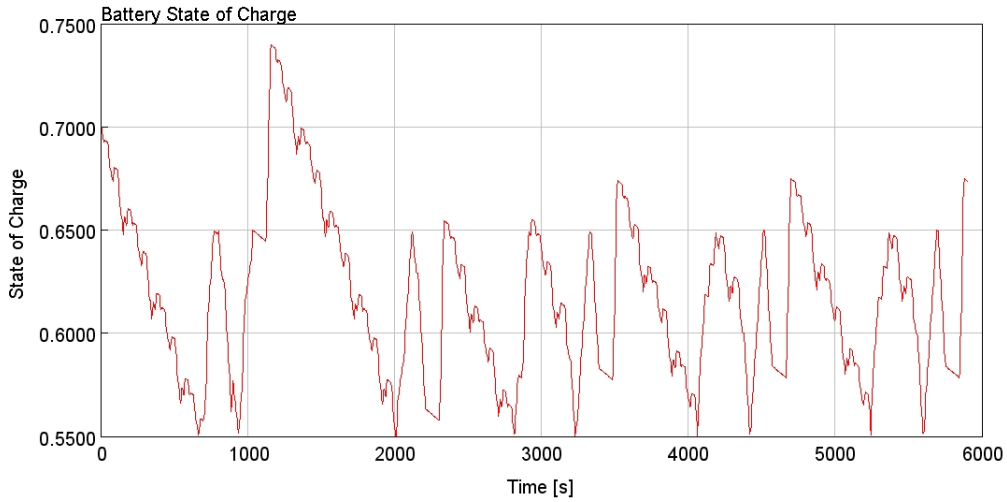

Figure 4.35: Battery SOC for the Fuel Cell-HEV driving NEDC 5 times consecutively with initial SOC 70%.

In Table 4.4, one can observe the hydrogen consumption for the modeled Fuel Cell-HEV in different driving cycles. Compared with the hydrogen consumption in the NEDC driving cycle with the same initial battery SOC, the hydrogen consumption increases 20.6% when running in the WLTC cycle. The result indicates that for the Fuel Cell-HEV, hydrogen consumption has a direct correlation with the driving cycle.

Table 4.4: The Hydrogen consumption for the Fuel Cell-HEV.

Vehicle Model	Hydrogen Consumption
Fuel Cell-HEV (WLTC 5 times, initial SOC 70%)	0.82 kg/100 km
Fuel Cell-HEV (NEDC 5 times, initial SOC 70%)	0.68 kg/100 km

According to [54], the combined hydrogen consumption for some reference Fuel Cell-HEV on the market can be observed in the Table 4.5 below.

For the reference Fuel Cell-HEV on the market, although the initial SOC does not have an enormous influence, the combined driving cycles used and the driving conditions are unknown. Therefore, the hydrogen consumption cannot be compared. However, it can be listed as a reference and give the reader a general idea about the hydrogen consumption for Fuel Cell-HEV.

Table 4.5: The Hydrogen consumption for the reference Fuel Cell-HEV on the market

Vehicle Model	Hydrogen Consumption
Toyota Mirai (Combined)	0.76 kg/100 km
Hyundai ix35 (NEDC/NEFZ)	1.0 kg/100 km
Hyundai NEXO (NEDC/NEFZ)	0.84 kg/100 km
Honda Clarity (Combined)	0.86 kg/100 km

4.10 Cost comparison based on different combinations

This section will present the results of a simple cost comparison among different combinations of power sources. The parameters in Table 4.6 were used in the calculation.

Table 4.6: Parameters used in general cost comparison

U.S Dollars to Swedish Krona (2019.5.16)	Fuel cell system efficiency	Battery efficiency	Battery cost($/kwh)
1:9.6	0.5	0.9	190
Hydrogen on-board storage cost($/kwh)	Fuel cell system cost($/kw)	Hydrogen cost($/kg)	Electricity Price in Sweden($/kwh)
17	50	11.8	0.21

4.10.1 Initial cost comparison

Figure 4.36 shows the cost comparison of energy source based on energy capacity. It is important to note that this cost comparison is only for energy source, and the precondition of it is the rest components are the same for both fuel cell vehicles and BEV. The contents for fuel cell vehicles are hydrogen onboard storage tank, fuel cell system, and battery PHEV and HEV. As for BEV, it only contents the cost of the battery.

In Figure 4.36, the x-axis is the energy capacity of the energy source, and the y-axis is the cost of energy source. With the increase of energy capacity, the cost of BEV has a vast increase, which is because of the high price of battery per kWh($ 190/kWh). However, the cost of onboard hydrogen storage is only $17/kWh, which is much cheaper than battery. It is no need to ask crystal-ball to find that when the request of energy capacity is high, the cost gap between BEV and fuel cell vehicle is enormous.

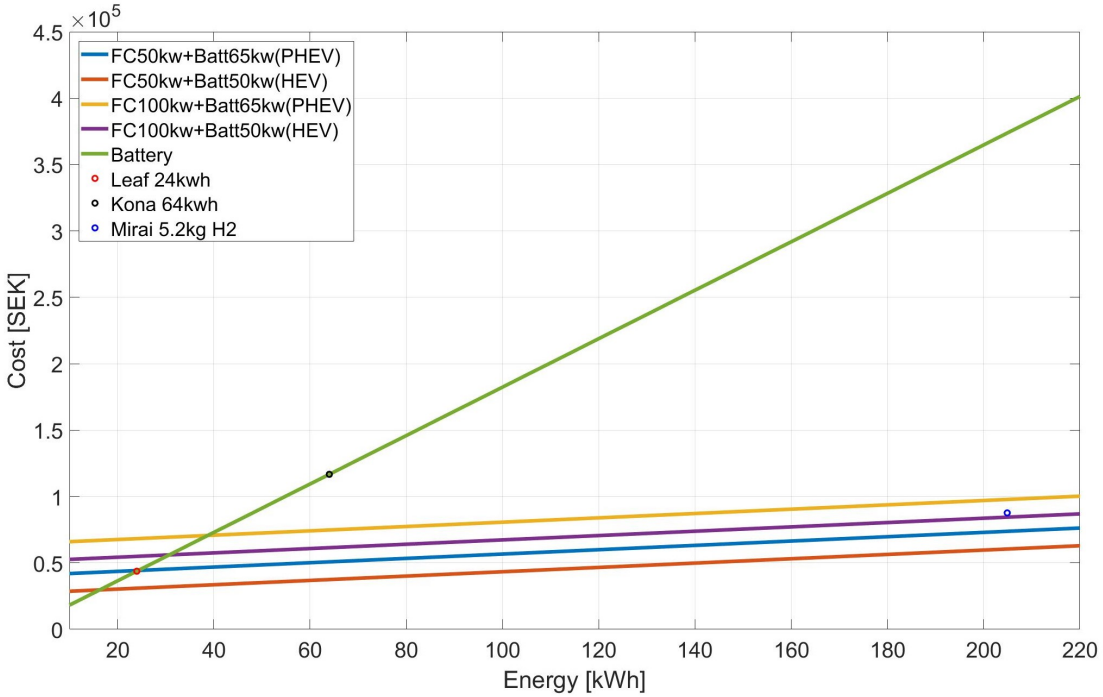

Figure 4.36: Cost comparison based on energy capacity

4.10.2 Total cost comparison

The total cost contents initial cost and using cost, the ratio between using electricity and hydrogen has been set as around 2:1. In other words, 2/3 of the trips will be covered by electricity and 1/3 of the trips will be covered by hydrogen, this is based on the data from U.S Department of Transportation Federal Highway Administration which mentioned in section 3.6. Meanwhile, most of conventional ICE Plug-in hybrid vehicles have set the pure electric range as 50 km. Therefore the ratio for using electricity and hydrogen has been set as 2.

As from Figure 4.37, the x-axis is the life span of a vehicle which is expressed as a range in km and y-axis is the total cost in Swedish Kronor. The starting point of the curve represents the initial component cost, which is based on the 78.5 kWh energy source and cooresponding to 500 km driving range, and there is a significant initial cost advantage for fuel cell vehicles compared to BEV. For using cost, it is still cost-efficient for using electricity instead of hydrogen currently. For fuel cell HEV which are blue and green lines, even it has an apparent initial cost advantage from BEV, but the total cost is still higher than BEV when the expected lifespan is higher than 150,000 km or 200,000 km for 150 kW HEV and 100 kW HEV respectively. According to the data from U.S Department of Transportation, the typical lifespan of a household vehicle is around 150,000 miles (241,400 km), it is easy to see that based on current state-of-play of hydrogen cost BEV still has cost advantage than fuel cell HEV. However, the total cost of fuel cell PHEV is still lower than BEV.

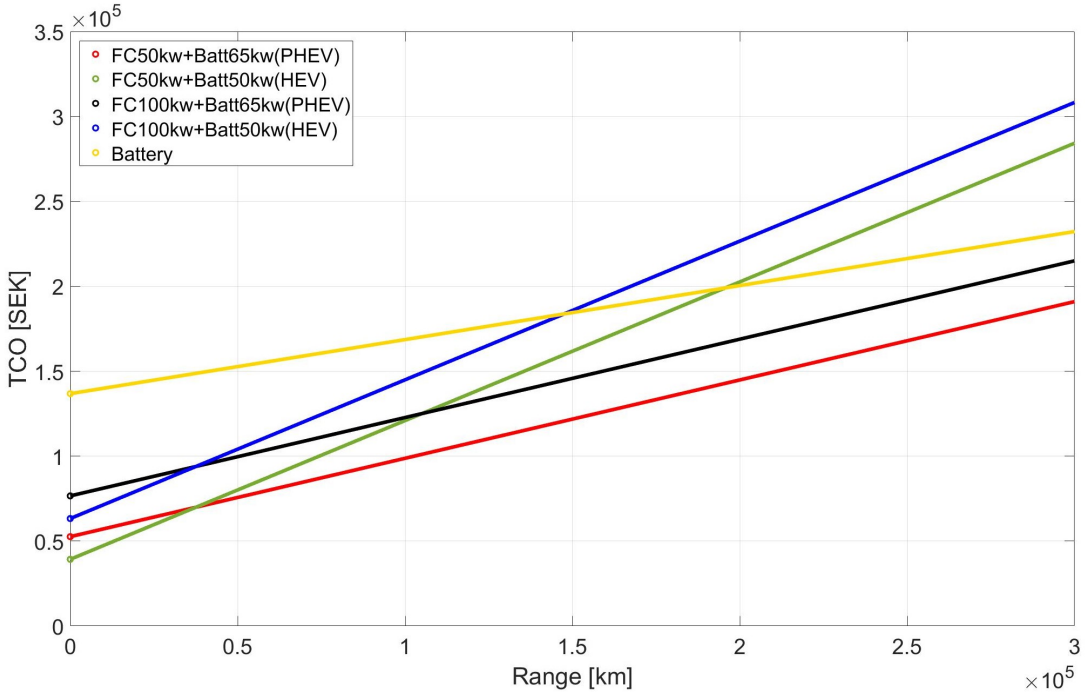

Figure 4.37: Total cost

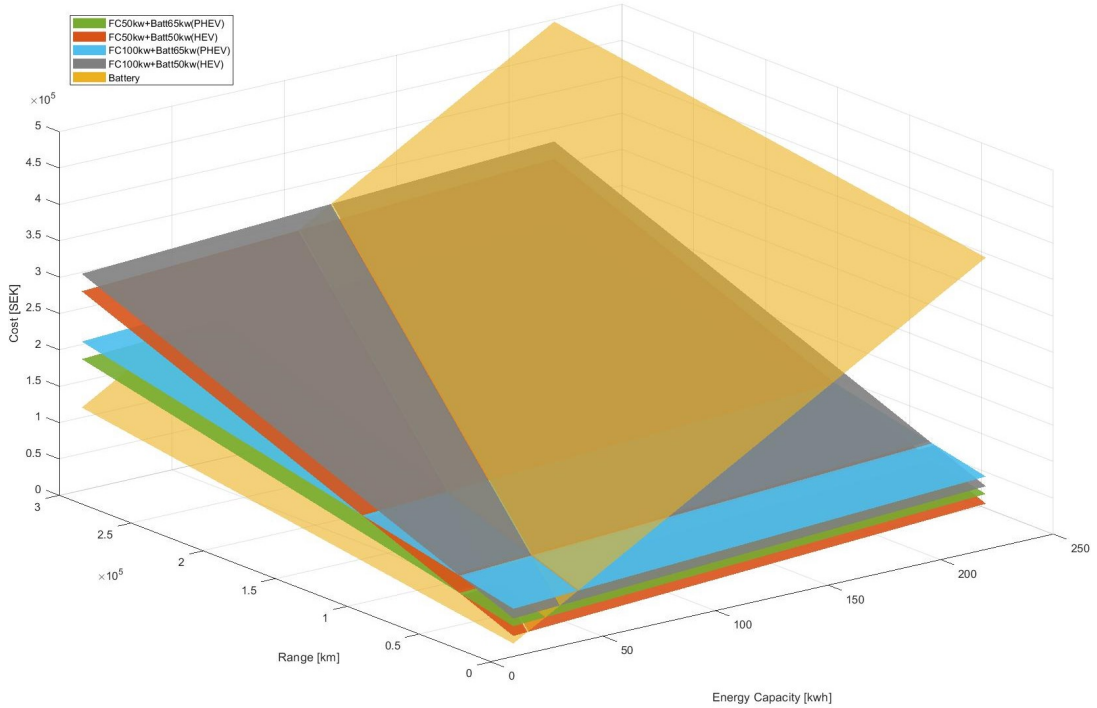

Figure 4.38: Total cost of ownership

Sum the results of initial cost and using cost, an XYZ plot can be defined, and Figure 4.38 is the XYZ plot for total cost regarding energy source capacity and

total driving range. The x-axis represents the energy source capacity, and the y-axis is the total driving range through the whole lifespan. From this XYZ plot, it can be found that for a specific size of energy capacity, the relationship between total cost and different total lifespan. Alternatively, the total cost difference of different size of energy source capacity for a specific lifespan.

4.11 Battery size determination for PHEV

Battery energy capacity determination method is presented in section cost model (3.7), this section will present the result for the best battery size from cost aspect.

Table 4.7: Parameters for U.S market

Vehicle energy consumption(kwh/km)	Fuel cell system efficiency	Battery efficiency	Battery SOC window
0.157	0.5	0.85	0.2-0.95
Battery cost($/kwh)	Hydrogen on-board storage($/kwh)	Hydrogen cost($/kg)	Electricity cost($/kwh)
190	17	11.8	0.13

Table 4.7 presents the parameters used for the battery size determination. Among the parameters, vehicle energy consumption and battery SOC window come from this project simulation. Besides, the data of cost of hydrogen and hydrogen on-board storage(if manufacturing volumes of 100,000 systems/year) came from U.S Department of Energy. Furthermore, the cost of the battery is based on the data from *Bloomberg NEF*.

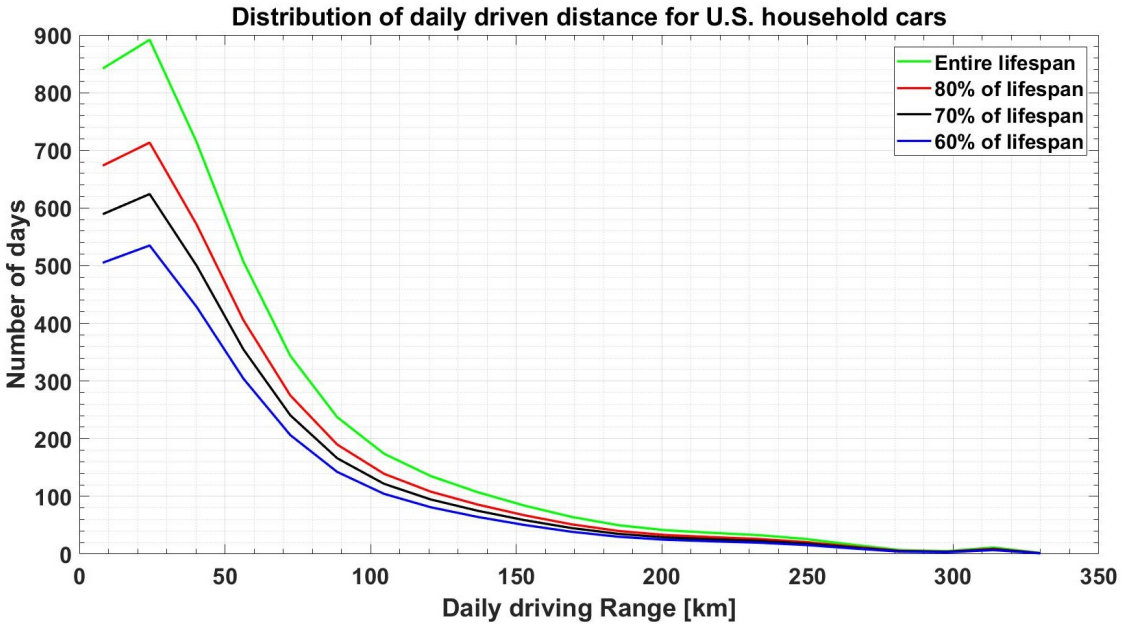

Figure 4.39: Distribution of the daily driven distance for U.S.household cars in days

Figure 4.39 illustrate the daily driving distribution of U.S market, based on the cost model in section 3.7 the result is 593 days, and the optimal battery size for entire lifespan, 80% lifespan, and 70% lifespan are 10.5 kWh, 8.37 kWh, and 6.28 kWh respectively.

The parameter used in the cost model is changing at any time; a discussion of how the parameters will affect the result will be presented. It can be predicted that the cost of hydrogen and hydrogen on-board storage will have a massive decrease in the future when large-scale production is implemented, and the decrease in either of them will have a positive effect for battery downsizing. While the cost reduction of battery and electricity will push the battery size going up. Therefore, what is the optimal battery size should be based on the data at the moment. Meanwhile, the distribution of daily driven distance for the different market is also different, which is another critical factor for the battery size determination. In general, specific analysis is required for the specific market.

5
Conclusion

In this thesis project, one Fuel Cell-PHEV and one Fuel Cell-HEV model, as well as their different components and control strategies have been modeled using GT-Suite software to analyze the hydrogen consumption under various driving cycles and scenarios. One cost analysis model has been developed using Matlab to find the optimal battery size for the Fuel Cell-PHEV. The conclusions of the study can be summarized as follows:

[1] The initial cost comparison for energy source components has been made in this project; The results of the initial cost comparison based on current data show the ranking from the cheapest to the most expensive powertrain is FC-HEV, FC-PHEV, and BEV.

[2] Using electricity from the grid is still much cheaper than using hydrogen to propel the vehicle. For FC-HEV it has no cost advantage compared with BEVs for the total cost of ownership through the whole vehicle lifespan since the only energy source of it is hydrogen. However, the total cost of ownership through the entire lifespan for FC-PHEV has advantages, that is because the energy source of FC-PHEV includes both electricity from the grid and hydrogen. The ranking of the total cost of ownership, including running cost from the cheapest to the most expensive is FC-PHEV, BEV, and FC-HEV.

[3] A summary of the hydrogen consumption for the modeled Fuel Cell-PHEV and Fuel Cell-HEV can be seen in Table 5.1 and Table 5.2 below

Table 5.1: The Hydrogen Consumption from the modeled Fuel Cell-PHEV.

	Range in CD-mode	**Hydrogen Consumption in CS-mode**	**Combined Hydrogen Consumption**
NEDC	43.4 km	0.78 kg/100 km	0.29 kg/100 km
WLTC	39.7 km	0.89 kg/100 km	0.34 kg/100 km

Table 5.2: The Hydrogen Consumption from the modeled Fuel Cell-HEV.

	Hydrogen Consumption
NEDC	0.68 kg/100 km
WLTC	0.82 kg/100 km

Since the FC-PHEV use both electricity from the grid and hydrogen as energy source. Therefore, the combined hydrogen consumption of FC-PHEV is much lower than that of FC-HEV configuration.

[4] A summary of the advantages and disadvantages of the different powertrain configurations can be seen in the Table 5.3, where '+' represents 'Better', '-' represents 'Worse' and '0' represents 'Middle'.

Table 5.3: The Comparison Summary.

	BEVs	**Fuel Cell-HEV**	**Fuel Cell-PHEV**
Emissions	+	+	+
Recharging/Refueling time	-	+	+
Range	-	+	+
Initial cost of energy source	-	+	**0**
Total cost of ownership	-	-	+
Fuel consumption	++	-	+

Overall, the Fuel Cell Plug-in Hybrid Electric Vehicle could be the best choice based on the current data.

[5] This project also present a simple mathematical cost model for determining the optimal energy capacity of the battery pack in FC-PHEV from economic aspect through the whole vehicle lifespan, it shows the optimal battery size of FC-PHEV based on the data of this model in the U.S market is around 10.5 kWh which equals to a 50 km driving range roughly.

6

Future Scope

This chapter will present some ideas which can be further developed but exceed time limitation or beyond the project scope.

6.1 PEM fuel cell system

The PEM fuel cell system in this project is a simplified model aiming to mimic the whole working process of the fuel cell system, but there are still lots of developments that need to be implemented in the future.

In the supplying system for both anode and cathode side, the compressors were modeled as ideal models. This part can be modeled as a detailed model and inserting the real measurements to improve the model dependency. In real condition, the compressor is connected to a motor through mechanical connections, and the future work needs to model a detailed motor model to get the reasonable lagging time of fuel cell system power-output. Moreover, the lagging time is an essential factor for energy management system implementation.

Overall, the PEM fuel cell system is lacking model validation. Until the whole model has been submitted, the model was only built but without validation since the limited time. The future work will cover the data collecting and model validation.

6.2 Electrical connection instead of power flow connection

In the project model, so far, all the components were connected by wireless signals instead of real electrical connections. If all the component models within the completed electrical architecture are available in the future, the model should be connected with electrical connections.

Fig.6.1 is an example to connect the components with electrical connections, but the results were not accurate and due to lacking necessary components model, the results were not present. This is where future work can modify.

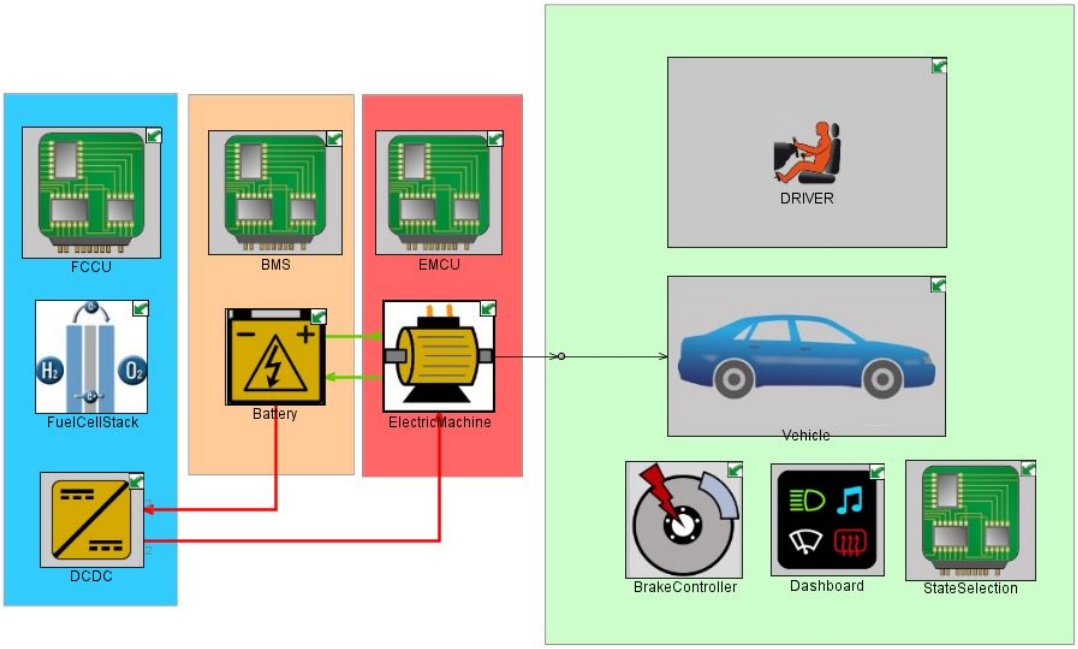

Figure 6.1: Electrical connection instead of power flow connection in GT-Suite

6.3 Different control strategies

In this thesis project, mainly rule-based control strategies are used to manage the energy and power flow. However, there are many other control strategies which can be further developed and implemented in the Fuel Cell-HEV and Fuel Cell-PHEV models. The following control strategies can be implemented and analyzed in the future:

· The ECMS (Equivalent Consumption Minimization Strategy) aims to minimize a sum of power from fuel and battery at each timestep [55]. The power from the battery is converted into fuel consumption by using an equivalence factor.

· The stiffness-coefficient-model (SCM) determines the fuel cell power according to the actual SOC of the battery and the power demand. The charging and discharging behaviors of the battery are triggered by the adjustment of the stiffness coefficients. The basic ideas of the SCM for fuel economy are to operate the fuel cell in high-efficiency areas and in doing so also in load following modus and that the battery has to cope with the dynamic charging and discharging conditions [56].

· Fuzzy-logic-controller (FLC) makes the transition between quantized steps smooth, and also weighs the control signals in such a way that the best representative, according to certain rules, is picked [57]. The input variables P_{demand} and SOC are

assigned to membership functions and passed to the FLC [56].

6.4 Using supercapacitor instead of battery

Another configuration of Fuel Cell Vehicle powertrain is using the PEM fuel cell system as the main power source to handle the steady-state conditions and using supercapacitor as the secondary or auxiliary power source to handle transient conditions. In report [58], the simulation results showed that the hybridization of FC and supercapacitor has the better performance due to the more effective assistance of the supercapacitor for FC, since the high charge current and discharge current can be obtained in the supercapacitor. Moreover, the supercapacitor can remove the peaks from the required drive power, which makes the power supplied by FC flatter, leading to a longer lifetime of the FC. In the future, this kind of powertrain configuration can be modeled and simulated.

6.5 The fuel cell vehicle drivability evaluation

The term driveability describes the driver's complex subjective perception of the interactions with the vehicle [59]. However, for a fuel cell vehicle, it may face a problem called fuel cell starvation, the compressor motor for replenishing oxygen is not easy to be regulated during power generation. This task needs to be achieved rapidly and efficiently to avoid oxygen starvation and degradation of the stack voltage [60], which could affect the rapid power response of the fuel cell vehicle. In the future, the simulation results can be implemented into the driveability evaluation tool AVL-DRIVE to predict the vehicle driveability without using the vehicle [61].

6.6 Driver mode selection

In the future, the active driver mode selection system can be further studied, where the driver can select the driving or charging mode following the current driving condition or the future driving conditions are known a priori. For the fuel cell vehicle, besides modes like ECO, Sport, and Normal. One could add a range-extend mode, which the fuel cell system will charge the battery until the SOC upper limit when this mode is selected. For example, when the driver will have a long journey and the driver is going to the hydrogen station. After selecting the range-extend mode, the fuel cell system will start charging the onboard battery until refilling. Therefore, the driving distance can be extended significantly.

6.7 Battery size determination

About the battery size determination, the method in this project is only from the economic aspect. The future work can investigate more factors into the analysis to make the result more accurate. Meanwhile, the results were based on the data from current U.S market which needs to be updated at any time to get a reasonable result of the moment and collecting data from a different markets to get the result for a specific market.

Bibliography

[1] B. T. Lokesh and J. T. Hui Min, "A Framework for Electric Vehicle (EV) Charging in Singapore", *Energy Procedia*, vol. 143, pp. 15–20, Dec. 2017, ISSN: 18766102. DOI: 10.1016/j.egypro.2017.12.641. [Online]. Available: https://linkinghub.elsevier.com/retrieve/pii/S1876610217364056.

[2] L. Zhang, J. Yu, J. Ren, L. Ma, W. Zhang, and H. Liang, "How can fuel cell vehicles bring a bright future for this dragon? Answer by multi-criteria decision making analysis", *International Journal of Hydrogen Energy*, 2016, ISSN: 03603199. DOI: 10.1016/j.ijhydene.2016.08.044.

[3] "Global Energy & CO 2 Status Report", Tech. Rep., 2017. [Online]. Available: https://www.connaissancedesenergies.org/sites/default/files/pdf-actualites/geco2017.pdf.

[4] I. E. A. International and E. Agency, "Global EV Outlook 2018", 2018, ISSN: 16738527. DOI: 10.1787/9789264302365-en. [Online]. Available: https://www.oecd-ilibrary.org/energy/global-ev-outlook-2018_9789264302365-en.

[5] Wikipedia, *Phase-out of fossil fuel vehicles*. [Online]. Available: https://en.wikipedia.org/wiki/Phase-out_of_fossil_fuel_vehicles.

[6] ——, *Energy density*. [Online]. Available: https://en.wikipedia.org/wiki/Energy_density.

[7] Solar Journey USA, *Can EVs handle the distances we drive? • A Study*. [Online]. Available: http://www.solarjourneyusa.com/EVdistanceAnalysis3.php.

[8] M.-R. de Valladares and G. M. I. H. T. C. P. (Mary-Rose de Valladares, "Global Trends and Outlook for Hydrogen", Tech. Rep. December, 2017, p. 20. DOI: ISBN-13:978-1-945951-07-7. [Online]. Available: http://ieahydrogen.org/pdfs/Global-Outlook-and-Trends-for-Hydrogen_WEB.aspx.

[9] Z. Xin, *Hydrogen vehicles on their way*, 2019. [Online]. Available: http://global.chinadaily.com.cn/a/201904/11/WS5cae817fa31048422-60b5819.html.

[10] P. Brooker, "Fuel Cells as Electric Vehicle Range Extenders", Tech. Rep., 2015. [Online]. Available: http://www.fsec.ucf.edu/en/publications/pdf/FSEC-CR-1995-14.pdf.

[11] C. Mi and A. Masrur, *Hybrid electric vehicles : principles and applications with practical perspectives*, ISBN: 9781118970560.

[12] V. Freyermuth, E. Fallas, and A. Rousseau, "Comparison of Powertrain Configuration for Plug-in HEVs from a Fuel Economy Perspective", Tech. Rep., 2007.

[Online]. Available: https://www.autonomie.net/docs/6%20-%20Papers/HEVs%20&%20PHEVs/Powertrain%20Configurations/comparison_of_powertrain.pdf.

[13] H. Banvait, S. Anwar, and Y. Chen, "A rule-based energy management strategy for Plug-in Hybrid Electric Vehicle (PHEV)", in *2009 American Control Conference*, IEEE, 2009, pp. 3938–3943, ISBN: 978-1-4244-4523-3. DOI: 10.1109/ACC.2009.5160242. [Online]. Available: http://ieeexplore.ieee.org/document/5160242/.

[14] Union of Concerned Scientists, *How Do Hydrogen Fuel Cell Vehicles Work?* [Online]. Available: https://www.ucsusa.org/clean-vehicles/electric-vehicles/how-do-hydrogen-fuel-cells-work.

[15] G. (Pistoia, *Electric and hybrid vehicles : power sources, models, sustainability, infrastructure and the market*. Elsevier, 2010, p. 652, ISBN: 9780444535665.

[16] matthew, *The World's First Mass-Production of FCEV - - BusinessKorea*. [Online]. Available: http://www.businesskorea.co.kr/news/articleView.html?idxno=552.

[17] HYUNDAI Media Center, *Hyundai ix35 Fuel Cell - Hyundai Newsroom*. [Online]. Available: https://www.hyundainews.com/en-us/releases/1624.

[18] H2.LIVE, *Fuel Cell Cars Models Overview*. [Online]. Available: https://h2.live/en/wasserstoffautos.

[19] Wikipedia, *Toyota Mirai*. [Online]. Available: https://en.wikipedia.org/wiki/Toyota_Mirai.

[20] INSIDEEVs, *Hydrogen Shortage Hits Hard: Toyota Mirai Owners Urged To Top Up Frequently*. [Online]. Available: https://insideevs.com/news/338465/hydrogen-shortage-hits-hard-toyota-mirai-owners-urged-to-top-up-frequently/.

[21] HYUNDAI Media Center, *Hyundai ix35 Fuel Cell - Hyundai Newsroom*. [Online]. Available: https://www.hyundainews.com/en-us/releases/1624.

[22] Green Motion, *Green Motion | News*. [Online]. Available: https://greenmotion.com/news.

[23] Madeleine Herdlitschka, *Mercedes-Benz GLC F-CELL: Market launch of the world's first electric vehicle featuring fuel cell and plug-in hybrid technology - Daimler Global Media Site*. [Online]. Available: https://media.daimler.com/marsMediaSite/en/instance/ko/Mercedes-Benz-GLC-F-CELL-Market-launch-of-the-worlds-first-electric-vehicle-featuring-fuel-cell-and-plug-in-hybrid-technology.xhtml?oid=41813012.

[24] INSIDEEVs, *Mercedes-Benz GLC F-CELL Combines Fuel Cell With Plug-In Capability*. [Online]. Available: https://insideevs.com/news/340241/mercedes-benz-glc-f-cell-combines-fuel-cell-with-plug-in-capability/.

[25] *The GLC F-CELL: First electric vehicle featuring fuel cell and plug-in hybrid technology | Daimler*. [Online]. Available: https://www.daimler.com/products/passenger-cars/mercedes-benz/glc-f-cell.html.

[26] P. Nikolaidis and A. Poullikkas, "A comparative overview of hydrogen production processes", *Renewable and Sustainable Energy Reviews*, vol. 67, pp. 597–611, Jan. 2017, ISSN: 1364-0321. DOI: 10.1016/J.RSER.2016.09.044. [On-

line]. Available: https://www.sciencedirect.com/science/article/pii/S1364032116305366.

[27] P. Corbo, F. Migliardini, and O. Veneri, *Hydrogen Fuel Cells for Road Vehicles*, ser. Green Energy and Technology. London: Springer London, 2011, ISBN: 978-0-85729-135-6. DOI: 10.1007/978-0-85729-136-3. [Online]. Available: http://link.springer.com/10.1007/978-0-85729-136-3.

[28] "GLOBAL TRENDS AND OUTLOOK FOR HYDROGEN 2 IEA Hydrogen", Tech. Rep., 2017. [Online]. Available: http://ieahydrogen.org/pdfs/Global-Outlook-and-Trends-for-Hydrogen_Dec2017_WEB.aspx.

[29] M. Ehsani, Y. Gao, A. Emadi, Y. Gao, and A. Emadi, *Modern Electric, Hybrid Electric, and Fuel Cell Vehicles*. CRC Press, Dec. 2017, ISBN: 9781315219400. DOI: 10.1201/9781420054002. [Online]. Available: https://www.taylorfrancis.com/books/9781420054002.

[30] M. E. Demir and I. Dincer, "Cost assessment and evaluation of various hydrogen delivery scenarios", *International Journal of Hydrogen Energy*, vol. 43, no. 22, pp. 10 420–10 430, May 2018, ISSN: 0360-3199. DOI: 10.1016/J.IJHYDENE.2017.08.002. [Online]. Available: https://www.sciencedirect.com/science/article/pii/S0360319917331579.

[31] Hydrogen Europe, *Hydrogen storage | Hydrogen*. [Online]. Available: https://hydrogeneurope.eu/hydrogen-storage.

[32] Wikipedia, *Hydrogen storage*. [Online]. Available: https://en.wikipedia.org/wiki/Hydrogen_storage.

[33] TOYOTA, *Toyota Mirai: Faktan om vår vätgasdrivna bränslecellsbil*. [Online]. Available: https://www.toyota.se/nya-bilar/mirai/faktan.

[34] Bengt Jacobson, *Vehicle Dynamics Compendium 2017*. 2017.

[35] L. A. Mohammed Saeed and L. Andersson, "Real Driving Emissions (RDE) of a Gasoline PHEV", 2018. [Online]. Available: http://studentarbeten.chalmers.se/publication/256029-real-driving-emissions-rde-of-a-gasoline-phev.

[36] "THE BENEFITS OF WLTP", Tech. Rep. [Online]. Available: https://wltpfacts.eu/wp-content/uploads/2017/04/WLTP_Leaflet_FA_web.pdf.

[37] Wikipedia, *Worldwide harmonized light vehicles test procedure - Wikipedia*. [Online]. Available: https://en.wikipedia.org/wiki/Worldwide_harmonized_light_vehicles_test_procedure.

[38] Diesel Net, *Emission Test Cycles: WLTC*. [Online]. Available: https://www.dieselnet.com/standards/cycles/wltp.php.

[39] Volvo Cars, *XC90 Twin Engine*. [Online]. Available: https://www.volvocars.com/en-ca/support/cars?pc=V526T8HBAT&my=2016&sw=15w46&&tab=ownersmanualonline&category=0f0050265f381217c0a801517550b725-om-en-ca-v526t8hbat-2016-15w46&article=65d5624f16a7c095c0a8015133-99886c-om-en-ca-v526t8hbat-2016-15w46.

[40] L. Pipkorn, "XC90 Plug-in Hybrid Customer Usage", Tech. Rep. [Online]. Available: https://publications.lib.chalmers.se/records/fulltext/254650/254650.pdf.

[41] Argonne NATIONAL LABORATORY, "Technology Assessment of a Fuel Cell Vehicle: 2017 Toyota Mirai Energy Systems Division", Tech. Rep. [Online]. Available: https://publications.anl.gov/anlpubs/2018/06/144774.pdf.

[42] M. Ehsani, Y. Gao, S. E. Gay, and A. Emadi, "Modern Electric, Hybrid Electric, and Fuel Cell Vehicles: Fundamentals, Theory, and Design", Tech. Rep. [Online]. Available: http://ceb.ac.in/knowledge-center/E-BOOKS/Modern%20Electric,%20Hybrid%20Electric%20&%20Fuel%20Cell%20Vehicles%20-%20Mehrdad%20Ehsani.pdf.

[43] C. Kunusch, P. Puleston, and M. Mayosky, "PEM fuel cell systems", in *Advances in Industrial Control*, 9781447124306, Springer International Publishing, 2012, pp. 13–33. DOI: 10.1007/978-1-4471-2431-3{_}2.

[44] *The Ideal Gas Law - Chemistry LibreTexts*. [Online]. Available: https://chem.libretexts.org/Bookshelves/Physical_and_Theoretical_Chemistry_Textbook_Maps/Supplemental_Modules_(Physical_and_Theoretical_Chemistry)/Physical_Properties_of_Matter/States_of_Matter/Properties_of_Gases/Gases_(Waterloo)/The_Ideal_Gas_Law.

[45] S. Gottesfeld and T. A. Zawodzinski, "Polymer Electrolyte Fuel Cells", in, John Wiley & Sons, Ltd, Mar. 2008, pp. 195–301. DOI: 10.1002/9783527616794.ch4. [Online]. Available: http://doi.wiley.com/10.1002/9783527616794.ch4.

[46] NIST|U.S Department of Commerce, *Thermophysical Properties of Fluid Systems*. [Online]. Available: https://webbook.nist.gov/chemistry/fluid/.

[47] E. Grunditz, "BEV Powertrain Component Sizing With Respect to Performance, Energy Consumption and Driving Patterns", PhD thesis, May 2014.

[48] Deloitte Sverige, *Deloitte Sverige | Revision, Consulting, Financial Advisory, Risk Management & Tax*. [Online]. Available: https://www2.deloitte.com/se/sv.html.

[49] A. Santos, N. Mcguckin, H. Y. Nakamoto, D. Gray, S. Liss, A. Santos, N. Mcguckin, H. Y. Nakamoto, D. Gray, S. Liss, and C. Systematics, "SUMMARY OF TRAVEL TRENDS - 2009 National Household Travel Survey", Tech. Rep., 2011. [Online]. Available: https://nhts.ornl.gov/2009/pub/stt.pdf.

[50] NISSAN, *Ample driving range for everyday deeds. Nissan Motor Corporation*. [Online]. Available: https://europe.nissannews.com/en-GB.

[51] L.-H. Kullingsjö and S. Karlsson, "The Swedish car movement data project", 2012. [Online]. Available: https://research-chalmers-se.proxy.lib.chalmers.se/publication/165497.

[52] statista, *Projected U.S. vehicle age from 2017 to 2019*. [Online]. Available: https://www.statista.com/statistics/738667/us-vehicles-projected-age/.

[53] "Too low to be true? How to measure fuel consumption and CO2 emissions of plug-in hybrid vehicles, today and in the future", Tech. Rep., 2017. [Online]. Available: https://www.theicct.org/sites/default/files/publications/EU-PHEV_ICCT-Briefing-Paper_280717_vF.pdf.

[54] *Toyota MIRAI Fuel Cell Car - H2.LIVE*. [Online]. Available: https://h2.live/en/wasserstoffautos/toyota-mirai.

[55] A. Sciarretta, M. Back, and L. Guzzella, "Optimal Control of Parallel Hybrid Electric Vehicles", *IEEE Transactions on Control Systems Technology*, vol. 12, no. 3, pp. 352–363, May 2004, ISSN: 1063-6536. DOI: 10.1109/TCST.2004.824312. [Online]. Available: http://ieeexplore.ieee.org/document/1291406/.

[56] C. Weyers and T. Bocklisch, "Simulation-based investigation of energy management concepts for fuel cell – battery – hybrid energy storage systems in mobile applications", *Energy Procedia*, vol. 155, pp. 295–308, Nov. 2018, ISSN: 1876-6102. DOI: 10.1016/J.EGYPRO.2018.11.048. [Online]. Available: https://www.sciencedirect.com/science/article/pii/S1876610218309950.

[57] J. Persson and T. Lundberg, "Hybrid Powertrain Control A Predictive Real-time Energy Management System for a Parallel Hybrid Electric Vehicle", Tech. Rep. [Online]. Available: https://publications.lib.chalmers.se/records/fulltext/87881.pdf.

[58] Q. Xun, Y. Liu, and E. Holmberg, "A Comparative Study of Fuel Cell Electric Vehicles Hybridization with Battery or Supercapacitor", in *2018 International Symposium on Power Electronics, Electrical Drives, Automation and Motion (SPEEDAM)*, IEEE, Jun. 2018, pp. 389–394, ISBN: 978-1-5386-4941-1. DOI: 10.1109/SPEEDAM.2018.8445386. [Online]. Available: https://ieeexplore.ieee.org/document/8445386/.

[59] L. Castellazzi, A. Tonoli, N. Amati, A. Piu, and E. Galliera, "Vehicle Driveability: Dynamic Analysis of Powertrain System Components", Apr. 2016. DOI: 10.4271/2016-01-1124. [Online]. Available: https://www.sae.org/content/2016-01-1124/.

[60] J. T. Pukrushpan, A. G. Stefanopoulou, and H. Peng, "Control of Fuel Cell Breathing: Initial Results on the Oxygen Starvation Problem", Tech. Rep. [Online]. Available: https://pdfs.semanticscholar.org/588d/b1d4e2da88c5a-2fd310546cf0e375b146de6.pdf.

[61] H. O. List and P. Schoeggl, "Objective Evaluation of Vehicle Driveability", Feb. 1998. DOI: 10.4271/980204. [Online]. Available: https://www.sae.org/content/980204/.